A DESIGN AND IMPLEMENTATION OF P300 BASED BRAIN-COMPUTER INTERFACE

A THESIS SUBMITTED TO
THE GRADUATE SCHOOL OF NATURAL AND APPLIED SCIENCES
OF
MIDDLE EAST TECHNICAL UNIVERSITY

BY

HASAN BALKAR ERDOĞAN

IN PARTIAL FULFILLMENT OF THE REQUIREMENTS
FOR
THE DEGREE OF MASTER OF SCIENCE
IN
ELECTRICAL AND ELECTRONICS ENGINEERING

SEPTEMBER 2009

Approval of the thesis

A DESIGN AND IMPLEMENTATION OF P300 BASED BRAIN-COMPUTER INTERFACE

submitted by **HASAN BALKAR ERDOĞAN** in partial fulfillment of the requirements for the degree of **Master of Science in Electrical and Electronics Engineering, Middle East Technical University** by,

Prof. Dr. Canan Özgen
Dean, Graduate School of **Natural and Applied Sciences** _____

Prof. Dr. İsmet Erkmen
Head of Department, **Electrical and Electronics Engineering** _____

Prof. Dr. Nevzat Güneri Gençer
Supervisor, **Electrical and Electronics Engineering, METU** _____

Examining Committee Members:

Prof. Dr. Murat Eyüboğlu
Electrical and Electronics Engineering, METU _____

Prof. Dr. Nevzat Güneri Gençer
Electrical and Electronics Engineering, METU _____

Prof. Dr. Uğur Halıcı
Electrical and Electronics Engineering, METU _____

Assoc. Prof. Dr. Tolga Çiloğlu
Electrical and Electronics Engineering, METU _____

Assoc. Prof. Dr. Süha Yağcıoğlu
Biophysics Dept., Faculty of Medicine, Hacettepe University _____

Date: 11.09.2009

I hereby declare that all information in this document has been obtained and presented in accordance with academic rules and ethical conduct. I also declare that, as required by these rules and conduct, I have fully cited and referenced all material and results that are not original to this work.

Name, Last name: Hasan Balkar Erdoğan

Signature :

ABSTRACT

A DESIGN AND IMPLEMENTATION OF P300 BASED BRAIN-COMPUTER INTERFACE

Erdoğan, Hasan Balkar
M.S., Department of Electrical and Electronics Engineering
Supervisor: Prof. Dr. Nevzat Güneri Gençer
Coadvisor: Dr. Ali Bülent Uşaklı

September 2009, 161 Pages

In this study, a P300 based Brain-Computer Interface (BCI) system design is realized by the implementation of the Spelling Paradigm. The main challenge in these systems is to improve the speed of the prediction mechanisms by the application of different signal processing and pattern classification techniques in BCI problems.

The thesis study includes the design and implementation of a 10 channel Electroencephalographic (EEG) data acquisition system to be practically used in BCI applications. The electrical measurements are realized with active electrodes for continuous EEG recording. The data is transferred via USB so that the device can be operated by any computer.

Wiener filtering is applied to P300 Speller as a signal enhancement tool for the first time in the literature. With this method, the optimum temporal frequency bands for user specific P300 responses are determined. The classification of the responses is performed by using Support Vector Machines (SVM's) and Bayesian decision. These methods are independently applied to the row-column intensification groups of P300 speller to observe the differences in human perception to these two visual stimulation types. It is observed from the investigated datasets that the prediction accuracies in these two groups are different for each subject even for optimum classification parameters. Furthermore, in these datasets, the classification accuracy was improved when the signals are preprocessed with Wiener filtering. With this method, the test characters are predicted with 100% accuracy in 4 trial repetitions in P300 Speller dataset of BCI Competition II. Besides, only 8 trials are needed to predict the target character with the designed BCI system.

Keywords: Brain Computer Interface (BCI), Spelling Paradigm, P300 Speller, Electroencephalography (EEG), Hardware Design, Human Perception to Visual Stimulations, Wiener Filtering, Support Vector Machines (SVM).

ÖZ

P300 TABANLI BEYİN-BİLGİSAYAR ARAYÜZÜNÜN TASARIMI VE UYGULAMASI

Erdoğan, Hasan Balkar
Yüksek Lisans, Elektrik-Elektronik Mühendisliği Bölümü
Tez Yöneticisi: Prof. Dr. Nevzat Güneri Gençer
Tez Yardımcı Danışmanı: Dr. Ali Bülent Uşaklı

Eylül 2009, 161 sayfa

Bu çalışmada, Heceleme Paradigması uygulaması ile P300 tabanlı bir Beyin-Bilgisayar Arayüzü (BBA) sisteminin tasarımı gerçekleştirilmiştir. Bu sistemlerdeki temel hedef, BBA problemlerine farklı işaret işleme ve örüntü sınıflandırma yöntemleri uygulayarak, problemlerdeki tahmin mekanizmalarının hızını arttırmaktır.

Bu tez çalışması, BBA uygulamalarında pratik olarak kullanılmak üzere, 10 kanallı bir Elektroensefalografik (EEG) veri toplama sistemi tasarımı ve kurulumunu içermektedir. Elektriksel ölçümler, süreğen bir EEG kaydı için aktif elektrotlar ile gerçekleştirilmektedir. Sayısal veri iletimi, sistemin herhangi bir bilgisayarda kontrol edilebilmesi için Evrensel Seri Yol (USB) aracılığıyla sağlanmaktadır.

Wiener süzgeçleme yöntemi, P300 Heceleme Uygulaması'na bir sinyal işleme aracı olarak literatürde ilk defa uygulanmıştır. Bu yöntem ile kişiye özel P300 tepkilerinin algılanması için optimum zamansal frekans bantları belirlenmiştir. Tepkilerin sınıflandırılması, Destek Vektör Makineleri (DVM) ve Bayes karar yöntemleri kullanılarak gerçekleştirilmiştir. Bu yöntemler, P300 Heceleticisi'ndeki satır-sütun yanma gruplarına bağımsız bir şekilde uygulanmış ve kişinin bu iki görsel uyarana olan algısı incelenmiştir. İncelenen P300 Heceleticisi veri kümelerine göre, sınıflandırıcıların optimum parametrelerle bile bu iki gruptaki tahmin başarısının farklı olduğu gözlemlenmiştir. Ayrıca, bu veri kümelerinde, işaretler Wiener süzgeçleme yöntemi ile işlendiğinde sınıflandırma başarısı artmıştır. Bu yöntem ile 2. BBA Yarışması'ndaki P300 Heceleticisi veri kümesindeki test karakterler, 4 tekrar kullanılarak %100 başarıyla tahmin edilmiştir. Tasarlanan BBA sistemi ile ise hedef karakterin tahmini sadece 8 tekrar ile mümkündür.

Anahtar Sözcükler: Beyin Bilgisayar Arayüzü (BBA), Heceleme Uygulaması, P300 Heceleticisi, Elektroensefalografi (EEG), Donanım Tasarımı, İnsanın Görsel Uyaranlara Olan Algısı, Wiener Süzgeçleme, Destek Vektör Makinaları (DVM)

To my Family

ACKNOWLEDGEMENTS

I would like to express my gratitude to my supervisor Prof. Dr. Nevzat G. Gençer for his invaluable help in my academic career. Studying with him and in his laboratory for the last two years was a great privilege for me. I would like to thank to Dr. Ali Büşent Uşaklı for sharing his critical ideas and experience in designing the EEG system.

I would like to thank to my family for their lovely support throughout this thesis. They were always nearby me even if they live far away. There is my beloved Berna who had seen all the dark sides of my mind and taken care of everything with her patience and encouragement during the last few months. I always feel the peace when I remember that their love will never fade no matter what happens.

Also, I would like to express my special thanks to Didem Menekşe for her invaluable friendship. There was always a cup of warm tea when I was concentrated on solving a problem or soldering the components on the circuit board during the integration of the EEG instrumentation. I would like to thank to Alper Çevik, Ajdan Küçükçiftçi, Yusuf Sayıta, Erdem Tosun and Azadeh Kamali, for their lovely friendship and wonderful nights they share with us.

I would like to utter my apologies to my colleagues Koray Özdal Özkan, Feza Carlak and Reyhan Zengin for the noise I have made during the implementation process of the EEG board. I would like to thank to Erman Acar for helping me to solder the components on the board and also, I would like to express my special thanks to Koray Özdal Özkan for the instrumentation I was supported during the

design of the EEG system and for the practical answers he shared with me in numerous problems. He has invaluable support in the design, implementation and test phases of the system.

Furthermore, there is Hemosoft who has been my second family after my graduation. It was never an ordinary workplace for me. Here, I would like to utter my gratitude to Dr. Güçlü Ongun for his key answers in most frustrating problems that I have encountered in this thesis. I believe that I have learned how to deal with problems in analytical point of view from him and Dr. Altan Koçyiğit.

Finally, I would like to express my thanks to Dr. Murat Özgören and Dr. Adile Öniz from 9 Eylül University for allowing me to use their EEG Laboratories during the experimentation of the P300 Speller. It was a great opportunity for me to gather a realistic EEG data for the thesis in such an excellent measuring environment.

TABLE OF CONTENTS

LIST OF TABLES

LIST OF FIGURES

CHAPTER 1

INTRODUCTION

Interaction with the outside world by means of communication is one of the most indispensible gifts of the human being. We all need our hands to control or use anything around us, legs to move and other necessary limbs that are crucial for continuing our lives. Unfortunately, these abilities can be lost due to possible accidents or diseases. As examples, Amyotrophic Lateral Sclerosis (ALS), brainstem stroke and multiple sclerosis are some of the diseases in which the motor neural pathways are damaged causing people to be locked into their bodies. In such a case, the voluntary control is lost fully or partially over the body [1]. With full consciousness, the patients suffering from these diseases can not even realize a physical movement or communicate with their environment. Therefore, it is impossible for these people to live and fulfill their daily needs without external help.

Fortunately, with the advancements in technology, researchers have developed innovative solutions to facilitate and improve the life quality of these patients. Among these, a well known emerging technology and research field is the Brain Computer Interface (BCI), in which people are able to communicate with their environment and control prosthetic or other external devices by using only their brain activity. In a BCI system, the brain activity is translated into simple commands using brain activity measurement systems, signal processing methods and classification techniques with the help of neurophysiologic experimental

paradigms. There are also other human computer interaction systems that rely on the movement of healthy limbs (eye-gaze etc.) as the controller of basic actions and these systems are still more efficient than currently existing BCI systems. However, for patients suffering from degenerative diseases like ALS, BCI is considered as the only way of communication with the outside world.

Over the last two decades, there have been numerous studies performed on BCI. Researchers proposed various methodologies, extended the application fields of BCI and investigated the physiological nature of the experimental paradigms [1]. However, the main challenge in BCI is to improve the usability and practicality of these systems. Thus, researchers put most of their effort on developing new algorithms to improve the speed and accuracy of the prediction mechanisms in BCI applications. Due to the nature of existing BCI's, the applications are considered as pattern recognition problems and variety of signal processing, feature extraction and pattern classification techniques are being experimented in these systems [2]. Moreover, despite the technological developments, current BCI systems are only usable in the laboratory environment. Current studies aim to improve these systems by building intelligent house systems in order for BCI to be available for daily use according to the needs of the patients [11 – 15].

1.1 Scope of the Thesis

This thesis is restricted to one of the applications of BCI which is known as the Spelling Paradigm (also known as the P300 Speller). First introduced by Farwell and Donchin in 1988 [3], Spelling Paradigm enables paralyzed people to express their thoughts and feelings by spelling the words on a computer screen (see chapter 3 for a detailed description of the paradigm and previous studies). In this application, it is aimed to predict the characters that the subject thinks of by presenting some visual stimuli to the subject. In order to accomplish this task, the brain activity is acquired by using biopotential measurement devices (usually via Electroencephalography - EEG) and further analyzed with advanced signal

processing and classification methods. Like in all other BCI applications, the main challenge here is to improve the accuracy and the speed of the prediction mechanisms so that the subject can express his thoughts in a fluent manner.

In this thesis, it is intended to develop a P300 based BCI by realizing the spelling application which can also be used in out-of-laboratory environments. The thesis includes the design of a portable 10 channel EEG data acquisition system, the development of signal processing methods and application of machine learning techniques on this paradigm.

1.2 Focus and Contributions of the Thesis

The thesis focuses on some key points that are believed to be open for progress in this application. These are stated as follows:

- *Investigation of the human perception to row and column intensifications:*
  Existing P300 Speller systems employ row and column intensification principle for increasing the speed of the application (see Chapter 3). In the studies performed for this application, the responses for both row and column stimuli are treated in the same preprocessing and classification scheme [4-10]. However, no study has been performed on the application of signal processing and classification methods separately on these two intensification types. In this thesis, it is aimed to investigate the difference in human perception to row and column intensifications in P300 Speller according to the differences in classification accuracy.

- *Investigation of optimal frequency bands for the P300 Speller:*
  The EEG signals acquired for this application are usually filtered with a preprocessing stage. The signal processing methods applied for this study are mainly simple filtering techniques. In this thesis study, the optimal temporal

frequency bands for user specific P300 responses will be investigated by the application of Wiener filtering in this problem.

- *Estimation of probability densities in binary classification between trials:*
  The determination of the focused character in Spelling Paradigm is performed by using repetitive trials and ensemble averaging in order to reduce the errors in prediction. Unlike the common approach of assigning classification score between trials [4], the class conditional probability density of the predicted characters is estimated by using the Maximum Likelihood Estimation and the target character is predicted with Bayesian decision techniques.

- *Experimenting Active Electrodes in EEG measurements:*
  Existing BCI systems use commercial EEG devices in which the electrodes are usually made up of ring shaped silver chloride (AgCl) leads. These electrodes are passive conductive elements and the quality of their material highly affects the performance of the measuring system. Moreover, employing these in EEG measurements requires a preparation stage in which the electrodes are covered with a conductive paste. This paste usually dries out in a 2-3 hours of time which makes the passive electrodes unsuitable for continuous EEG recording in BCI applications. In this thesis work, a design of active electrodes for EEG measurements is performed to improve the quality of the recorded EEG signals, eliminate the preparation stage required in their passive counterparts and therefore realize a continuous EEG measurement in BCI applications.

- *EEG cap design:*
  Commercial EEG systems also provide electrode caps to attach the conductive leads to the scalp of the subject. These EEG caps are usually made of elastic silk material which can be easily stretched and fit to the subject's head. However, it is hard to attach the designed active electrodes on these caps. In addition, some modifications are possible that can theoretically improve the

quality of the measurements in the system. Therefore, in this thesis, a shielded EEG cap design is performed which allows easy placement of the active electrodes on the scalp while reducing the electrical noise in the measurements.

1.3 Outline of the Thesis

The thesis is composed of two introductory parts discussing the current BCI systems and spelling application and three main chapters including the methodologies performed for P300 Speller in this study.

The Brain-Computer Interface systems are introduced in chapter 2. The brain activity measurement techniques, neurophysiologic phenomenon underlying the principle of these systems and some BCI applications are briefly explained in this chapter.

In chapter 3, the application of P300 Speller is presented. The experimental setup and the review of the methodologies in the literature are provided discussing the complexity of the approaches and success of these in literature.

The approach of Wiener filtering is discussed in chapter 4. The derivations in Wiener filtering model and the application procedures related to P300 Speller are explained.

In chapter 5, the classification methods used in this study are explained. The basics of the algorithms are discussed providing correlations to the P300 Speller.

Chapter 6 is reserved for the description of the Electroencephalographic data acquisition system designed in this study. In this chapter, the parts of the designed system are explained briefly.

Chapter 7 provides the results of the proposed methodologies on one of the Spelling Paradigm datasets in the literature and on two P300 Speller experimentations performed in this study.

Finally in chapter 8, all of the work performed during this study is summarized. General observations are outlined with a discussion part. The advantages of the methods suggested in the thesis are stated and concluding remarks are given on the experimental results. The future studies are presented by discussing the possible modifications and improvements to implement a compact BCI system.

CHAPTER 2

BRAIN COMPUTER INTERFACES

In chapter 1, a brief introduction is given on Brain-Computer Interface (BCI) technology. A formal definition of a BCI is given in [44] as a system that does not depend on normal neural or muscular peripheral pathways of the brain. This definition discriminates BCI from other Human-Machine Interaction (also called Human-Machine Interface – HMI, Human-Computer Interface - HCI) systems which rely on the movement of some healthy limbs of the body as discussed previously. A BCI system interprets the brain activity as simple commands and transforms these into prescribed actions within its applications (for the control of a wheelchair as an example). Furthermore, the BCI technology is not restricted only to the activity of the brain. The research topics also include the neural prosthesis in which the damaged neurons can be replaced with artificial ones or unhealthy limbs are assisted by prosthetic devices [45].

In this chapter, it is aimed to provide the necessary information related to the underlying principles of BCI, approaches in detecting the brain activity and the applications of BCI in real life. The chapter is concluded with a comparison of existing BCI systems providing the efficiency and usability of these in real world applications. The reader can find detailed information about existing BCI systems in [1] and [46].

2.1 Framework of a BCI system

The functional model usually employed in many BCI systems is demonstrated in Figure 2-1.

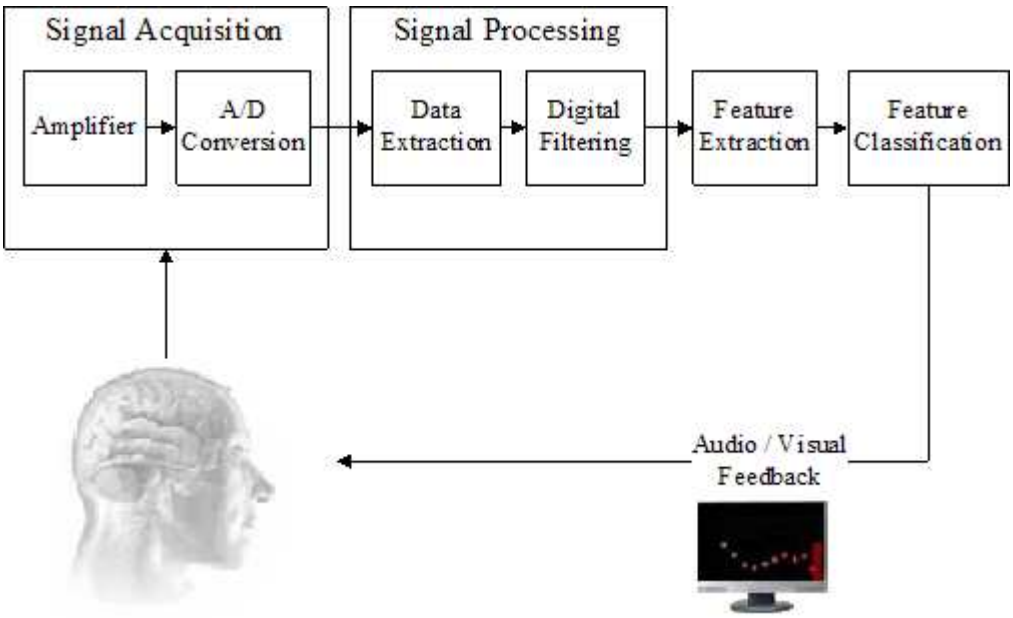

Figure 2-1 : Functional Model of a BCI System. The signals are obtained by a signal acquisition system, processed by signal enhancement methods and classified in a specific BCI application.

First stage of this framework is the signal acquisition phase in which the brain activity is extracted by a biosignal measurement device. Electroencephalography (EEG), Magnetoencephalography (MEG), Functional Magnetic Resonance Imaging (fMRI) and Near Infrared Spectroscopy (NIRS) are some biosignal measurement systems which are briefly discussed in the scope of BCI in section 2.2. At this stage, the brain signals are usually enhanced with an amplification system and digitized to be further processed on a computer.

The data extracted within the acquisition block is the raw data and might contain redundant information for the BCI application. For this purpose, the signals are

digitally filtered in the preprocessing stage. In this block, the unnecessary information is eliminated by data selection (e.g. channel selection in EEG) and several other operations (noise reduction, downsampling etc.) are performed to improve the signal quality.

The feature extraction is the stage in which the most relevant information for classifying the EEG patterns is investigated. Depending on the complexity of the BCI application, the feature extraction is performed either manually or with the application of optimization algorithms (see section 5.2.3). The aim of this stage is to improve the classification performance of the BCI system and it is usually performed together with the classification stage. Therefore, it can also be considered as a preprocessing or classification method. However, it is usual to express this stage in a separate block indicating the connection with the preprocessing and classification phases.

The features extracted from the feature extraction block are classified in the classification stage in order to decide which action should be taken. This block is the main part of the system in which pattern recognition algorithms are used to learn and model the input-output relationship of the BCI application. The performance of a BCI system usually depends on the accuracy of the employed classifiers.

Some BCI applications require feedback mechanisms in which some visual or auditory signals are presented to the subject indicating the decision taken by the classifier. The subject may need to manipulate his/her actions in performing the mental tasks according to the given feedback in order to present accurate signals for that application. Therefore, a feedback block may be realized with a graphical user interface on the computer screen in a BCI application.

There are also other blocks like the external device in which the control of a wheelchair or a prosthetic arm can be realized. These are secondary mechanisms

which may be integrated in the feedback stage. The presented building blocks in Figure 2-1 are considered as the main identifiers of a BCI system and used by many BCI researchers [14], [46], [47].

2.2 Measuring the Brain Activity

Depending on the purpose, there are several methods to measure the brain activity. These are mainly electrical, magnetic or hemodynamic activity measurements which are discussed briefly in the following subsections. A review of these methods in BCI can be found in [63].

2.2.1 Electromagnetic Activity of the Brain

2.2.1.1 Electroencephalography

Electroencephalography (EEG) is one of the methods to measure the electrical activity of the brain. The name was given after a German scientist named Hans Berger who announced the first EEG recording in 1924 [74]. It is used widely in clinical applications and preferred by many BCI communities as the EEG instrumentation is relatively cheaper and portable. Furthermore, the application procedure of EEG takes comparably less amount of time which makes it easy to operate for BCI applications in any environment.

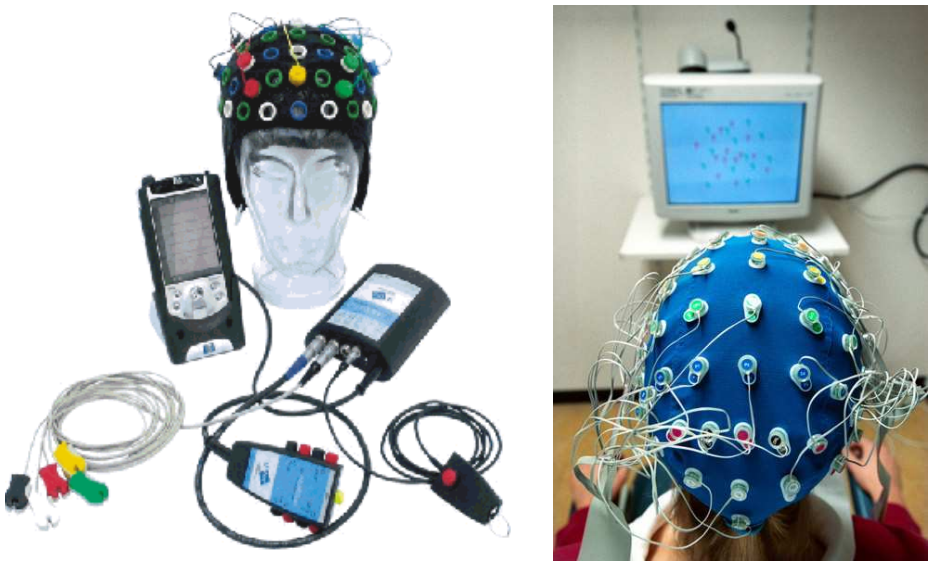

(a) (b)

Figure 2-2 : Instrumentation used in EEG systems. The measurement system consists of a number of electrodes, a biopotential amplifier and recording/monitoring devices [49], [48].

The electrical activity of the brain is measured with silver or silver chloride electrodes (Ag/AgCl) which are located on the scalp of the subject according to the standard 10-20 system [43], [41] (see Figure 6-4). An elastic cap (electrode cap) is used to attach the electrodes on the scalp (Figure 2-2).

The maximum amplitude of the measured electrical signals in EEG is on the order of several hundred microvolts (see also chapter 6). As the signals are have very low amplitudes, they are highly affected by disturbances (changes in contact impedance, power line noise, ocular and muscular artifacts etc.). To overcome this problem, several operations are applied either mechanically (using a conductive paste), electronically (analog filtering) or mathematically (digital signal processing). To improve the contact impedance between the skin and the electrodes, the electrodes are usually covered with conductive gel. This requires a preparation time depending on the number of electrodes employed. Furthermore, one can also employ the active electrodes instead of passive Ag/AgCl leads which will eliminate the need for preparation before the operation.

2.2.1.2 Electrocorticogram and Cortical Microelectrodes

Electrocorticogram (ECoG) is an invasive method in which the electrical signals of the brain are measured under the skull, from the surface of the cortex (Figure 2-3).

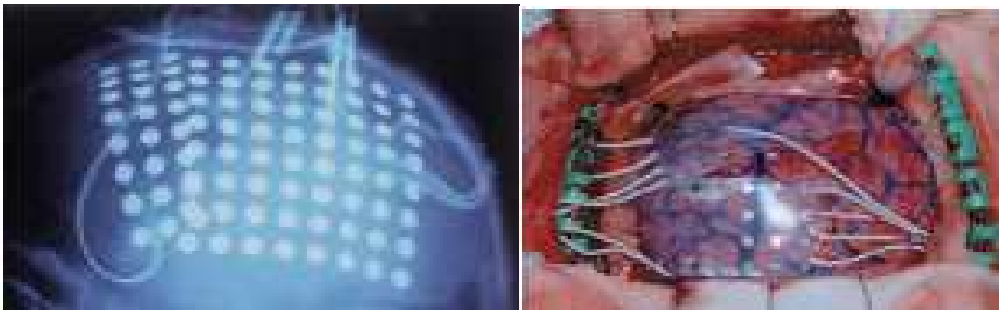

(a) (b)

Figure 2-3 : (a) Electrodes used in an ECoG system. (b) The electrodes are placed on the cortex surface with a surgical operation [53].

The electrodes are usually made up of a conductive biocompatible needle or a grid of needles and are implemented on the cortex surface with a surgical operation. The electrical measurements are performed with the same amplification procedure as in EEG. However, the skull is a low conductive material and in ECoG, it is penetrated by the implementation of the electrodes [27]. Therefore, the signals are less affected by conductivity of the skull as compared to EEG and the measured signals are on the order of millivolts [42]. As it provides higher ranges of amplitude, the signals recorded by ECoG contain less ocular or muscular artifacts which makes it a suitable alternative to EEG in BCI applications [50], [51], [52].

Cortical microelectrodes are similar to ECoG in which the electrical activity of the brain is measured inside the cortex (Figure 2-4).

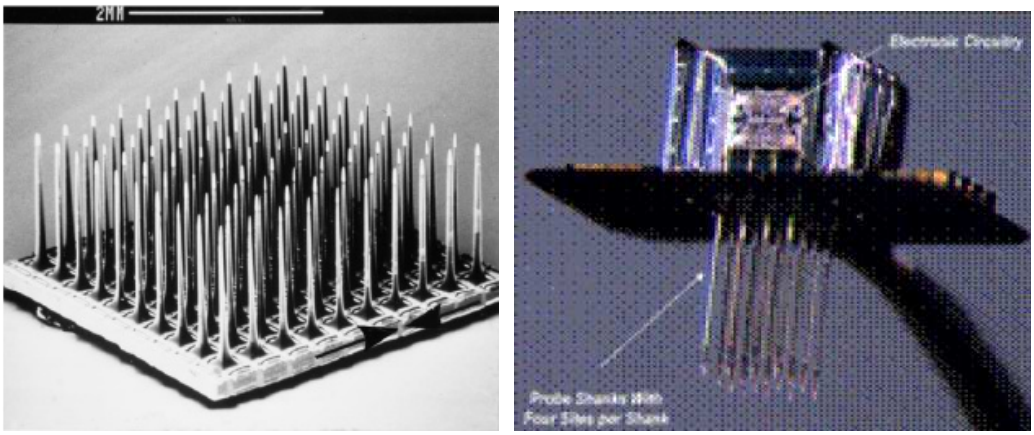

(a) (b)

Figure 2-4 : Microarray electrode for cortical electrical measurements. The electrodes are developed with VLSI technology and can be assisted with additive electronic components [53].

The electrodes used to measure the electrical signals are developed with the VLSI technology and the signal quality is improved by integrating analog circuits in their design. As the electrical signals are recorded inside the cortex, it is possible to detect the activity of a single neuron with high spatial resolution and excellent signal-to-noise ratio (SNR) [27].

Despite the advantages of ECoG and cortical microelectrodes, there are also several handicaps of these systems such as they need a surgical operation before use. The possibility of infection and incompatibility between the brain cells and the electrodes are the major risks in these systems. Therefore, these methods are only applicable on unhealthy subjects when necessary or on animal subjects. The reader can find detailed information on these systems in [54].

2.2.1.3 Magnetoencephalography

Magnetoencephalography (MEG) is a method to noninvasively measure the magnetic field strength generated by the flow of electrical currents through the pyramidal neurons in the cortex. The signals are measured with superconducting quantum interference devices (SQUID) which are extremely sensitive to the changes in the magnetic field [55]. The use of MEG in BCI is limited in a few studies [56], [57]. It is reported that this method can also be used in BCI applications when considered in communication speed [27]. However, as the instrumentation in MEG systems are relatively larger in size, unportable and more expensive as compared to EEG, it is usually not preferred for real world applications of BCI.

Figure 2-5 : The picture of a Magnetoencephalographm. Due to the size of the instrumentation, MEG systems are impractical in BCI applications for daily use [58].

2.2.2 Hemodynamic Activity of the Brain

2.2.2.1 Functional Magnetic Resonance Imaging

Functional Magnetic Resonance Imaging (fMRI) is a method used to measure the amount of oxygen in the blood flowing through the brain. When the neurons are active, the consumption of oxygen increases in these cells. Therefore, this gives an idea about the neural activity in different regions of the brain. The spatial resolution in this technique is comparably higher than that of others. In fact, the neural activity can be detected not only from the cortex but also any other regions of the brain. On the other hand, the fMRI systems have a poor temporal resolution; the response of hemodynamic activity is extracted within a few seconds [27]. In addition, the equipments in these systems are larger in size and much more expensive. Therefore, it is nearly impossible to employ fMRI in BCI applications for daily use. Nevertheless, researchers investigated fMRI to observe the hemodynamic activity in BCI applications [59], [60], [61].

2.2.2.2 Near Infrared Spectroscopy

Similar to fMRI, Near Infrared Spectroscopy (NIRS) is used to measure the hemodynamic activity of the brain. The principle of this technique is to detect the amount of blood oxygen in the brain from the reflection of the emitted infrared light. As the hemodynamic activity is measured, the temporal resolution is poor in NIRS systems, which makes the method impractical for BCI applications. However, few BCI studies were performed with NIRS which basically investigate the suitability of this brain activity measuring method in BCI applications [27], [62].

2.3 Neurophysiologic Background of BCI

There are various implementations of BCI, relying on different physiological activities related to human brain. Basically, there are three main approaches employed in existing BCI systems. The first approach is based on the responses of the subject to some external stimuli which are known as Event Related Potentials. In the second approach, the subject regulates the brain activity by concentrating on specific mental tasks. Slow Cortical Potentials (SCP) is the final method which is based on the slow potential shifts in the brain observed according to the mental state of the subject. Here, only the first two approaches will be briefly described as the method of SCP is not of interest in current BCI studies.

2.3.1 Event Related Potentials

Event Related Potentials are specific patterns occurring after or during the presentation of an auditory or visual stimulus. These include the P300 patterns and Steady State Visual Evoked Potentials (SSVEP).

2.3.1.1 P300 Signals

P300 is a peaking signal pattern which occurs after the presentation of a rare audio/visual event [3], [16] (Figure 2-6). It is observed nearly 300ms after the stimulus onset which gives the name to the signal pattern. Such a phenomenon occurs when the subject is asked to focus attention on a specific stimulus (also named as the target or odd-ball) which is rarely encountered among a large number of other irrelevant stimuli (non-target). Furthermore, the evoked P300 response is more distinctive when the occurrence of the event is random. The idea is first investigated in BCI in [3] with a spelling application which is explained in chapter 3 in detail.

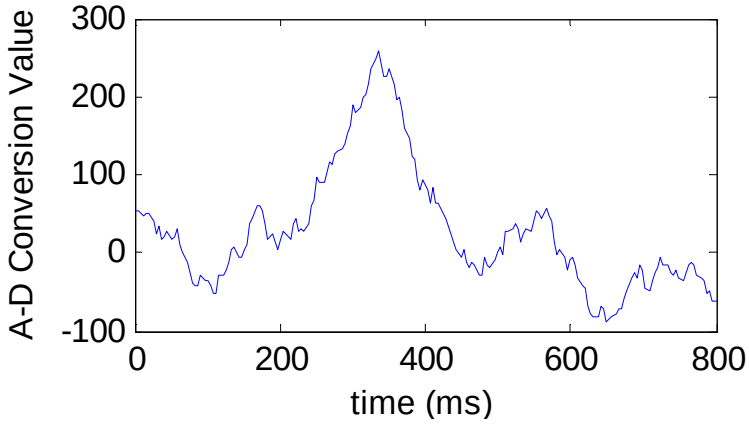

Figure 2-6 : A typical P300 signal. A rising pattern occurs nearly 300ms after the presentation of the target stimulus. The data used to represent the pattern is obtained from [18].

2.3.1.2 Steady State Visual Evoked Potentials

Steady State Visual Evoked Potentials (SSVEP) are oscillating signal patterns elicited in the brain according to the frequency of the presented periodic visual stimulation. These signals are more distinctive in occipital regions of the brain which is believed to be related to visual activities. SSVEP is employed in BCI applications by the presentation of several flickering light sources with different frequencies [64], [65], [66]. In such a paradigm, the focused light elicits a signal pattern of the same frequency or harmonics with that of the source (Figure 2-7). Therefore, an SSVEP based BCI system can be realized by the detection of the focused light sources from these signal patterns. As an example, a wheelchair can be controlled by using only four light sources to perform a movement on the main directions.

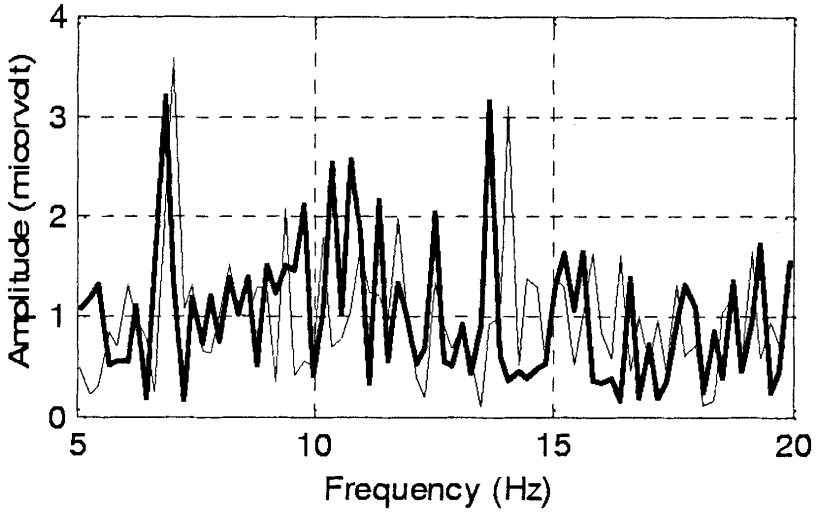

Figure 2-7 : Amplitude spectra of SSVEPs induced by two flickering light sources; 6.83Hz (thick) and 7.03-Hz (thin) [64].

2.3.2 Event Related Oscillatory Activity of the Brain

In general, the brain signals are represented with oscillating patterns categorized in specific frequency bands which are shown in Table 2-1. The amplitude of the signals (or the energy) changes over time according to the mental activities performed by the subject. For example, the amplitude of the μ-rhythm decreases when the subject is concentrated on a specific task (imagination of movement [67], [68], calculation, imagination of a rotating an object [69]) and the oscillating activity in the α band increases when the subject is in relaxed state. Furthermore, the energy change in these frequency bands may not be the same in every region of the brain. For example, the imagination of the right hand movement reduces the amplitude of the μ-rhythm over the sensorimotor cortex of the left hemisphere (Figure 2-8). In BCI applications, synchronization and desynchronization of these rhythms (Event Related Synchronization/ Desynchronization – ERS/ERD) are used to determine the mental state of the subject by analyzing the energy changes over the sensorimotor cortex [67], [70]. However, these systems require a long training period for the subject to obtain a

successful performance. The subject is required to learn to regulate his brain activity with feedback mechanisms in these training sessions.

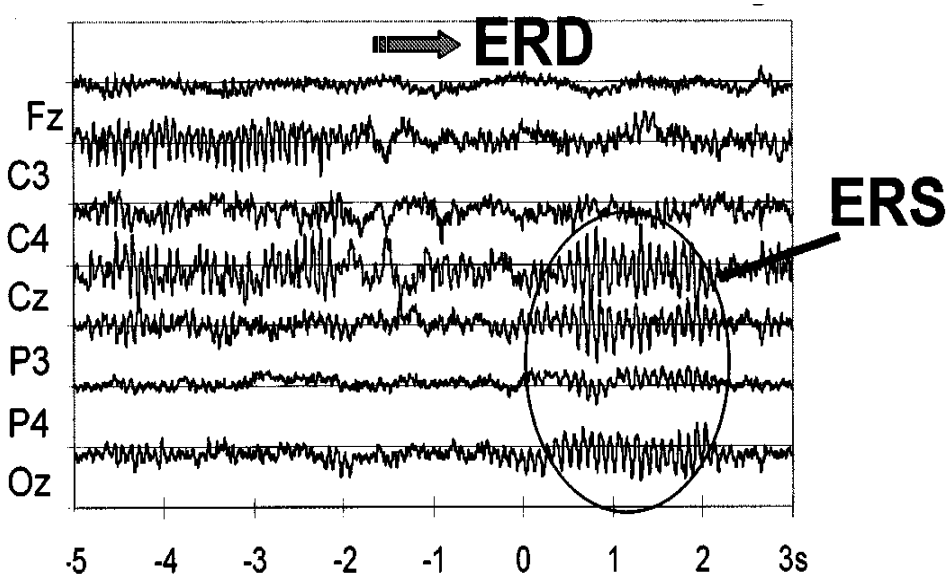

Figure 2-8 : ERD/ERS activity during the right hand movement in ongoing EEG. After the cue, the activity of alpha band increases over the right posterior region more than the left hemisphere [67].

Table 2-1: Oscillatory EEG wave patterns and their frequency ranges [74].

Wave	**Frequency Range**	**Characteristics**
delta - δ	0 – 4 Hz	• slow wave sleep for adults • seen in babies
theta - θ	4 – 7 Hz	• seen in young children • drowsiness or arousal in older children and adults • idling, meditation
alpha - α	8 – 12 Hz	• relaxed/reflecting • occurs usually when closing the eyes
beta - β	12 – 30 Hz	• alert state, working • active, busy or anxious thinking, active concentration
gamma - γ	30 – 100 Hz	• alert state, working • seen when a certain cognitive or motor functions is employed
mu - μ	~10Hz	• alpha range activity indicating the imagination of movement when it is attenuated.

2.4 Applications and Potential Users of BCI

Depending on the purpose, a BCI system can find many different application fields (bioengineering, military, gaming industry etc.). As its primary objective, a BCI can be used to assist a disabled person by providing a control on an external device so that he/she can realize specific actions like movement via wheelchair, control of a prosthetic arm and house control systems or communication with other people. Potential users of BCI can vary from healthy subjects to severely disabled ones like ALS patients.

Table 2-2: Potential Users of BCI in the world [42].

Type of the Disease	Number of Patients
Amyotrophic Lateral Sclerosis (ALS)	400,000/3,000,000
Multiple Sclerosis	2,000,000
Muscular Dystrophy	1,000,000
Brainstem Stroke	10,000,000
Cerebral Palsy	16,000,000
Spinal Cord Injury	5,000,000
Postpolio Syndrome	7,000,000
Guillain-Barre Syndrome	70,000
Other types of Stroke	60,000,000

A BCI system can also be used in rehabilitation of these patients by encouraging and motivating them to life with virtual reality and gaming applications [72], [73]. Although these applications do not provide primary needs of the subjects, they improve the life quality of these patients in psychological point of view.

(a) (b)

Figure 2-9 : Control of external devices by BCI. (a) the wheelchair application [75], (b) prosthetic robot arm [76].

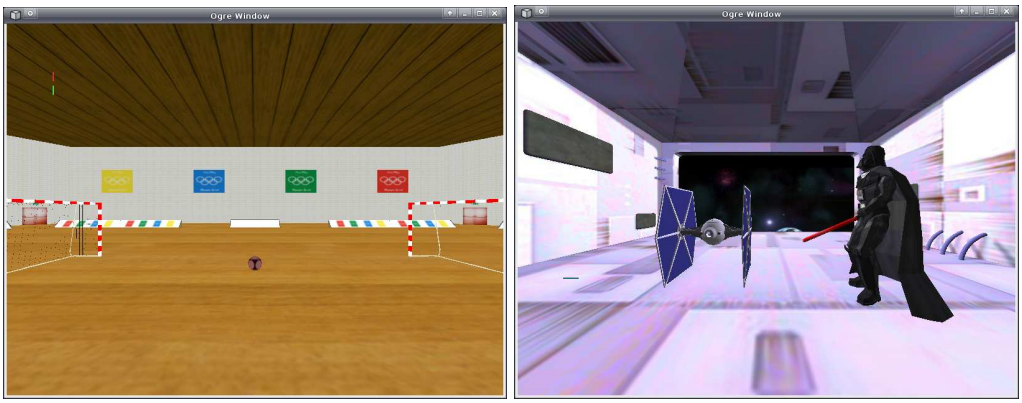

(a) (b)

Figure 2-10: Virtual gaming examples: (a) Hand ball, (b) Use the Force [73]. Patients can be rehabilitated psychologically by games and therefore they can be more motivated to life.

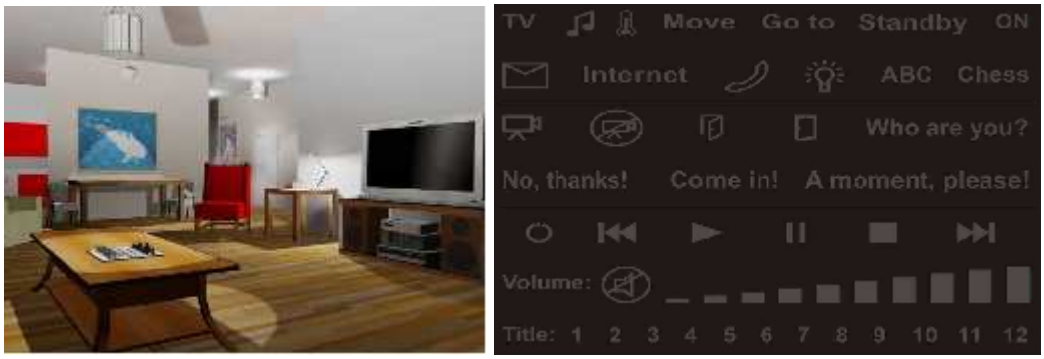

Figure 2-11: Home control applications with Virtual Reality [42].

2.5 Conclusion

As existing BCI systems are compared to each other, all approaches explained in section 2.3 have similar performances in prediction accuracy and speed in most of the subjects. Each approach has a different advantage regarding the implementation of the applications or time required to operate the BCI. For example, it is difficult and impractical to control a wheelchair with a P300 based BCI; an ERD/ERS or SSVEP based BCI can provide a faster control on a wheelchair or prosthetic hand application. However, P300 based BCI's do not require subject training as in the case of motor imagery BCI systems. The training time required in motor imagery BCI's can be as long as 6 months to successfully operate the system [42].

The major drawback of P300 and SSVEP based BCI's is that a visual stimulation is needed to operate these systems. When considered in that point of view, ERD/ERS based BCI systems have the advantage of operation without external stimulation. On the other hand, it is usually harder to detect the ERD/ERS activity than P300 responses. Furthermore, P300 based systems provide higher degrees of freedom in the applications. That is, with SSVEP or motor imagery BCI, it is impractical to implement an application that includes 36 or more different possibilities (the spelling application or smart home control). Regarding all these points, one can decide on the type of the BCI in order to implement a specific paradigm. Therefore, the main consideration here is to determine the feasibility of the approaches on the BCI application that is to be implemented.

CHAPTER 3

SPELLING PARADIGM

Although chapter 1 provided an introductory description of the P300 Speller, here, it is aimed to explain this BCI application within a separate chapter. The chapter starts with a detailed explanation of the experimental setup and then continues with a brief review of the previous studies performed on this title. Finally, a concluding section is provided at the end of the chapter discussing the accuracy and complexity of reviewed methodologies.

3.1 Experimental Setup

In the experimental paradigm proposed by Farwell and Donchin [3], a 6 by 6 matrix of alphanumeric characters is presented to the subject on a computer screen (see Figure 3-1 for a spelling matrix example). The rows and columns of this matrix are sequentially intensified in a random order with a predefined duration and interstimulus interval (the duration between two consecutive intensifications). The subject is asked to focus attention on a specific character and is assumed to count the number of intensifications whenever the row or column containing the focused character is flashed. The focused characters here will be named as the *target characters* and consequently, the row and column intensifications containing the target character will be referred as the *target intensifications* throughout the thesis.

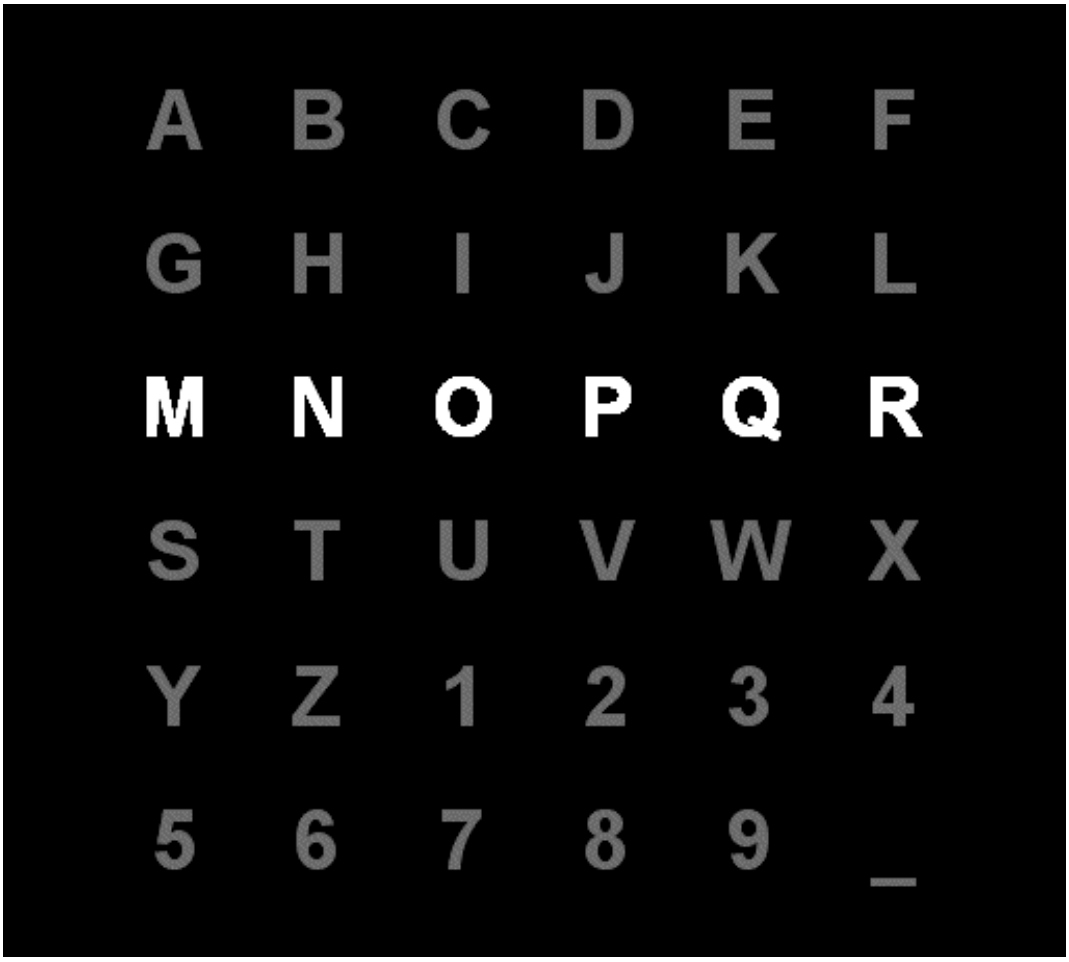

Figure 3-1: P300 Speller Matrix used in the datasets in [18] and [20].

The row and column intensifications in fact constitute the visual stimulations in this paradigm. Moreover, there are few target stimulations as compared to the non-target ones. For example, for a 6 by 6 matrix of characters, there is only one target row intensification and one column intensification since the target character is in the intersection of these two stimuli. The other five rows and five columns constitute the non-target intensifications and the responses of the subject to these stimulations are supposed to be different than that of the target ones. The underlying principle of the spelling application is that the subject produces specific responses to the target intensifications as they occur less than the non-target ones. The target stimulations are expected to evoke the so called P300 potential which is described in section 2.3.1.1.

The very aim of this application is to predict the target character such that the subject expresses his/her thoughts fluently by spelling the words on the screen. In order to accomplish this task, the algorithms try to determine the stimulations that evoked the P300 responses (i.e. the target responses) and therefore predict the character that the subject focused. However, usually it is difficult to make this prediction in one trial which corresponds to the duration that all the rows and columns of the matrix are intensified only once. The reason is that the measured EEG signals are highly affected by noise and this makes it impossible to distinguish the target responses from the non-target ones within a single trial. Therefore, several trials are performed for the same target character in order to decrease the error in prediction.

Employment of trial repetition comes with the main disadvantage of duration of prediction. That is, the more trial repetition, the longer it takes to predict the target character which makes it unsuitable for the subject to fluently express his or her thoughts. As an example, for the dataset of [18] experimented in this study, the trial duration corresponds to 4.5 seconds. Using at least 5 trial repetitions for guessing the character takes 22.5 seconds which takes a few minutes to complete a 5-10 letter word[1]. Therefore, the challenge in this application is also to decrease the time for prediction of the target characters (use less number of trial repetitions to predict) and thus improve the usability of the system.

[1] The spelling of a character in the paradigm actually depends on many factors which are explained in the results chapter. One can decrease the timing parameters which can affect the speed of the prediction mechanism. However, the consideration stated here is to minimize the number of trial repetitions which is the main factor assessing the speed of the system.

3.2 Preceding the Analysis

The common procedure before designing a classification model for the P300 Speller is to follow a few steps to extract the relevant information from the provided training dataset. This involves the selection of a set of EEG channels that are likely to exhibit the presence of a P300 response, extraction of EEG time segments of predefined length after the stimulus onset from these channels and the combination of stimulus code and the class label information with the extracted EEG segments. After that, one usually applies low-pass or band-pass filtering for better signal to noise ratio (SNR) and may employ downsampling operation to reduce the dimensionalty of the signal.

3.3 Review of the Methodologies

As mentioned before, in BCI studies, the researchers focused mainly on the application of different classification and signal enhancement methods in existing BCI problems. Here, the methodologies will be briefly reviewed for P300 Speller in terms of classification and signal processing aspects. Detailed review for the classification problem in BCI applications can be found in [9] and [2].

3.3.1 Review of Studies in Machine Learning

Earlier studies in P300 Speller approached the pattern classification problem in unsupervised aspects like the application of peak picking algorithms and decision principle according to area of the EEG segment in the time domain [3], [8]. In their pioneering work, Farwell and Donchin investigated four different classification methodologies for categorizing the target and non-target responses [3]. They have compared Stepwise Discriminant Analysis (SWDA), peak detection, classification according to the area of the responses and covariance methods for the P300 Speller. However, with the advances in technology and increase in computation power, the application of supervised classification

techniques became more popular in which the algorithms are developed on a training dataset.

Kaper *et al*. investigated the application of Support Vector Machines (SVM's) with Gaussian kernel transformation on the paradigm and obtained successful results while using only a few number of EEG channels [4]. They have been elected as one of the winners in BCI Competition II [17], [18] due to the success and the simplicity of the method they have proposed. SVM has also been applied in numerous studies for the classification of P300 responses [6], [21], [22] and in other BCI applications [23], [24], [25]. In their work, Rakotomamonjy *et al.* trained several SVM's on different partitions of the training dataset while recursively selecting the optimal subset of EEG channels as features [6]. They won the BCI Competition III [19], [20] with the highest prediction accuracy on the test set in P300 Speller.

Linear Discriminant Analysis (LDA) or more specifically Fisher's LDA has been investigated for P300 speller by Bostanov [7] in which the aim is to separate the data by constructing a hyperplane between the classes. The classification method has shown a relatively well performance for the P300 speller dataset in BCI Competition II and elected as one of the winning methods in this contest.

In order to predict the target character in Spelling Paradigm, additional decision methodology is needed after the application of the discriminative classifiers. This procedure can be simply the scoring of the classifier output [4] or a more probabilistic approach in which the classification is performed regarding the distribution of the discriminative classifier outcome. Guan *et al.* conducted research on the statistical modeling of P300 responses by analyzing the stimulus output distribution of the main classifier [26]. They proposed probabilistic methods for the multi-trial EEG signals and employed assumed distributions for the discriminative classifier output (mainly Gaussian) in prediction of the target character. Hoffman [27] studied the Bayesian algorithms in his doctoral thesis

work providing a well understanding of the applied procedure. He applied the evidence framework for Bayesian regression in P300 speller [29] and proposed a combined discriminative method named as Bayesian Discriminant Analysis (BDA) for this problem [28]. Moreover, Lin and Zhang investigated the classification problem in P300 Speller regarding the perceptual characteristics of the paradigm [21]. They approached the problem in three category classification task considering also the intensifications adjacent to target stimuli. In their study, the accuracy of the prediction was reported to be improved when the probabilistic model included the confusion of the subject due to these nearby target intensifications.

3.3.2 Studies on Signal Enhancement and Feature Extraction

The preprocessing algorithms for improving the EEG signal quality play an important role in accurate prediction of the target character in Spelling Paradigm as well as the classification methods applied this context. Especially, the feature extraction methods reduce the complexity of the problem by optimizing the computational effort needed for the classifiers. These methods can be as simple as usual low-pass or band-pass filtering or more complicated procedures which require a solution of an optimization problem.

The method of Principle Component Analysis (PCA) has been applied in [5], [30] to reduce the dimensionality of the data extracted from the selected EEG channels. The idea in PCA is to determine the maximum eigenvalues which elicit the principle components of the signal. In other words, PCA removes the relatively irrelevant parts of the data while retaining the most powerful components of the signal. This provides the dimensionality reduction of the feature vector which usually improves the performance of the employed classifier.

Another signal processing technique called the Independent Component Analysis (ICA) has been investigated in numerous studies in BCI [8], [9], [31]. Being one

of the blind source separation algorithms, ICA has been widely employed for removing the desired signal from the background noise. For the case of Spelling Paradigm, the signals other than P300 responses are considered as the background noise. ICA was successfully verified by Xu *et al.* [8] in BCI Competition II and was elected as one of the winning algorithms in the P300 Speller problem.

The t-statistics has been investigated for feature extraction purposes in the studies performed by Bostanov [7] and Hu *et al.* [30]. In his work, Bostanov applied t-Value Scalogram together with Continuous Wavelet Transform (t-CWT) to automatically select the features according to student's t-test. In [30] the features are detected according to t-weight method in the training phase after the application of PCA. Both methods have shown successful performance in the P300 speller dataset of BCI Competition III.

3.4 Conclusion

There are numerous other studies related to the application of similar feature extraction and classification techniques in BCI applications described here. One can find a detailed comparison of these in [2] and [9]. As the performance of the system highly depends on the employed classification algorithms, it is reasonable to consider the most successful approach in the problem. In order to complete the objective of the thesis, it is also important that the considered methodology is easy to implement. Therefore, due to its success in BCI competition datasets, SVM is selected as a primary classification tool in this study [77]. Furthermore, the feature extraction techniques described in the review are not employed in this study as the performance of the P300 Speller is more than satisfactory when using only SVM for a fixed number of EEG channels [4]. Instead, the effect of Wiener filtering on the classifier performance is to be investigated in this thesis.

CHAPTER 4

WIENER FILTERING

As it constitutes the major subject in this thesis in terms of signal enhancement, the method of Wiener filtering and its application to the P300 Speller are explained in this chapter. The chapter begins with a description of the Wiener model, and continues with the derivations required to design the optimal Wiener filter. Finally, the Wiener approach on the spelling application is given at the end of the chapter, explaining the application procedure for this problem.

4.1 Introduction

In many practical applications, it is of interest to reconstruct a signal from noisy observations. However, it may be impossible to achieve this task with simple, classical filtering techniques. In such cases, it is necessary to take the statistics into account and apply more complex signal processing methods. Wiener filtering is a statistical signal processing technique, in which, it is aimed to construct a filter to estimate the desired signal from noisy observations [32]. It is a kind of optimal filtering in the sense that it minimizes the error in the estimation of the desired signal [33].

Depending on purpose, Wiener filter can be applied to numerous signal processing problems. For example, in the simple filtering case, the aim is to estimate the desired signal by designing a causal filter. There is also a noncausal

filter type which is usually used in image processing, in smoothing or unblurring the images distorted by noise. Prediction is another important application of Wiener filtering where the filter produces the future values of the observation using its past values [32].

4.2 Wiener Filter Model

In the framework of Wiener filtering, the following discrete time model will be assumed which is valid for many practical applications.

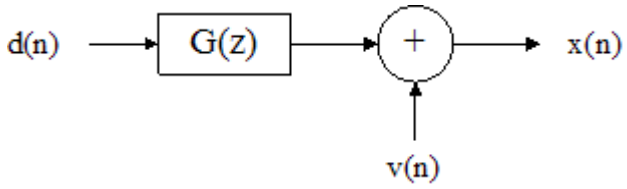

Figure 4-1: The Discrete Time Model of a Practical Application. G(z): The transfer function of the process in z-domain. d(n), x(n) and v(n) represent the desired signal, noisy observations and the additive noise respectively.

Here, $G(z)$ is the transfer function of a system (in z-domain) which can be realized as a recording device or a communication system. Since $G(z)$ is a known system function, it can be considered as a unity or an identity transfer function to simplify the formulations. Assuming $G(z) = 1$,

$$x(n) = d(n) + v(n) \tag{4.1}$$

where

$x(n)$: The observations in the system,

$d(n)$: The desired signal,

$v(n)$: The noise present in the observations.

The starting assumption is that the desired signal $d(n)$ and the observations $x(n)$ are jointly wide sense stationary processes (WSS) with known autocorrelations, $r_x(k)$, $r_d(k)$ and crosscorrelation $r_{dx}(k)$. The goal is to design a linear, shift-invariant filter $w(n)$ that would produce the minimum square error (mse) estimate of the desired signal from the observations, considering the statistics of each signal [32].

The squared error to be minimized is defined as:

$$\xi = E\{|e(n)|^2\} \tag{4.2}$$

where

$$e(n) = d(n) - \hat{d}(n). \tag{4.3}$$

Here, $\hat{d}(n)$ represents the estimated signal and $e(n)$ is the difference between the desired signal and the estimated signal, i.e. the error. The model is illustrated in Figure 4-2.

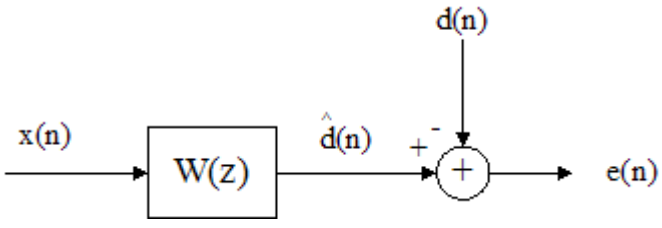

Figure 4-2: Wiener filter model, W(z): Wiener filter to be constructed. The observations are filtered with the estimated Wiener filter which minimizes the difference between the desired signal $d(n)$ and the filter output $\hat{d}(n)$.

Depending on the requirements in the filter design, Wiener filter takes different forms considering the finite-infinite impulse response (FIR or IIR) and causality in the filter: causal-FIR, noncausal-FIR, causal-IIR and noncausal-IIR Wiener filter. Here, the noncausal and IIR form of the Wiener filter will be investigated in the explanation framework of [32]. The formulations derived for the noncausal IIR Wiener filter are also valid for other types. Detailed explanation and derivations can be found in [32] and [33] for each type of design.

4.3 Noncausal IIR Wiener Filter Design

The noncausal IIR form of the Wiener filter can be represented in the z-domain as:

$$W(z) = \sum_{n=-\infty}^{n=\infty} w(n) z^{-n} \tag{4.4}$$

The estimate of the desired signal in Figure 4-2 is the convolution of $x(n)$ and $w(n)$,

$$\hat{d}(n) = w(n) * x(n) = \sum_{l=-\infty}^{\infty} w(l) x(n-l) \tag{4.5}$$

In order to find the filter coefficients optimally in the mean square sense (mse), the derivative of the squared error defined in (4.2) with respect to $w^*(n)$ or $w(n)$ should be equal to zero for all samples of the filter [32]. Thus,

$$\begin{aligned} \frac{\partial \xi}{\partial w^*(k)} &= \frac{\partial}{\partial w^*(k)} E\{e(n)e^*(n)\} \\ &= E\left\{ e(n) \frac{\partial e^*(n)}{\partial w^*(k)} \right\} = 0 \qquad -\infty < k < \infty \end{aligned} \tag{4.6}$$

Combining (4.3) with (4.5), $e(n)$ can be rewritten as

$$e(n) = d(n) - \sum_{l=-\infty}^{\infty} w(l)x(n-l) \tag{4.7}$$

Then the partial derivative expression in (4.6) reduces to

$$\frac{\partial e^*(n)}{\partial w^*(k)} = -x^*(n-k) \tag{4.8}$$

Substituting the derivative expression in (4.6) with the result found in (4.8),

$$E\{e(n)x^*(n-k)\} = 0 \qquad -\infty < k < \infty \tag{4.9}$$

Equation (4.9) is referred as the orthogonality principle or the projection theorem [32] which implies that all of the samples of the observation are orthogonal to the error in estimation of the desired signal. Thus, if $e(n)$ in (4.7) is substituted in (4.9), we obtain

$$E\{d(n)x^*(n-k)\} - \sum_{l=-\infty}^{\infty} w(l)E\{x(n-l)x^*(n-k)\} = 0 \tag{4.10}$$

Since it is assumed that $x(n)$ and $d(n)$ are jointly WSS processes, the expectation expressions in (4.10) are equal to the cross-correlation of $x(n)$ with $d(n)$ and autocorrelation of $x(n)$ respectively. Therefore, equation (4.10) can be rewritten as

$$r_{dx}(k) = \sum_{l=-\infty}^{\infty} w(l)r_x(k-l) \qquad -\infty < k < \infty \tag{4.11}$$

Equation (4.11) is known as the Wiener-Hopf equation for the noncausal IIR Wiener filter. It differs from the FIR case by the limits of the summation and the range for k for which the equation should hold [32]. Unlike the FIR Wiener filter, the solution for $w(k)$ can not be found directly from (4.11), since there are infinite number of equations with infinite number of unknowns in the IIR case. However, if the equation is turned into a convolution expression between $w(k)$ and $r_x(k)$, finding a solution for $w(k)$ will be much easier:

$$r_{dx}(k) = w(k) * r_x(k) \tag{4.12}$$

If the Fourier transform is applied to (4.12), the variables can be expressed in the frequency domain as

$$P_{dx}(jw) = P_x(jw)W(jw) \tag{4.13}$$

Thus, the frequency response of the noncausal IIR Wiener filter is

$$W(jw) = \frac{P_{dx}(jw)}{P_x(jw)} \tag{4.14}$$

where $P_{dx}(jw)$ is the cross-power spectral density of the desired and observation signals and $P_x(jw)$ is the power spectral density (psd) of the observation signal. According to equation (4.14), the optimum Wiener filter depends only on $P_x(jw)$ and $P_{dx}(jw)$. Thus, when these are calculated, the design of the Wiener filter will be complete.

Here, it can be assumed that $d(n)$ and $v(n)$ are statistically independent processes and also $v(n)$ is a zero mean random process. Usually, independence is a reasonable assumption in practical applications since the desired signal may not

necessarily be related to the noise. Therefore, from the independence assumption it can be inferred that they are also uncorrelated. Then, if we would like to express the autocorrelation of $x(n)$,

$$\begin{aligned} r_x(k) &= E\{x(n)x^*(n-k)\} \\ &= E\{(d(n)+v(n))(d^*(n-k)+v^*(n-k))\} \\ &= E\{d(n)d^*(n-k)\}+E\{v(n)v^*(n-k)\}+E\{d(n)v^*(n-k)\} \\ &\quad + E\{v(n)d^*(n-k)\} \\ &= r_d(k)+r_v(k)+r_{dv}(k)+r_{vd}(k) \end{aligned} \tag{4.15}$$

Since $d(n)$ and $v(n)$ are uncorrelated, their cross-correlation $r_{dv}(k)$ or $r_{vd}(k)$ reduces to zero. Therefore,

$$r_x(k) = r_d(k) + r_v(k) \tag{4.16}$$

and the power spectral density of $x(n)$ becomes

$$P_x(jw) = P_d(jw) + P_v(jw) \tag{4.17}$$

When we consider the cross-correlation between $x(n)$ and $d(n)$, it can be found that

$$\begin{aligned} r_{dx}(k) &= E\{d(n)x^*(n-k)\} \\ &= E\{d(n)d^*(n-k)\}+\underbrace{E\{d(n)v^*(n-k)\}}_{=0} \\ &= r_d(k) \end{aligned} \tag{4.18}$$

Thus,

$$P_{dx}(jw) = P_d(jw) \tag{4.19}$$

which is valid under the assumption that $v(n)$ is zero mean and $d(n)$ and $v(n)$ are uncorrelated WSS random processes. This assumption is important especially for the optimality of the Wiener filter. When one of the signals is found to be non-stationary, the use of linear, shift invariant Wiener filter will not be optimum [32]. Moreover, if the noise signal has non-zero mean, then a few more terms will be added to the cross-power spectral density, which will certainly affect the frequency characteristics of the Wiener filter when ignored. Then, the IIR Wiener filter takes the final form:

$$W(jw) = \frac{P_{dx}(jw)}{P_x(jw)} = \frac{P_d(jw)}{P_x(jw)} = \frac{P_d(jw)}{P_d(jw) + P_v(jw)} \tag{4.20}$$

To construct the Wiener filter in a specific application, one can choose any equality expression in (4.20), considering to the computational difficulty in evaluation of these parameters.

After finding the optimum Wiener filter, we can now evaluate the mean square error in the estimation of the desired signal.

$$\begin{aligned} \xi &= E\left\{|e(n)|^2\right\} = E\left\{e(n)\left[d(n) - \sum_{l=-\infty}^{\infty} w(l)x(n-l)\right]^*\right\} \\ &= E\left\{e(n)d^*(n)\right\} - \sum_{l=-\infty}^{\infty} w^*(l)\underbrace{E\left\{e(n)x^*(n-l)\right\}}_{=0} \end{aligned} \tag{4.21}$$

If $w(n)$ is the solution of Wiener-Hopf equations in (4.11) satisfying the minimum mean squared error, then due to the orthogonality principle defined in (4.9), the last expectation term in the summation drops to zero. Therefore,

$$
\begin{aligned}
\xi_{\min} &= E\{e(n)d^*(n)\} = E\{(d(n)-\hat{d}(n))d^*(n)\} \\
&= E\left\{\left[d(n)-\sum_{l=-\infty}^{\infty} w(l)x(n-l)\right]d^*(n)\right\} \\
&= \underbrace{E\{d(n)d^*(n)\}}_{=r_d(0)} - \sum_{l=-\infty}^{\infty} w(l)\underbrace{E\{x(n-l)d^*(n)\}}_{=r_{dx}^*(l)} \\
&= r_d(0) - \sum_{l=-\infty}^{\infty} w(l)\, r_{dx}^*(l)
\end{aligned}
\tag{4.22}
$$

Evaluation of the minimum mean squared error in (4.22) requires a lot of computation due to infinite samples in the summation. However, if Parseval's theorem is applied to the summation in (4.22) calculations will become much easier in the frequency domain.

$$
\xi_{\min} = r_d(0) - \frac{1}{2\pi}\int_{-\pi}^{\pi} W(jw)P_{dx}^*(jw)dw \tag{4.23}
$$

From the same reasoning, we can also express $r_d(0)$ as,

$$
r_d(0) = \frac{1}{2\pi}\int_{-\pi}^{\pi} P_d(jw)dw \tag{4.24}
$$

Therefore, the minimized mean square error becomes,

$$
\xi_{\min} = \frac{1}{2\pi}\int_{-\pi}^{\pi}\left(P_d(jw) - W(jw)P_{dx}^*(jw)\right)dw \tag{4.25}
$$

4.4 Application of Wiener Filtering in P300 Speller

As discussed in chapter 3, the identification of P300 patterns from EEG is the main goal in Spelling Paradigm. In this subchapter, the Wiener filtering approach for the signal enhancement problem will be investigated in this context. Here, we will treat the problem as in the following: we will construct a Wiener model for target signals, i.e. the class of P300 patterns, and another one for non-target signals. Then, we will combine these two systems and construct a single model that will enhance the target signals while suppressing the non-target ones.

To begin with, the model in Figure 4-1 is assumed for the signal acquisition phase of the P300 speller, where $x(n)$ represents the recorded EEG data. As defined before, $d(n)$ and $v(n)$ are the desired and the noise signals, respectively. However, the desired signal here will be either the target signal, or the non-target signal waveform depending on the system of concern. For the sake of simplicity and clarity, we will consider the target signal system first and then continue with the non-target one. The EEG data used for demonstrating the target and non-target signals is from the dataset IIb of BCI Competition 2003 [18].

As averaging-between-trials is a common approach in classification in this problem, it is natural to obtain the main target response or P300 response by averaging all signals belonging to the target class. By averaging all target signals in the dataset, we in fact, obtain the least square solution for P300 pattern measured from related EEG channels. This is a well known technique for reducing the noise present in the measurements.

Therefore, when the ensemble averaging is performed between the observations, we obtain the target responses as given in Figure 4-3.

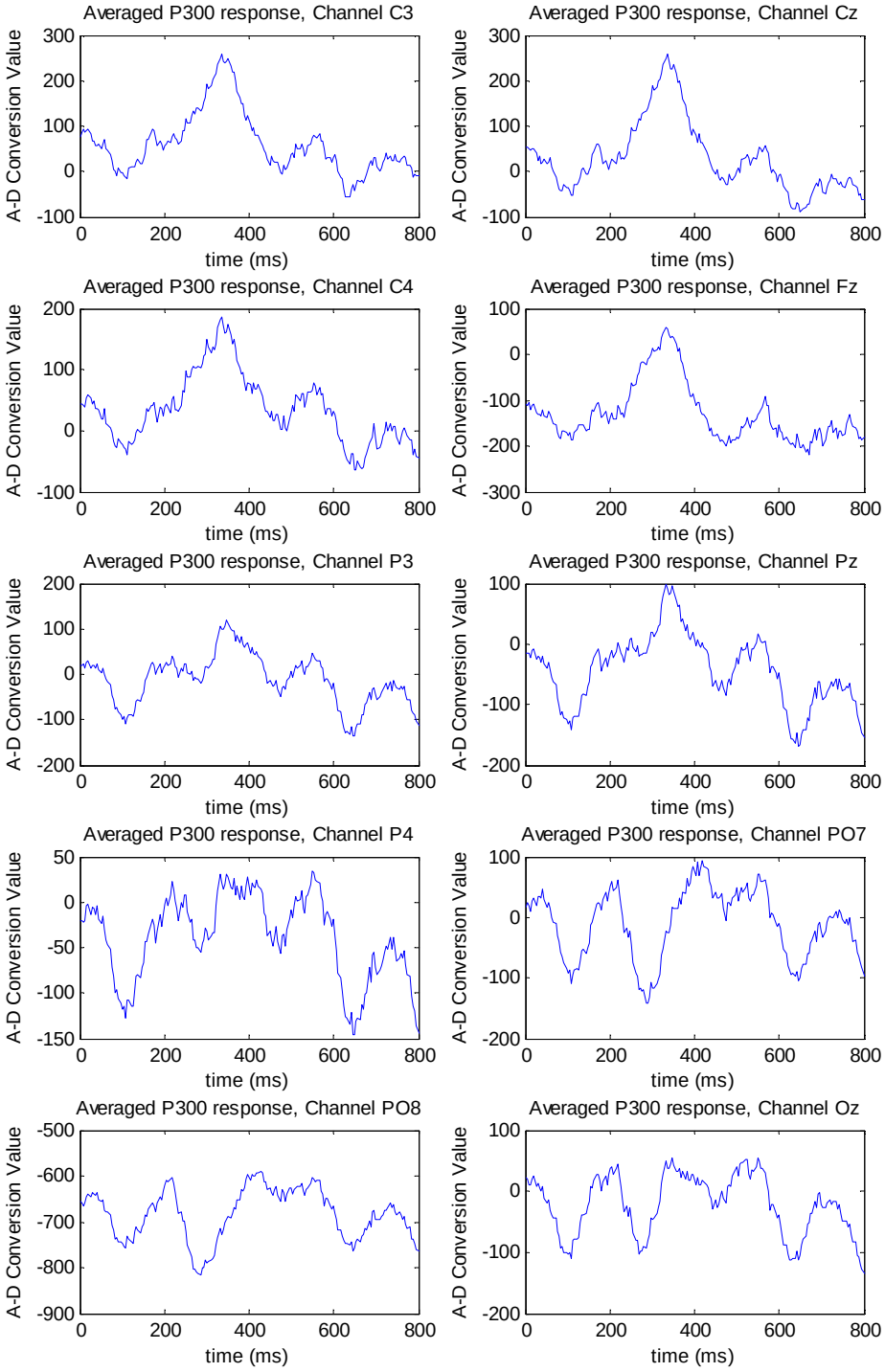

Figure 4-3: Averaged target responses from 10 EEG channels. The signals averaged over parietal and central locations exhibit the presence of P300 activity. The data of [18] is used for the demonstration of the P300 signals.

To construct the Wiener model, we will consider the P300 response as the desired signal $d(n)$. Despite the fact that $d(n)$ has a stochastic behavior in Wiener model, the P300 signal discussed here is somewhat a deterministic signal. In order to take the P300 response as the desired signal, a more statistical model should be included in the P300 response.

Therefore, we can model the P300 signal as a random process as follows:

$$x_{target}(n) = \sum_i A_i \sin(w_i n + \phi_i) \qquad i = 0,1,.....,k \qquad (4.26)$$

Here, the P300 signal is expressed as a sum of sinusoids, where A_i and w_i represent the amplitude and a set of frequencies comprising the P300 signal respectively. ϕ_i's are the phase parameters which, in fact, add a randomness property in the P300 signal; they form a set of random variables letting the signal be a random process. The latency of the P300 signal mainly depends on ϕ_i's and this latency varies according to the perception of the subject which actually is the random phenomenon in this problem. It can be assumed here that ϕ_i's are independent and have uniform distributions with means μ_{ϕ_i}'s. Expressing the desired signal as in (4.26) with these assumptions also satisfies the requirements for $d(n)$ being a wide sense stationary (WSS) process (Appendix A).

The noise in the EEG measurements is known to be mainly due to the power network in the environment. However, there are also other sources of noise like electromagnetic noise caused by other devices, the motion of the subject during the EEG recordings; or even the brain signals for other activities like body regulation, heart beat etc. can also be considered as a noise affecting the EEG recordings in this scheme. Therefore, we will consider the noise as a random process, independent of the target and non-target responses.

One should note that, the Wiener filter model is applied to random processes satisfying at least the second statistics or wide sense stationarity. For those processes, there are some operations and valid assumptions such as ergodicity, which combines the time course of the signal and ensemble distribution of the random processes [32]. For example, calculation of the autocorrelation or mean of a WSS process is possible using a single example from a set of observations. Therefore, the Wiener model can be constructed using only one example of the observation signal and the desired signal. However, as will be discussed here, we will follow an alternative way in designing the optimal Wiener filter considering all the samples of the observation signal in the dataset to be used.

As all the WSS requirements for the Wiener filter model are satisfied, we can continue with the construction of the filter. According to (4.20), the optimal Wiener filter has the form, $W(jw) = \frac{P_{dx}(jw)}{P_x(jw)} = \frac{P_d(jw)}{P_x(jw)} = \frac{P_d(jw)}{P_d(jw) + P_v(jw)}$.

Due to its simplicity in evaluation, we will use the second form in (4.20), where the filter depends only on the power spectral densities of the desired and observation signals. As we have only one desired signal which is the averaged target response in Figure 4-3, and it is assumed to be a WSS process from (4.26), it is easy to obtain the autocorrelation and power spectral density from its time course. For the observation signal $x(n)$, however, we have many examples regarding the subject response to target row or column intensifications in the paradigm. This leads an ambiguity since one can calculate the power spectral density of the observation signal using any of the samples in the dataset. Here, we employ the following estimation in order to evaluate the autocorrelation and hence the power spectral density of the observation signal $x(n)$:

$$P_x(jw) = \frac{P_{x,1}(jw) + P_{x,2}(jw) + ... + P_{x,N}(jw)}{N} \tag{4.27}$$

where N and $P_{x,i}(jw)$ represent the number of target observations and power spectral density estimate of the i-th observation respectively.

By performing the approximation in (4.27), we in fact average the spectral power information regarding all the samples in the dataset and hence obtain an averaged psd of the observation signal. So, the whole operation in designing the Wiener filter can be summarized as follows:

Method 1: Estimation of the Wiener filter

- Approximate the noise free desired signal $d(n)$ by ensemble averaging the observations from the same class
- Calculate the autocorrelation and obtain the psd of the desired signal $P_d(jw)$ by evaluating the Fourier transform of the autocorrelation
- Estimate the average power spectral density of the observations by first computing the psd of each observation and then averaging all computed psd's. $P_x(jw) = \frac{P_{x,1}(jw) + P_{x,2}(jw) + ... + P_{x,N}(jw)}{N}$
- Obtain the optimal Wiener filter from $W(jw) = \frac{P_d(jw)}{P_x(jw)}$

Up to now, we have discussed the implementation of Wiener filter for the target response class which can be represented as $W_{\text{target}}(jw)$. One can also apply the same modality to the system of non-target responses where the desired signal is the response to the non-target row or column intensifications. For this case, the desired signal obtained by averaging all non-target observations for the employed EEG channels is given in Figure 4-4.

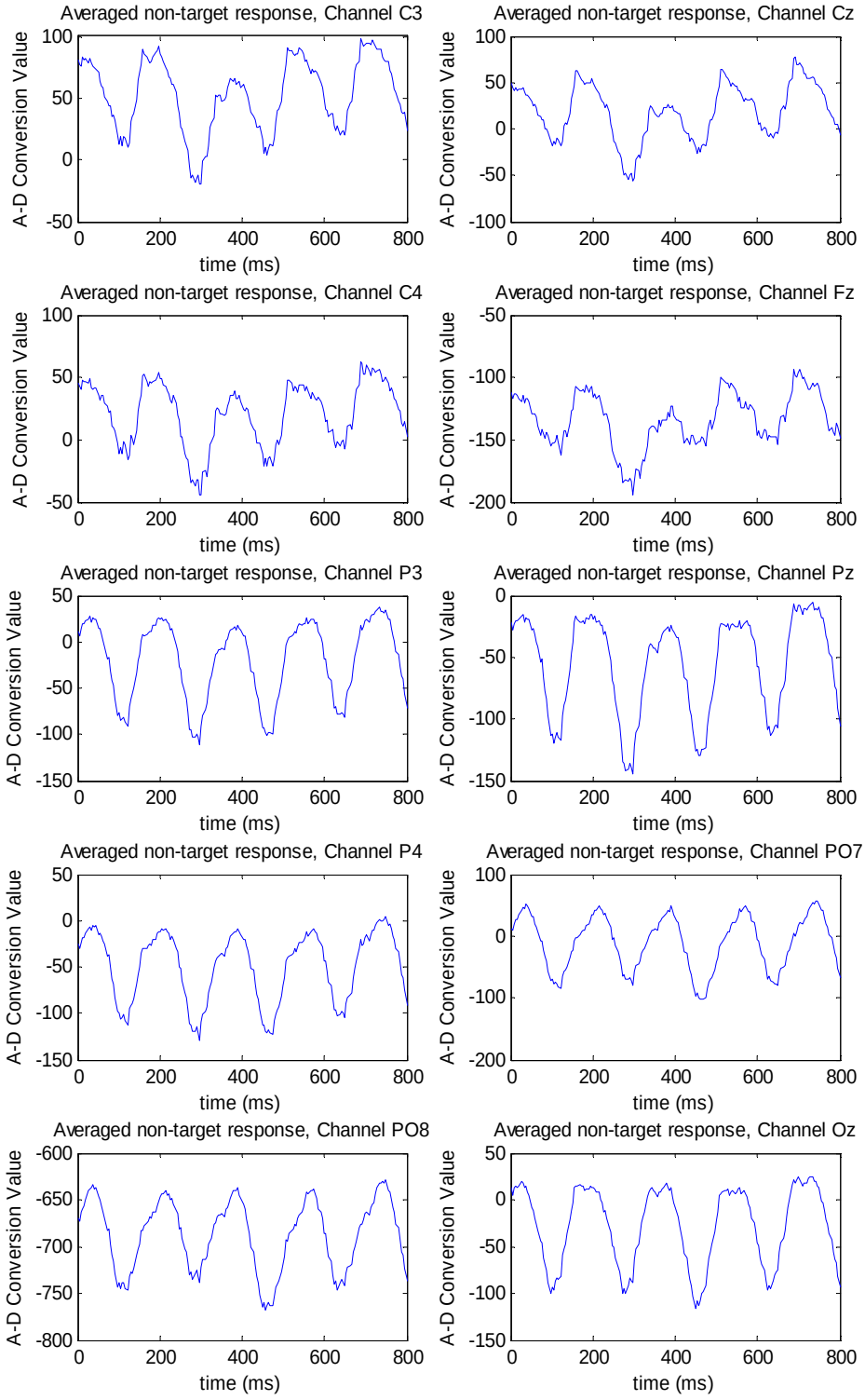

Figure 4-4: Averaged non-target responses from 10 EEG channels. The data of [18] is used to demonstrate the non-target responses.

Similar to equation (4.26), the averaged non-target signal is modeled as:

$$x_{\text{non-target}}(n) = \sum_i B_i \sin(w_i n + \phi_i) \qquad i = 0,1,....., p-1 \qquad (4.27)$$

which in this case depends only on p frequency components. Performing the same operations described in Method 1, we obtain the Wiener filter for the non-target system which can be represented as $W_{\text{non-target}}(jw)$.

After all, it is desired to identify the target responses. Therefore, we will define the final form of the filter as:

$$W_{\text{final}}(jw) = W_{\text{target}}(jw)\left(1 - W_{\text{non-target}}(jw)\right) \qquad (4.28)$$

Constructing the final filter as in (4.28) will enhance the target signals while suppressing the non-target ones.

When the behavior of the noise signal is considered, it is observed to be Gaussian distributed in this model. As an example, the histogram plots of the noise signal for the target column and non-target row groups (at random samples of time index n) are given in Figure 4-5 and Figure 4-6 respectively. From these figures, it is clear that $v(n)$'s are zero-mean random processes[2]. This is a trivial result since the desired signals are obtained by ensemble averaging the observations. Therefore, subtracting the desired signal from the observations to obtain the noise will definitely give us a zero mean signal.

[2] As there are two examples (target column and non-target row groups) given to illustrate the distribution of the noise signal, and therefore two separate Wiener filter models, it is more accurate to refer the noise signal separately for each group.

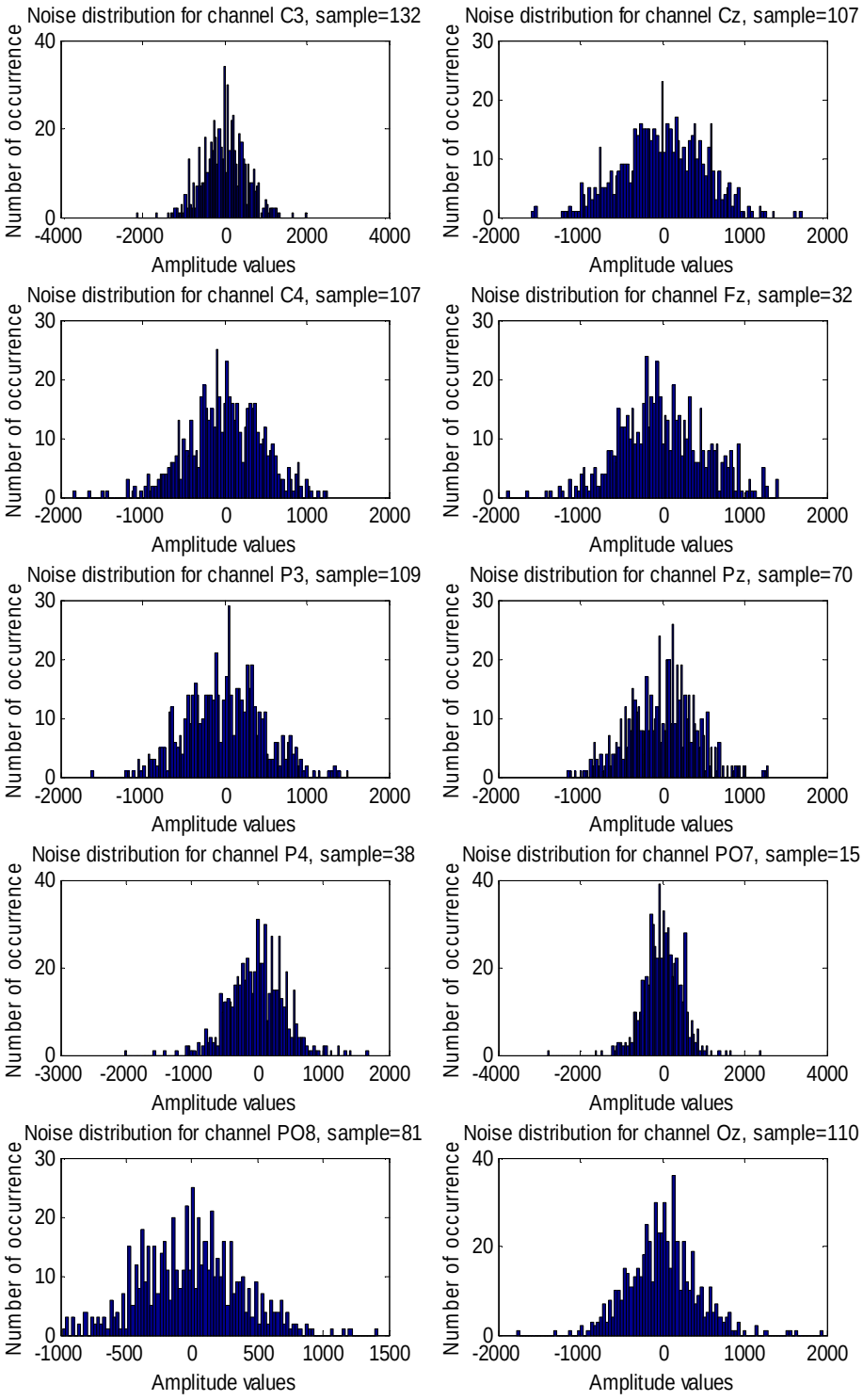

Figure 4-5 : Marginal distribution of the noise signal $v(n)$ at random time indices for the target column group. Each sample of $v(n)$ is Gaussian like distributed with means equal to zero.

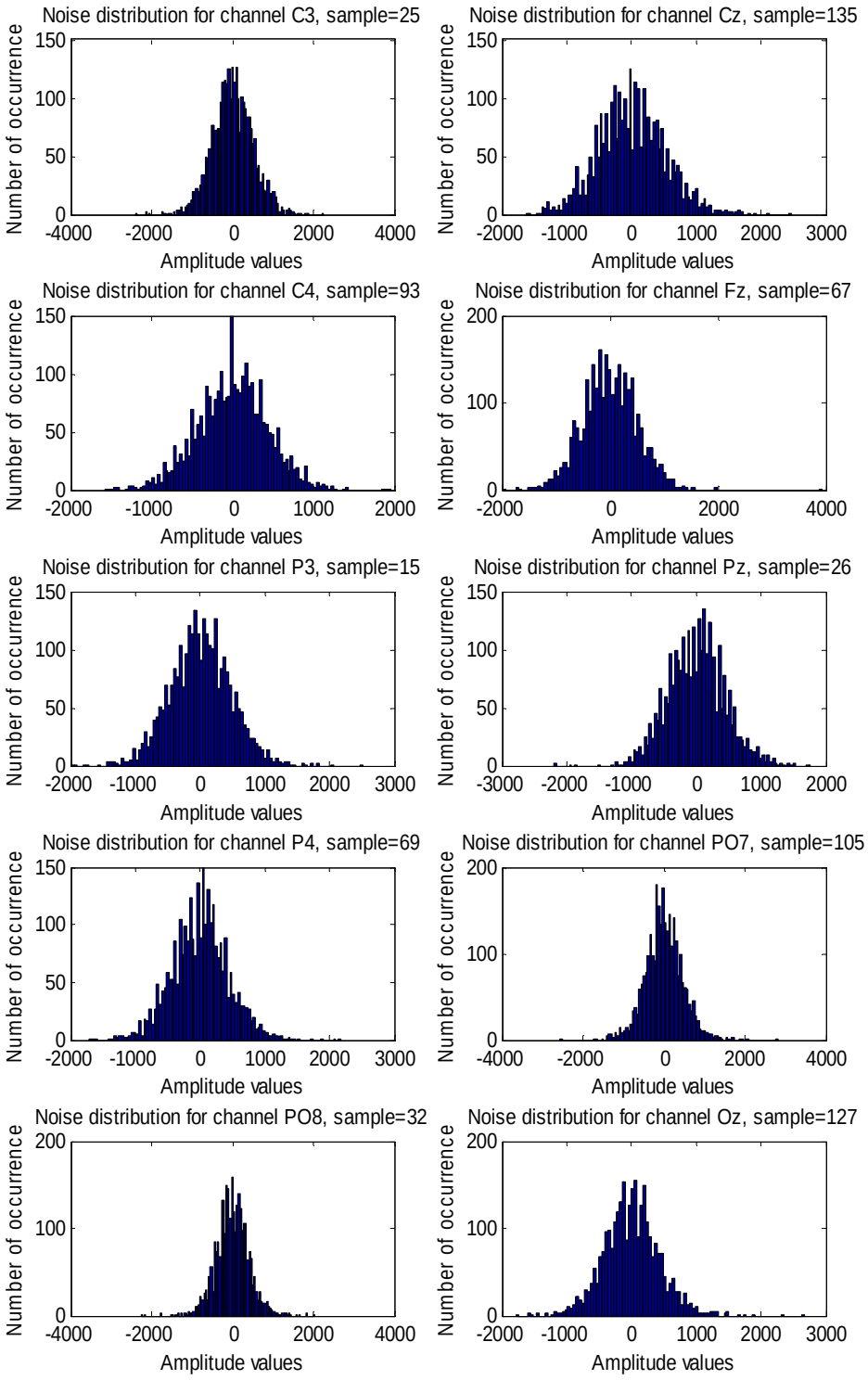

Figure 4-6 : Marginal distribution of the noise signal $v(n)$ at random time indices for the non-target row group. Each sample of $v(n)$ is Gaussian like distributed with means equal to zero.

Another observation regarding the noise signal is that the correlation coefficients of the noise signal are very small for two far samples of the signal (e.g. $v(k)$ and $v(k+100)$) which indicates that the noise signal in this dataset according to the described model is uncorrelated. The correlation coefficient increases as the samples get close to each other (for example $v(k)$ and $v(k+1)$ are highly correlated). However, it is impractical to show this observation with an illustrative tool. From these observations, it can be assumed that the noise signal is an independent random process as it is Gaussian distributed and also uncorrelated. Furthermore, it is observed to be zero mean. Therefore, it is natural to assume $v(n)$ as a white noise, which satisfies the requirements to be a wide sense stationary process. This suggests that the Wiener filtering model is well suited for this application.

To visualize the effect of Wiener filtering on the raw EEG data, two samples are randomly selected from the dataset (one from the target and one from the non-target group). These are filtered with the estimated Wiener filters and the outputs of these are shown in Figure 4-7 and Figure 4-8. The signals used in these figures are obtained from the Spelling Paradigm dataset of BCI Competition II [18].

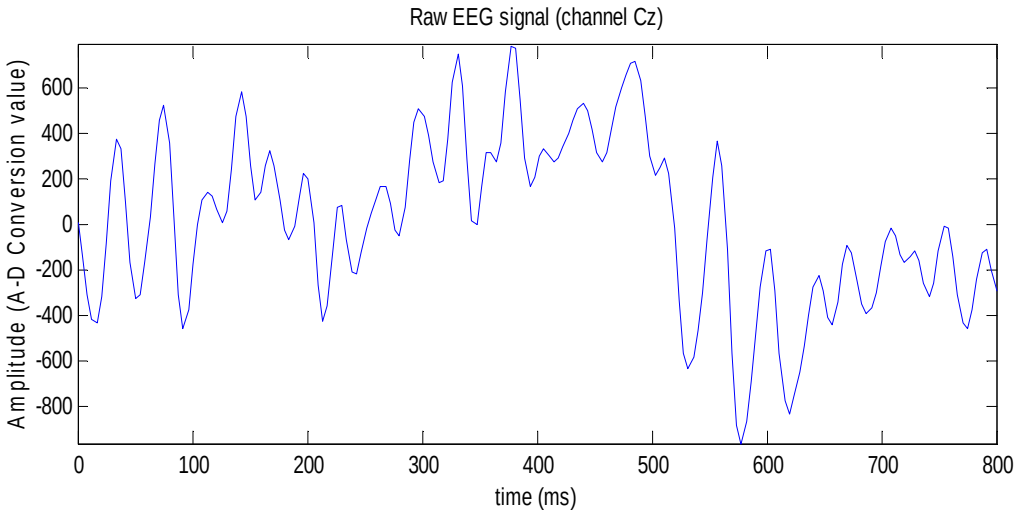

(a)

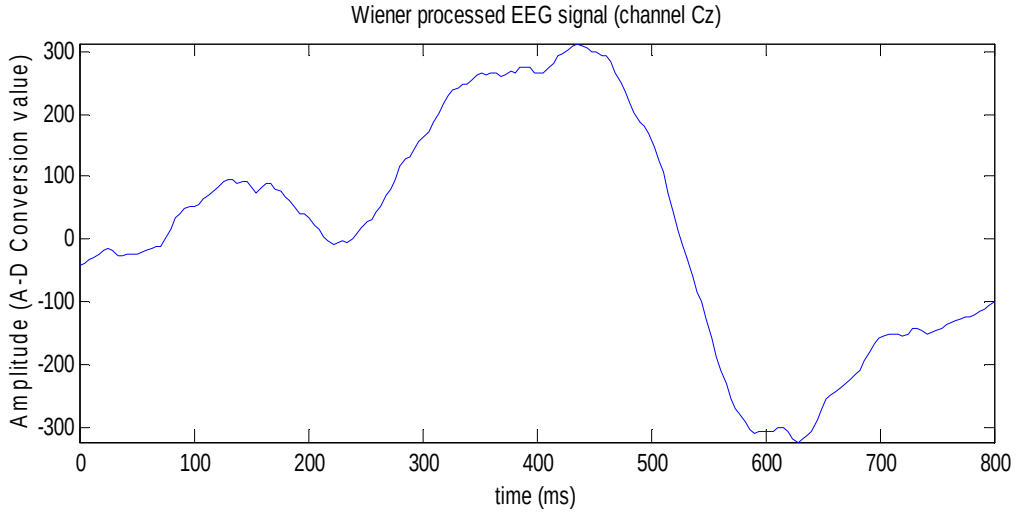

(b)

Figure 4-7: The effect of Wiener filtering on a randomly selected target response. (a) Raw target signal, (b) Processed target signal with the estimated Wiener Filter.

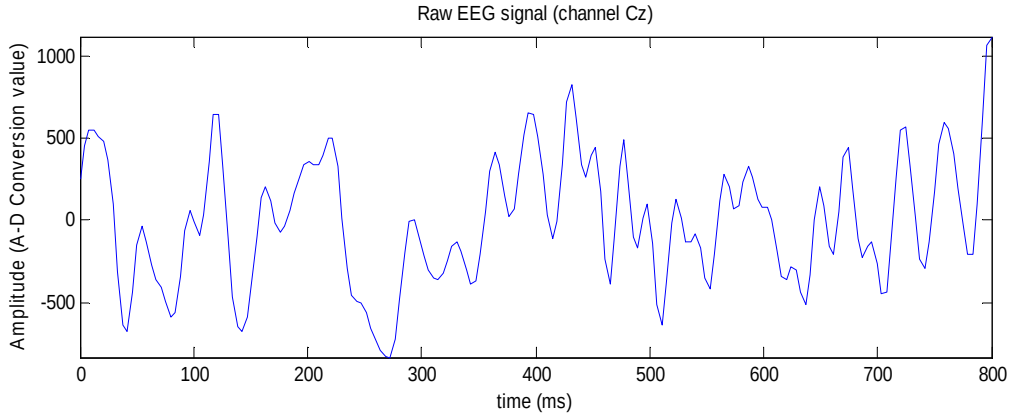

(a)

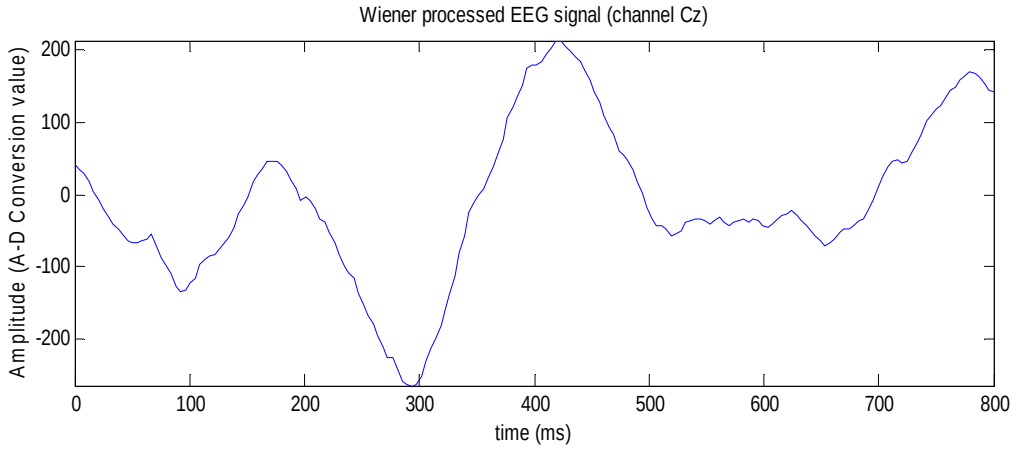

(b)

Figure 4-8: The effect of Wiener filtering on a randomly selected non-target response. (a) Raw non-target signal, (b) Processed non-target signal with the estimated Wiener Filter.

One can note that the amplitude of the Wiener processed target response in Figure 4-7 is comparably higher than that of Figure 4-8; the amplitude of the non-target signal has been considerably suppressed by the filter (consider the scale of the unfiltered signals). Moreover, the peaking time of each signal is preserved after the filtering operation which is also important in detection of P300 responses regarding the latency of these signals.

CHAPTER 5

CLASSIFICATION IN SPELLING PARADIGM

5.1 Introduction

The purpose of the BCI applications is to map the neurophysiologic signals to basic actions, like going on a specific direction in the cursor movement application. This mapping is performed with machine learning algorithms in which one or more classification methods are employed to form a classification model. The approaches in the classification methods can either be parametric or non-parametric depending on the information supplied by the problem. However, the common approach in BCI problems is to train the learning algorithm first within a training phase in which the subject is asked, for example in Spelling Paradigm, to focus on a character that is known by the algorithm. This is a supervised learning methodology that constitutes a major topic in pattern recognition.

In this chapter, the Spelling Paradigm will be considered in the classification point of view. First, a short explanation will be given on supervised learning describing the basic concepts about supervised classification. Then, the classification methods used in this study will be described in detail. Correlations and reference to the problem will also be given during the explanation of the concepts.

5.1.1 Classification Problem in Spelling Paradigm

As discussed in Chapter 3, the prediction of the target character in P300 Speller requires the determination of the target row and column intensifications. To visualize the problem in the classification aspect, there are 12 classes for a 6x6 speller matrix (6 row and 6 column intensification classes). However, one can use the intuitive idea that there are two independent groups, namely the row and column groups as the target character should be at the intersection of only one row and one column. Hence, there are 6 classes in each separate classification group.

Here, the problem may seem to be a 6 class classification task at first for each group. However, since the aim is to classify the stimulations as target or non-target, the task is realized as a binary classification problem. The presence of one target element out of six elements in a trial is just a constraint or a priori information supplied by the problem.

As discussed in chapter 2, the population of the non-target class should be higher than that of the target one in order to present a well behaved P300 pattern. If this case is considered in Bayesian classification point of view (see section 5.4.1), the probability of each stimulus to be the target character is 1/6. When one applies the Bayes decision rule for this problem, all new coming test samples will be assigned to the non-target class which provides a classification accuracy of 5/6 for each of the row and column groups. However, in this problem, the employed classification methods should determine at least one stimulus as from the target class for each trial. Therefore, the classification of these classes is usually performed using supervised learning techniques which will be discussed in the next section.

5.2 Supervised Learning

Most of the classification algorithms deal with a group of data that has some information about the dataset. In other words, the class label information is given within the dataset for training the classifier. This type of classification belongs to supervised learning, in which a supervisor instructs the classifier during the construction of the classification model. Linear Discriminant Functions (LDF), Support Vector Machines (SVM's) and Neural Networks (NN) are some well-known examples of supervised learning and commonly used in many classification problems.

In the supervised learning approach, there are pairs of examples in the given training dataset which can be mathematically expressed as $D = \{(x_1, y_1), (x_2, y_2), ..., (x_N, y_N)\}$. Here, $x_1, x_2, ..., x_N$ are the observations and $y_1, y_2, ..., y_N$ are the class labels of the observations. The observations can be any vector, whose elements are selected from a set of features (section 5.2.3). But for practical considerations, we usually have real valued observations and it is easy to assume $x \in X = R^M$. Also, one can choose any type of representation for the class labels. For simplicity, they are usually represented as real numbers, that is $y \in Y = R$. Therefore, in supervised learning, the aim is to find the transformation between the *feature* space X and the *class label* space Y, i.e. $f : X \to Y$. If the class space has a finite number of elements, i.e. $y \in \{1,2, ..., L\}$ then the problem is considered as a *classification task*. On the other hand, if there are infinite classes, then the case becomes a *regression problem*. For the case of Spelling Paradigm, it is a binary classification problem in which the classes are the target and nontarget classes. For clarity and conformity with the literature, these classes are represented as $Y = \{-1,+1\}$ where the negativity represents the nontarget case.

For such a problem, additional parameters underlying the classification rule can also be given such as the probabilistic distribution, or the form of the density function of the classes. When this is the case, the transformation of the observations to the class labels takes the form of $y = f(x, \theta)$. Whether these are provided or not, one can estimate the parameters or unknown densities of the class conditional probabilities by employing parametric or nonparametric estimation techniques. However, these will not be explained in this context. The reader can find detailed information about the estimation in supervised learning in [34].

5.2.1 Linear Discriminant Functions

A type of supervised learning called Linear Discriminant Functions (LDF) will be considered as a motivation to Support Vector Machine (SVM) which is used as the main classification method in Spelling Paradigm [77]. The importance of LDF is that they form the base of many discriminative classification methods and constitute a major subject in classification literature. It is a non-parametric supervised learning in which the form of the discriminating function is known or assumed instead of the probabilistic distribution of the classes. The form of the discriminating function may not essentially be linear in the feature vector; however, linearity brings additional properties that provide some advantages in analytical point of view [34]. Also, being easier to implement, LDF provide a well understandability of the discriminant classification with a simple model.

It is easy to demonstrate LDF in a two class case where the classes are also linearly separable as shown in Figure 5-1. The aim in LDF is to construct a hyperplane, or mathematically, to find the parameters defining the hyperplane that separates two classes by using the samples in the training dataset.

So, a linear discriminant function can be expressed in terms of the feature vector x as

$$f(x) = w^t x + w_0 \tag{5.1}$$

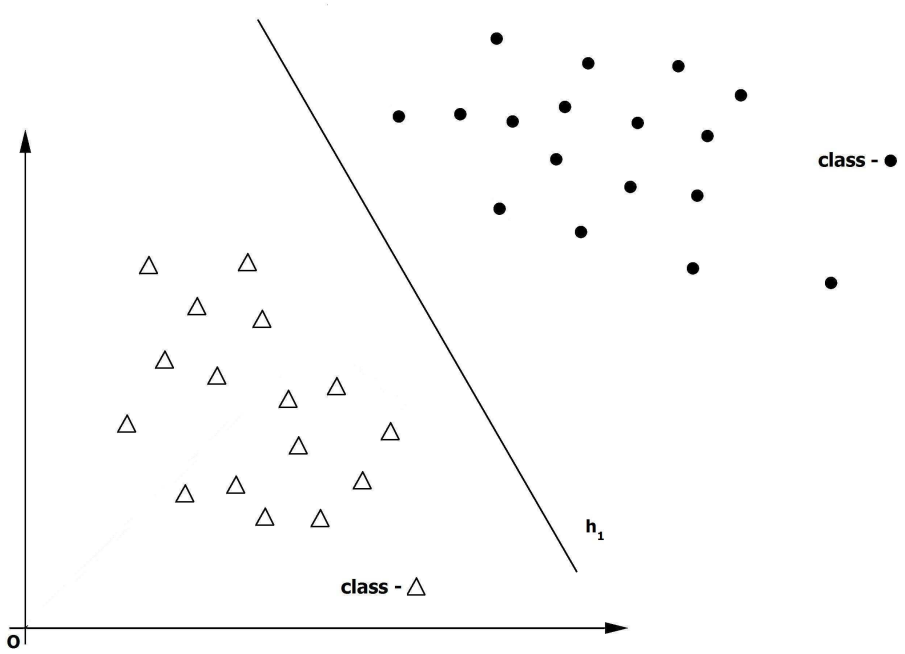

Figure 5-1: Visualization of a linear discriminant function for a 2-class separable problem.

where w and w_0 represent the weight and bias vectors respectively. Here, the classification of a new sample can be simply done according to the sign of the discriminant function f. That is if $f(x) < 0$ then the sample belongs to the triangle class and if $f(x) > 0$ then the sample is from the circle class. The boundary $f(x) = 0$ representing the separating hyperplane h_1, can be left undefined in terms of classification since the sample on the hyperplane can be from each class with the same probability.

Beside the sign of the discriminant function f, one can also consider the value $f(x)$ on the sample x. The value of the discriminant function provides a

measure of distance between the sample and the separating hyperplane. This can be seen if one uses the following expression for x:

$$x = \underbrace{w^t x}_{\hat{x}_p} + d\frac{w}{\|w\|} \tag{5.2}$$

where x_p and d represent the projection of the sample x on the hyperplane h_1 and distance of the sample to the hyperplane respectively. This distance is illustrated in Figure 5-2.

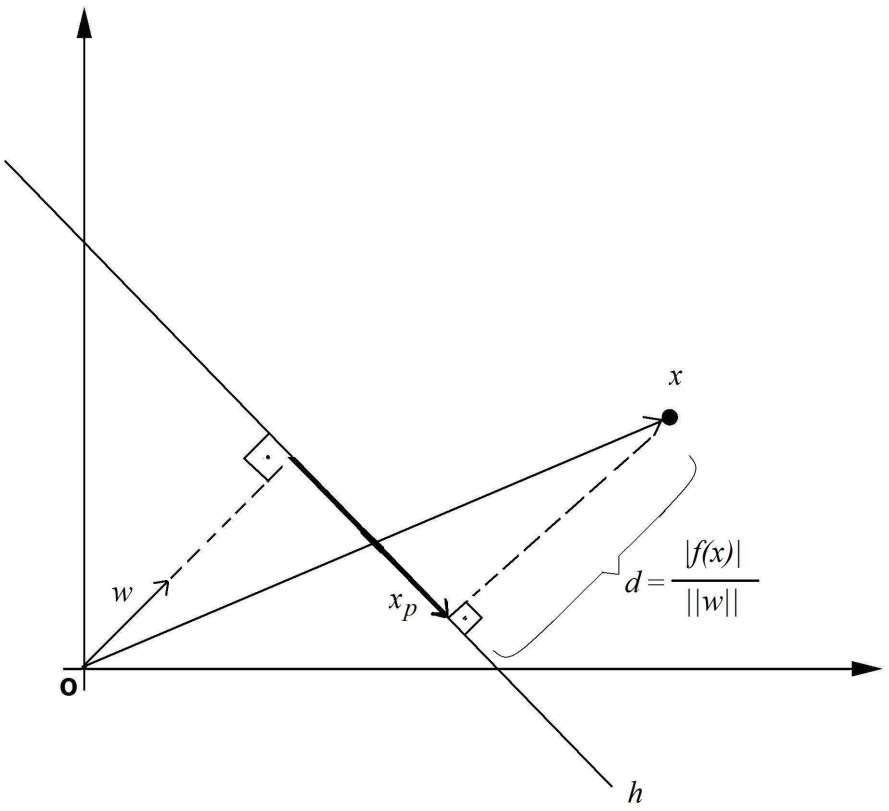

Figure 5-2: Relation between the function value of the sample *x* and its distance to the discriminating hyperplane.

Without going into detail, the distance d gives an idea of the probability value of the sample being in that halfspace. Although this is not always true, the larger value of d can be assumed to be the higher probability of right decision.

5.2.2 Error and Risk in Classification

Due to the stochastic nature of the problems, the error or the misclassification of samples is inevitable in pattern recognition. In fact, the principle of the classification methods is to minimize the error in classification or the risk in the decision. In this section, it is aimed to describe these concepts which are mentioned throughout following sections of this chapter. The explanations will be restricted to the binary classification problem which is the case in Spelling Paradigm. The reader can find detailed explanation for multiclass case in [34], and [35].

To begin with the error in classification, consider the Bayesian case where the decision is made according to the class conditional probabilities (discussed in section 5.4.1). That is, classify x as C_1 if $P(C_1|x) > P(C_2|x)$ or vice versa. In this case, one can not think of the error itself only, but the average probability of error which can be expressed as:

$$P(e) = P(x \in R_2, C_1) + P(x \in R_1, C_2) \tag{5.3}$$

where R_1 and R_2 represent the halfspaces separated by the decision surface. Applying the Bayes Theorem on (5.3) yields:

$$\begin{aligned} P(e) &= P(x \in R_2|C_1)P(C_1) + P(x \in R_1|C_2)P(C_2) \\ &= \int_{R_2} p(x|C_1)P(C_1)dx + \int_{R_1} p(x|C_2)P(C_2)dx \end{aligned} \tag{5.4}$$

which is also known as expected error or error rate and it is minimized by the Bayes decision rule stated above [34], [35].

Beside the average probability of error, one can also consider the risk in taking the decision in the problem. For example, in the P300 Speller case the risk of deciding the sample as target can be higher than the risk of deciding the sample as nontarget. Therefore, the risk or expected loss for taking an action α_i can be defined in a two class problem as follows:

$$R(\alpha_i|x) = \sum_{j=1}^{2} \lambda(\alpha_i|C_j) \int_{R_j} p(x|C_i)dx \tag{5.5}$$

In this scope, a loss function $\lambda(.)$ is introduced in the problem which is usually defined for two class case as:

$$\lambda(\alpha_i, C_j) = \begin{cases} 0, & i = j \\ 1, & i \neq j \end{cases} \qquad i, j = 1,2 \tag{5.6}$$

In this loss function, the cost of wrong decision in each class is equal. However, one can also define the loss function according to the nature of the classification problem. When defined as in this case, one can show that overall expected loss or risk becomes identical to the average probability of error defined in (5.4).

$$\begin{aligned} R &= \sum_{i=1}^{2} R(\alpha_i|x)P(C_i) \\ &= \int_{R_2} p(x|C_1)P(C_1)dx + \int_{R_1} p(x|C_2)P(C_2)dx \end{aligned} \tag{5.7}$$

However, the conditional probability densities are not always known in supervised learning methods like discriminant functions or SVM. The only information provided in supervised learning is a training dataset which includes

the class labels. Therefore, the evaluation and minimization of the risk is not possible by using the expressions above. Instead, one can employ empirical risk minimization to construct the discrimination function by using the training samples in the given dataset. The empirical risk in supervised learning is defined as follows:

$$R_{emp}[f] = \frac{1}{N}\sum_{j=1}^{N} \lambda\left(y_j, f(x_j)\right) \tag{5.8}$$

And the optimum discriminant function is the one which minimizes the empirical risk.

$$\hat{f}(x) = \arg\left(\min_{f \in H_n} R_{emp}[f]\right) \tag{5.9}$$

where H_n is the function space of interest.

One should note that the empirical risk makes sense only if it is equal to the expected risk if the number of elements in the training set goes to infinity. That is,

$$\lim_{N \to \infty} R_{emp}[f] = R \tag{5.10}$$

When this is not true, one can encounter some problems which will be mentioned in the next section.

5.2.3 Feature Space

The data given for training and testing the classifier are usually gathered from a recording device and contain raw data information. However, one can use some of the elements for classification instead of all from the supplied information. The

information extracted from the input space is called the feature space and usually represented with a transformation vector (Figure 5-3).

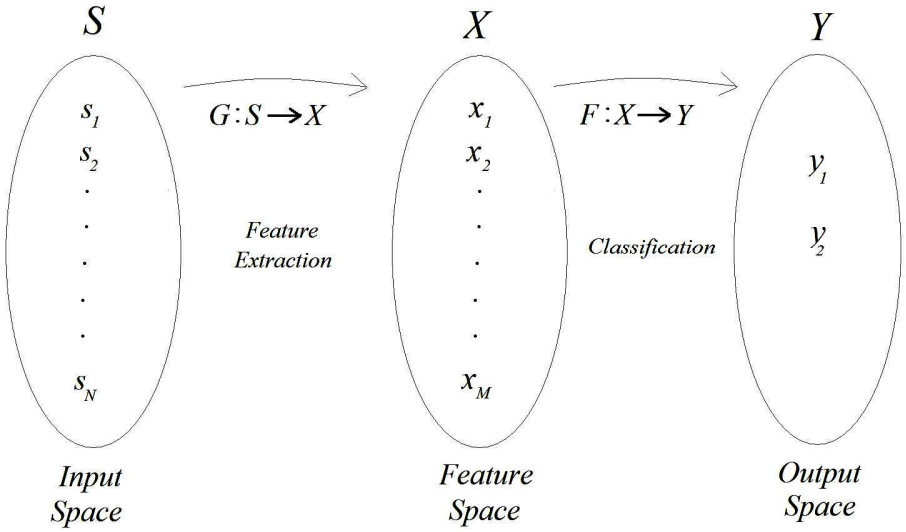

Figure 5-3 : Transformation between input, feature and output spaces. The feature space is constructed by performing preprocessing methods (*G(X)*) on the input space. Classification methods are applied on the feature space.

Although the data is processed with some signal processing techniques, it may not always be easy for the classification algorithm to distinguish the classes using the coarse information. The reason for this is usually related to the dimensionality of the feature space which is a well known problem in the classification literature. If the number of samples in the dataset is small as compared to the dimension of the feature space, the classifier suffers from the problem of overfitting which is a result of a large difference between the empirical risk and the expected risk defined in the previous section [27]. One can think of increasing the number of samples in the dataset as a solution to this problem. However, this can lead to a worse situation which is known as the curse of dimensionality. This problem arises from the statistical dependence of the features. The probability of error in the classification reduces as the independence between the features increases [34].

But when the features are statistically dependent, the classification performance is limited and can not be improved by adding new features.

A solution to this problem is to use other properties of the data by applying feature selection. For example, in a BCI problem, the band power of the EEG signal or coefficients of the autoregressive parameters might contain more useful information for the classifier than the signal itself in a mu-rhythm based BCI. As stated in chapter 3, there are also feature extraction algorithms that automatically select the elements for the feature space which improve the classification performance. However, in this study, due to the computational simplicity and conformity with the literature, the features are selected manually without any feature extraction method. As in [4], we have used the EEG time segments of 600 or 800 ms duration after the stimulus onset from the electrode locations Fz, Cz, Pz, Oz, C3, C4, P3, P4, PO7 and PO8 (Figure 7-3 (a)) and set the Wiener filtered signals as our feature vector. The dimension of the feature vector varies according to the sampling rate of the EEG recording device. For illustration purposes, the Wiener filtered EEG signals are concetanated by channel to form the feature vector as seen in Figure 5-4.

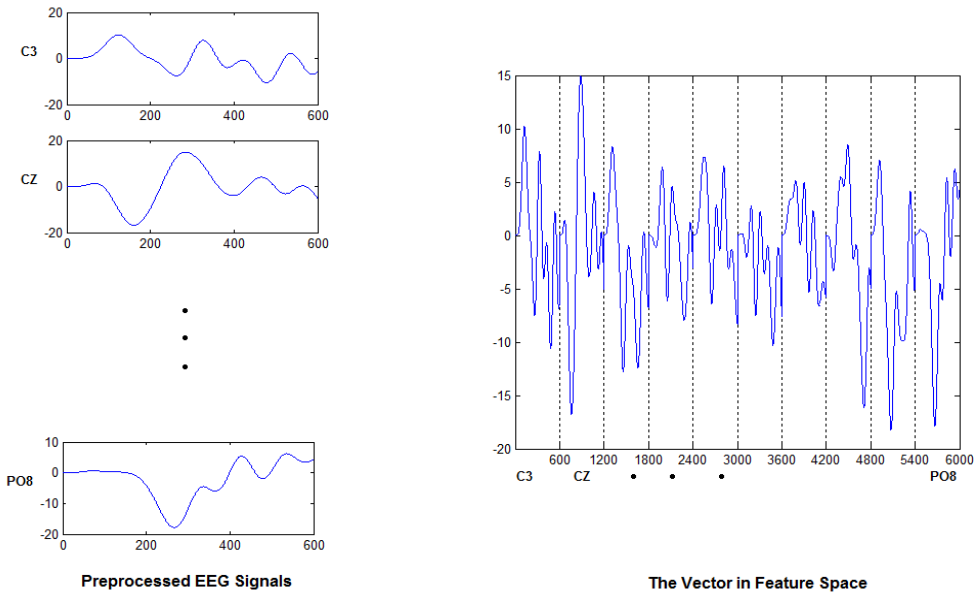

Figure 5-4 : Formation of the vector for the feature space as a concatenation of time segments from 10 EEG channels

5.3 Support Vector Machines

Support Vector Machine (SVM) is a supervised machine learning algorithm whose foundations have been developed by Vapnik [36], [37], [39]. Showing much similarity with the LDF, SVM provides better generalization than most of the discriminant methods due to the structural risk minimization it employs. SVM has also been successfully applied in numerous BCI applications [4], [6], [2] and excellent classification performances are reported in these studies. As it is preferred as the main classifier in this study, the basic concepts of SVM will be explained briefly in this section. A more detailed explanation and discussion on SVM can be found in [36], [38] and [39].

5.3.1 Support Vector Classification

To begin with the formulation of the classification problem, consider the two class case described in section 5.2.1, where the set of examples are to be separated

by a discriminating function. For such a problem, one can find infinitely many separating hyperplanes hence functions, as can be seen in Figure 5-5.

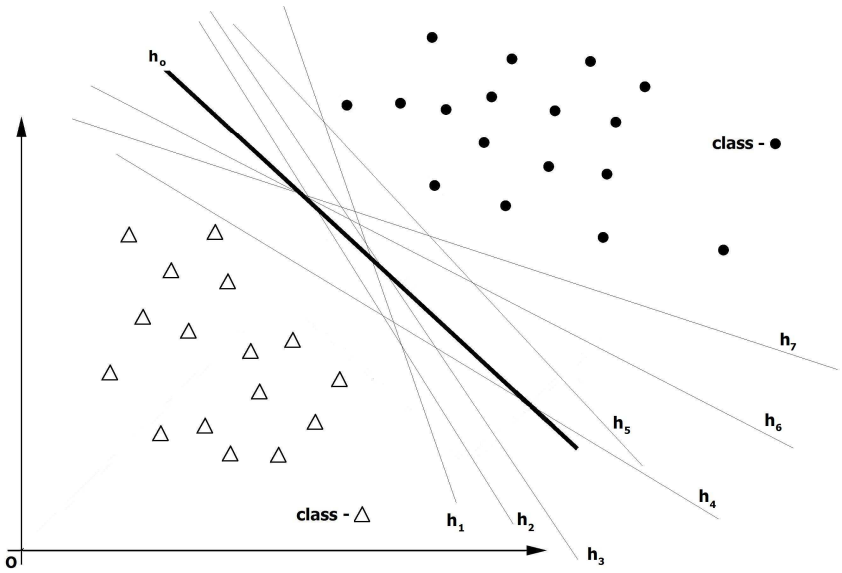

Figure 5-5 : Several solutions of the discriminating function for a linearly separable 2 category classification problem. The solution found by SVM (represented with h_0) is the one that maximizes the margin between the samples (support vectors) and the hyperplane.

However, among these hyperplanes, there is only one that separates the classes with the maximum margin. That is, SVM tries to find the separating hyperplane which maximizes the distance between the hyperplane and the nearest samples in each class. This idea intuitively provides optimality in the sense that it increases generalization capabilities [2], [38]. The optimum separating hyperplane is illustrated in Figure 5-6.

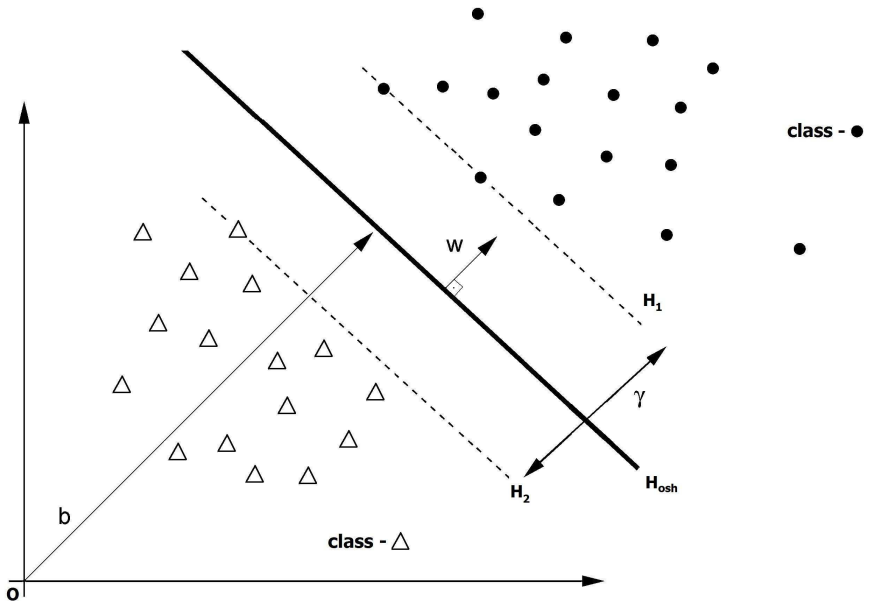

Figure 5-6: Optimum Separating Hyperplane (OSH) of SVM for a two class case. The closest samples to OSH from each class are called the support vectors.

The nearest elements to the hyperplane lying on H_1 and H_2 in Figure 5-6 are called the support vectors which give the name to the method. The solution procedure of the optimum separating hyperplane (OSH) reveals these elements and once these are found the classification in the test phase is done by using the support vectors.

The OSH for the linearly separable case can be mathematically represented with a line as:

$$w^t x + b = 0 \tag{5.11}$$

where the bias vector for the OSH is represented with b for conformity with the literature [38].

The solution for OSH requires the solution of an optimization problem where the goal is to maximize the margin γ. Here, if one sets the class labels as $y = \{-1,1\}$, then $y_i(w^t x_i + b) \geq 1$ becomes a constraint of this optimization problem. This constraint comes from the restriction that

$$\min_i \left| (w^t x_i + b) \right| = 1 \tag{5.12}$$

which simplifies the formulations in the problem. With these constraints one can show that the margin γ is related to the weight vector w with:

$$\gamma = \frac{2}{\|w\|} \tag{5.13}$$

Therefore, maximizing the margin γ is equivalent to minimizing the norm of the weight vector. So the quadratic support vector optimization problem is formulated as follows:

$$\begin{aligned} &\text{minimize} \quad \frac{1}{2}\|w\|^2 \\ &s.t. \qquad y_i(w^t x_i + b) \geq 1 \qquad i = 1,2,\ldots\ldots\ldots,N \end{aligned} \tag{5.14}$$

where N is the number of elements in the training set.

SVM can find the optimum solution for the separating hyperplane from (5.14) only if the classes are linearly separable. However, this is not usually the case. In real problems the data is inseparable even with the feature extraction methods and higher dimension mappings which will be discussed in the later sections of this chapter. To overcome this problem, (5.14) is modified by introducing a penalty function and positive slack variables into the optimization problem [39], [38]:

$$\begin{aligned} &\text{minimize} && \frac{1}{2}\|w\|^2 + C\sum_{i}^{N}\xi_i \\ &s.t. && y_i(w^t x_i + b) \geq 1 - \xi_i \qquad i = 1,2,\ldots\ldots,N \\ & && \xi_i > 0 \qquad\qquad \forall i \end{aligned} \tag{5.15}$$

where ξ_i's are the slack variables and C is the regularization parameter. This modification provides a more flexible situation which is named as the "soft-margin" SVM optimization problem [4]. The ξ_i parameters moderate the constraints by allowing violations and provide the penalty together with the regularization parameter in the cost function.

The solution for the optimum separating hyperplane is simplified when the cost function in (5.15) is expressed in the Lagrangian dual form:

$$\begin{aligned} &\text{maximize} && L_D \equiv \sum_i a_i - \frac{1}{2}\sum_{i,j} a_i a_j y_i y_j x_i^t x_j \\ &s.t. && 0 \leq a_i \leq C \\ & && \sum_i a_i y_i = 0 \end{aligned} \tag{5.16}$$

This formulation provides an advantage that one does not deal with the slack variables inside the cost function. One should also note that the solution is found in terms of the Lagrange multipliers a_i for all the training points x_i and the non-zero solutions for a_i's represent the coefficients of the support vectors. Therefore, the solution for the weight vector w of the OSH is found from:

$$w = \sum_{i}^{N_s} a_i y_i x_i \tag{5.17}$$

where x_i's and N_s represent the support vectors and the number of the support vectors respectively.

The solution for the threshold or the bias term b can be found from the Karush-Kuhn-Tucker (KKT) conditions for the primal Lagrangian form which states

$$a_i\left[y_i\left(x_i^t w+b\right)-1\right]=0, \qquad \forall i \tag{5.18}$$

Expression (5.18) is, in fact, a simplified case of the real KKT conditions. The slack variables ξ_i's are removed here by using the fact that $0<a_i<C$. This constraint implies that $\xi_i=0$ when the Lagrange multipliers are in this range. Therefore, from (5.18) one can use all the training points to compute the bias term b for which $0<a_i<C$ is satisfied. As there are at most N equations in (5.18) one may find N different solutions for b and the common approach is to average all these solutions to compute the bias vector [38].

5.3.2 Prediction in SVM

When the parameters defining the OSH are found, the class labels of the new coming vectors are determined by evaluating the sign of the function defined in (5.19).

$$f(x)=w^t x+b \tag{5.19}$$

The function is expressed in terms of the support vectors if the equation (5.19) is combined with (5.17) as:

$$f(x)=\sum_{i}^{N_s} y_i a_i x^t x_i+b \tag{5.20}$$

The sign of the function value indicates the side of the OSH on which the vector lies and the absolute value of the function gives the idea of distance of the vector to the hyperplane. In other words, the higher the absolute value of the function, the higher the probability of the vector being in that halfspace.

5.3.3 Kernel Functions

Up to here, SVM is discussed in the linear functions of the data, i.e. the discriminating function used in classification is a linear transformation of the feature vector to the output space. The Kernel operator used in the above SVM discussions is the usual dot product of the two vectors. However, one can also employ other transformations to generalize the SVM to the nonlinear case. The idea is to map the vectors into a higher dimensional space which provides some advantages in cases where the data is linearly inseparable [38]. So, one can express the Kernel operation as an inner product in the feature space as:

$$K(x_i, x_j) = \left\langle \Phi(x_i), \Phi(x_j) \right\rangle \tag{5.21}$$

where the operation $\langle .,. \rangle$ represents the inner product and the function $\Phi(.)$ provides the nonlinearity in the transformation of the feature vector. Therefore, the inner product in SVM discriminant function can be replaced by the generalized Kernel operator defined in (5.21).

$$f(x) = \sum_{i}^{N_s} y_i a_i K(x, x_i) + b \tag{5.22}$$

Some examples of the nonlinear Kernel functions used in SVM are defined in the following:

- **Polynomial Kernel:**

$$K(x_i, x_j) = \left\langle x_i, x_j \right\rangle^d \tag{5.23}$$

or

$$K(x_i, x_j) = \left(\left\langle x_i, x_j \right\rangle + 1\right)^d \tag{5.24}$$

- **Gaussian Radial Basis Function:**

$$K(x_i, x_j) = e^{-\frac{\left\|x_i - x_j\right\|^2}{2\sigma^2}} \tag{5.25}$$

- **Exponential Radial Basis Function:**

$$K(x_i, x_j) = e^{-\frac{\left\|x_i - x_j\right\|}{2\sigma^2}} \tag{5.26}$$

- **Dirichlet Kernel:**

$$K(x_i, x_j) = \frac{\sin\left(\left(N + \frac{1}{2}\right)\left(x_i - x_j\right)\right)}{2\sin\left(\frac{x_i - x_j}{2}\right)} \tag{5.27}$$

- **Sigmoid Function:**

$$K(x_i, x_j) = \tanh\left(\kappa x_i . x_j - \delta\right) \tag{5.28}$$

Among these kernel operators, the Gaussian Radial Basis Function (Gaussian RBF) is reported to provide excellent results in the classification and generalization performance of SVM as compared to other functions [40], [38].

The variance expression σ^2 in Gaussian RBF provides an additional control parameter that leads to a more suitable decision boundary for many classification problems. Also in BCI studies, the Gaussian RBF is preferred in SVM due to its success in classification [4], [2].

5.3.4 Normalization

Normalization is a data processing technique used in statistics, signal processing and machine learning applications. It is used to standardize the magnitude or decrease the variance of the elements in the set of interest. For classification point of view, the samples in a training set usually exhibit a large variance. It is sometimes necessary for removing the extremity of the samples and increasing the correlations between the samples from the same class when training the classifier.

There are several techniques for data normalization. The simplest one is to normalize the length or the magnitude of the vector; that is the normalized sample is equal to the unit vector pointing in the direction of the input sample.

$$\hat{x} = \frac{x}{\|x\|} \tag{5.29}$$

The norm operation in (5.29) is the L_2 norm which corresponds to the linear scaling of the input vector with its magnitude. There are also other normalization options like scaling the input vector with the difference between the maximum and minimum of the input vector:

$$\hat{x} = \frac{x - \min(x)}{\max(x) - \min(x)} \tag{5.30}$$

In (5.30), the input vector is linearly scaled to the interval $[0,1]$. This range can be modified according to the requirements of the classifier (if exists any) as:

$$\hat{x} = \frac{\max(\hat{x}) - \min(\hat{x})}{\max(x) - \min(x)}\left(x - \min(x)\right) + \min(\hat{x}) \tag{5.31}$$

Up to here, the normalization is explained by using only the properties of a single sample in the dataset. However, one can also employ ensemble normalization which is performed over the whole dataset. In this approach, the statistical properties of the dataset such as the means or the variances of the features are used to scale the samples. A well known type of ensemble normalization is the Gaussian normalization in which all the features are normalized with according to a normal distribution $N(\mu, \sigma)$.

$$\hat{x} = \frac{x - \bar{\mu}_x}{\bar{\sigma}_x^2} \tag{5.32}$$

where $\bar{\mu}_x$ and $\bar{\sigma}_x^2$ represent the mean and variance vectors of the features respectively.

5.3.5 Cross-Validation

Cross-validation is a testing method in supervised learning used for assessing the generalization performance of a classification model. The idea is to divide the training set into small partitions and use only one partition to train the classifier. The remaining subsets (validation set) are left to test the classifier where the result of classification could be justified. The cross-validation is performed by rotating the subsets used for training and the result of the prediction accuracy over the validation set is averaged for all combinations. Application of this technique allows the modification of the parameters that are used to construct the classifier and thus provides a generalization procedure for the classifier.

Two types of the cross-validation are commonly used in measuring the accuracy of the classification model which are the random sub-sampling and κ- fold cross-validation methods. In random sub-sampling cross-validation, the training set is randomly partitioned into training and validation sets and the classification model is tested on the validation set for each partitioning operation. The averaging is performed over the partitions to determine the average accuracy of the model. On the other hand, the κ- fold cross-validation divides the training set into κ subsets. The classifier is trained on $\kappa - 1$ of these subsets and then tested on the remaining subset. This operation is then repeated for κ times until all the subsets are used as a validation set for the classifier. The κ classification accuracy results obtained from the validation sets are then averaged to asses the overall performance of the classifier. In this study, the κ-fold cross-validation method is preferred for the comparison of the classifier performance with the results given in [4]. It is used to determine the optimal control parameters which are the regularization parameter in the penalty function of SVM defined in (5.15) and variance parameter of the Gaussian RBF kernel in (5.25).

5.4 Unsupervised Learning

The supervised learning techniques like SVM employ only the data to construct the classification model and the additional information supplied by the problem is not used in these methods. As described in section 5.1.1, for the case of Spelling Paradigm, the information given by the problem is that there exists only one target class in each of the row and column groups for a single trial. Discriminant classification, on the other hand, can decide as if there are multiple target classes in each group which is not true for the Spelling Paradigm case. For example, the classifier can predict two or more rows from the same trial as the target class or all columns as the nontarget class. To overcome this problem, unsupervised learning techniques are involved by using the probabilistic information supplied by the problem. Therefore, in this section, the Bayesian classification together

with the Maximum Likelihood Estimation (MLE) will be explained as the unsupervised learning technique in Spelling Paradigm.

5.4.1 Bayesian Classification

The Bayesian classification is the simplest machine learning technique that employs the a posteriori probabilities of the observations in the decision. It is used in both supervised and unsupervised learning depending on the information provided by the problem. In this section, Bayesian decision is explained for unsupervised learning in which only the state conditional probability density of the observations and the a priori probabilities of the classes are known.

To begin with the Bayes decision theory, classification for an observation x is done according to the Bayes Rule which is defined as:

$$P(C_j|x) = \frac{p(x|C_j)P(C_j)}{p(x)} \tag{5.33}$$

Here, $P(C_j|x)$ represents the a posteriori probability of x for the class C_j. In other words, it is the probability of an observation belonging to that class. It can be interpreted for the Spelling Paradigm case as the true probability of a row or column being from the target or non-target class once it is observed. Moreover, $p(x|C_j)$ is the class-conditional probability density of x for the j-th class which represents the distribution of x when the j-th class is observed. This can be interpreted as the probability of a row or column once it is decided (by the SVM classifier) as from the target or nontarget class.

If the case is restricted to the two class case, one can express the probability density of x in (5.33) as:

$$p(x) = \sum_{j=1}^{2} p\left(x\middle|C_j\right)P(C_j) \tag{5.34}$$

The Bayesian decision is performed according to the intuitive idea that if $P\left(C_j\middle|x\right) > P\left(C_i\middle|x\right)$ then the observation x belongs to the j-th class and this minimizes the risk in classification as discussed in section 5.2.2. Once the class-conditional densities are known, the Bayesian classification can be applied for prediction of the observations using the rule defined in (5.33). If the probability densities are unknown or depend on some parameters, then parameter estimation techniques can be applied to determine the distribution of the class-conditional probabilities. A common parameter estimation technique, known as the Maximum Likelihood Estimation (MLE) will be the topic of the next section.

5.4.2 Maximum Likelihood Estimation

Maximum Likelihood Estimation (MLE) is used in cases where the conditional probability density function is unknown, but the form of the function is known. The conditional probability in this case depends on some parameters $\theta = (\theta_1, \theta_2, ..., \theta_N)$ such as mean or variance of the distribution, and these parameters can be estimated using the MLE method. For the case of Spelling Paradigm, the unknown parameter θ will represent the trial dependency of the target class prediction. Here, the MLE is discussed on the estimation of the conditional probability density $p\left(x\middle|C_j\right)$ required in the Bayesian classifier.

To begin with, the dependence of the class-conditional probability density $p\left(x\middle|C_j\right)$ to the unknown parameter θ can be expressed in a joint density as $p\left(x\middle|C_j,\theta\right)$. For our case, $p\left(x\middle|C_j,\theta\right)$ represents the class-conditional probability density for each trial repetition. Since the form of $p\left(x\middle|C_j,\theta\right)$ is known (it can be

observed from each trial), the best estimate of the class-conditional density $p(x|C_j)$ is obtained by averaging[3] $p(x|C_j,\theta)$ over θ [34]:

$$p(x|C_j)=\int p(x|C_j,\theta)\,d\theta \tag{5.35}$$

The expression (5.35) in fact, provides the MLE of the class-conditional density provided by the SVM outputs for the spelled character. Kaper *et al.* considered this case as the scoring of the row and column intensifications regarding the SVM outputs [4] but did not formulate the problem in a probabilistic methodology.

At this point, one can think of a better estimation of $p(x|C_j)$ for a real world problem in P300 Speller. For example, consider the case that the subject wants to stop the spelling application and rest for a moment. In other words, he/she refuses to spell a character. In this case, a stopping criteria should be introduced into the problem. Therefore, one can modify the decision rule in prediction as follows:

[3] The expression $p(\theta|X)$ in [34] has been omitted here as it is obvious that it is equal to 1 for the P300 Speller (There is always a trial for any observation). However, for an online system in which the subject may not always desire to perform spelling, the form of the conditional density $p(\theta|X)$ should be considered.

Method 2: Decision Rule in Prediction of a Character

```
X = [0 0 0 0 0 0];          % Decision vector for a row or column group, assign 0 for all intensifications
X_svm = [0 0 0 0 0 0]; % The number of occurences of each stimuli predicted by SVM as from the target class
t_s = 0;                    % Total number of stimuli predicted by SVM as from the target class

for t = 1 to n              % For a predefined number of trial repetitions to be employed
    for s = 1 to 6          % For all stimuli of interest in a group
        if f(s) > 0         %if the stimulus is predicted as from the target class by SVM
            X(s) = X(s) + f(s)    % add the probability of prediction
            X_svm(s) = X_svm(s) + 1;  % increment the number of occurence
            t_s = t_s + 1;
        end if
    end for
end for
X = (X) .* (X_svm) / t_s;  %Multiply two probability distributions to obtain the realistic probability density
Decided stimulus = argmax(X);
```

The proposed decision mechanism is meaningful only when the single observation prediction accuracy of the discriminative classifier (SVM for our case) is satisfactory. For example, consider the case when the SVM could not predict any stimulus as from the target class in *n* trial repetitions. This will force the system in not taking an action to predict the character. Using this decision method will prevent false prediction of the character when the subject does not focus on any character. If the character prediction rule of [4] was employed, the stimulus with the maximum SVM score among *n* trials would be selected as the target stimulus even if it was not predicted as a target class by the SVM. Therefore, the decision rule in [4] is reasonable only when it is known that the subject is focused on a character. However, as it is impossible to know the state of the subject, it is practical to employ the prediction mechanism described in Method 2 for real world applications of P300 based BCI systems.

CHAPTER 6

THE DESIGN OF ELECTROENCEPHALOGRAPHIC DATA ACQUISITION SYSTEM FOR BCI APPLICATIONS

6.1 Introduction

Beside the signal processing techniques and classification methods, the mechanisms in measurement of the brain activity and decision in experimental paradigms are of quite importance. The quality of the signal detecting and recording devices considerably affect the performance of the BCI algorithms. As mentioned in Chapter 2, BCI systems usually use electroencephalogram to measure the brain activity due to its portability and practicality. In this chapter, we will present a prototype design of an EEG system to be used BCI applications. The design of the system mainly covers the design of an EEG amplifier, the data acquisition hardware, electrode and EEG cap designs and the software controller design for BCI experiments. Here, in this chapter, the designed system is explained briefly. Detailed information (system diagrams, performance tests etc.) can be found in the technical documentation of the EEG system [82].

6.1.1 EEG Design Requirements

- EEG systems are used in medical applications. They should first satisfy some safety requirements in order not to harm the subject. Therefore, electrical safety should be of primary consideration; isolations from the power network should be implemented properly.
- As stated in Chapter 2, the amplitude of EEG signals is on the order of several microvolts (~100μV). Therefore, the system should be capable of sensing the signals in this range. The gain of the amplifier system and the resolution of the analog to digital conversion should be taken into account.
- Since the signal amplitudes are very low, EEG systems are usually affected from noise, especially from the noise of the power network and the digital circuitry. The filters should reduce the noisy effects of the signals that are not related to EEG. The analog and digital grounds should be isolated properly.
- EEG signals cover a small frequency range in BCI applications. The system should sense the electrical activity of the brain for frequencies lower than 40Hz.
- Sampling rate should be high enough considering the EEG frequency range (Table 2-1).
- For the P300 based BCI applications like Spelling Paradigm, the system should support recording the epoch information synchronously with the signal.
- Regarding the previous studies performed on spelling paradigm, there should be at least 10 channels in the system [4].
- The system should be implemented with minimum number of hardware components.

6.2 System Specifications

The system design is performed according to the needs listed in the previous section. Basically, the system is designed satisfying the following specifications:

- The analog amplifier circuitry will be supplied by standard batteries in order to reduce the effect of noise caused by the mains supply. Also, the batteries are preferred due to electrical safety issues.
- Active electrodes will be used in the system.
- The amplifier system will be AC-coupled in order to eliminate the DC offsets.
- EEG measurements will be monopolar.
- The isolation between the analog and digital circuitries will be performed with analog isolators.
- ADC resolution is chosen as 12 bits.
- The digital data will be transferred to PC via USB.

6.3 Analog Hardware

The analog hardware is composed of an active electrode stage and an amplifier circuitry which mainly includes instrumentation amplifiers, filters and isolator components inside. These will be explained in detail in the following subsections. The circuit diagrams of the system can be found in Appendix B.

6.3.1 Active Electrodes

Instead of simple passive ring electrodes, in this design, the use of active electrodes is preferred due to their practicality. When using the passive electrodes in EEG, a preparation stage is needed in which the electrodes have to be covered with a conductive gel. This is a time consuming procedure especially when the number of the electrodes is high. Moreover, the conductive paste usually dries out after 2-3 hours of use and additional pasting is needed in order to continue to EEG recording. Active electrodes eliminate the need for pasting and thus can be used for the measurements much longer than the passive ones.

As EEG signals are very low amplitude signals, they are more prone to noise. Also, for the passive electrodes, it is difficult to match the contact impedance between the scalp and the electrode leads for all channels. This results in the amplification of the displacement currents in the preamplifier stage [83]. The active electrodes are usually used as voltage follower devices to improve the signal strength at the scalp by increasing the current driving capability of the signal. There are also studies on the design of active electrodes with gain. However, it is difficult to overcome the problem of DC offsets in EEG. Therefore, in this study, it is preferred to use active electrodes as simple voltage buffering elements. Additionally, a first order high pass filter with a low cutoff frequency is used to remove the DC component in the signal in order not to saturate the preamplifier. Figure 6-1 shows the simulations on frequency characteristics of the designed active electrodes.

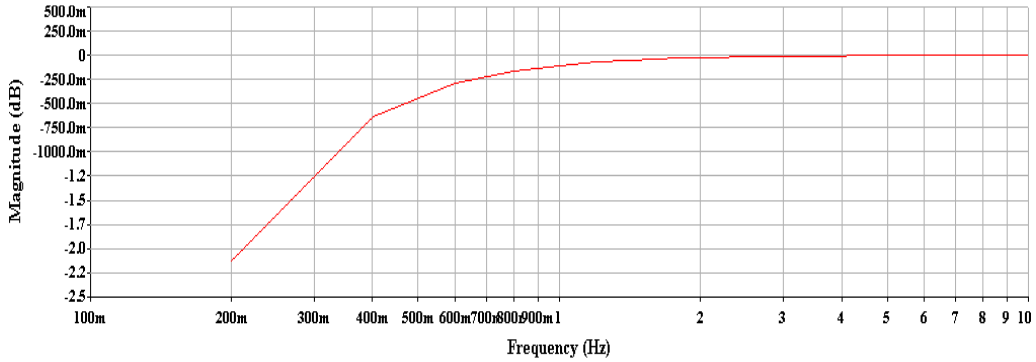

(a)

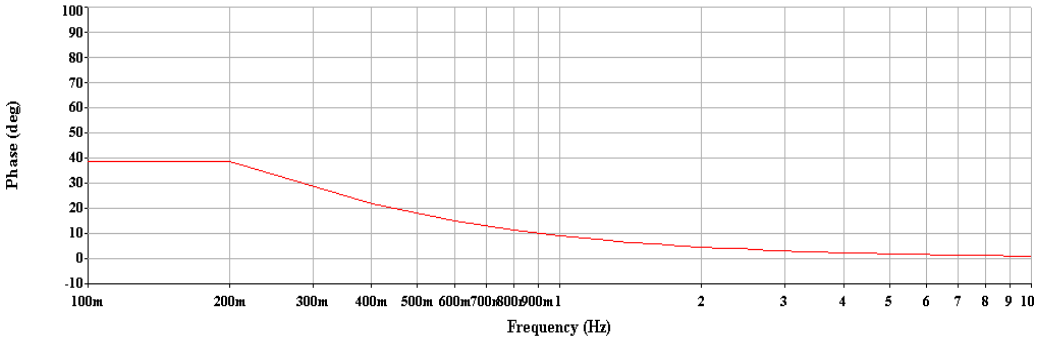

(b)

Figure 6-1 : Frequency characteristics of the designed active electrodes. a) Magnitude response (in dB), b) Phase response (in degrees)

6.3.2 Preamplifier

Since the amplitude of the signal to be measured is considerably low, special type of amplifiers are preferred in EEG systems. These are called instrumentation amplifiers (IA) and have a high common mode rejection ratio (CMRR) property in their design, providing a less noise affected signal in the amplification. There are usually two stages in the structure of IA. The first stage is the buffering stage where the signal is electrically isolated from the signal source and common mode voltage is reduced. In the second stage, there exists a difference amplifier in which the difference between two isolated signals is amplified [83].

Since instrumentation amplifier includes at least three operational amplifiers (op-amp) in its design, it occupies a larger size compared to other components in the circuits. However, there are also commercial instrumentation amplifiers that provide all the components in an instrumentation amplifier in a single package. These packages have comparatively smaller size and provide the gain adjustment with a single external resistor.

In this design, the commercial instrumentation amplifier package, LT1167 of Linear Technologies is used at the preamplifier stage which was also employed in the design of the 256 channel EEG system in [78]. For the elimination of high frequency signals, first order low pass filters are added to the inputs. Moreover, a high pass filter is used for AC coupling at the output of the amplifier.

6.3.3 Active Filters

Noise is the major problem in biopotential measurement devices. Especially, the noise caused by the power network affects these devices by imposing a common mode signal on the inputs of the amplifier blocks. Therefore, the need for filter use is inevitable in these systems.

In BCI applications, the algorithms use the frequency band between 0.1Hz and 45Hz. Signals out of this range should be removed by including either analog or digital filters in the design. Also, application of filters can solve possible aliasing problems in digitizing circuitry. Therefore, in this design, two active filters are used in the EEG amplifier circuitry: the first one is a band-stop filter to remove the effect of noise caused by the mains supply and the second one is a third order low pass Bessel filter with cutoff frequency 40Hz. The choice of Bessel filter is due to the flat group delay response in the pass band. The magnitude and phase response plots of these filters are given Figure 6-2 and Figure 6-3.

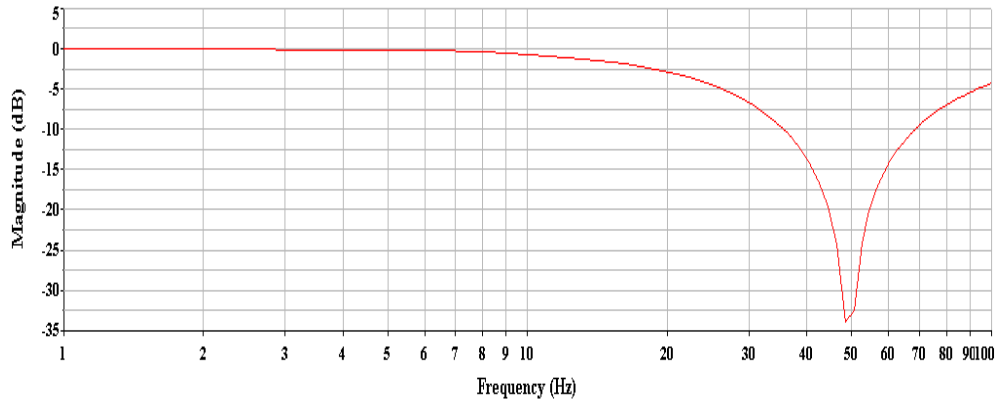

(a)

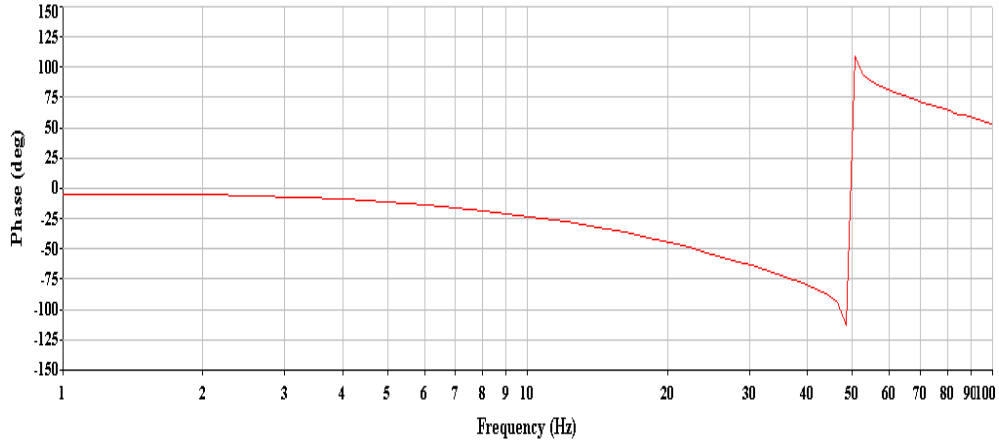

(b)

Figure 6-2 : Frequency characteristics of the employed active 50Hz band-stop filter. a) Magnitude response (in dB), b) Phase response (in degrees)

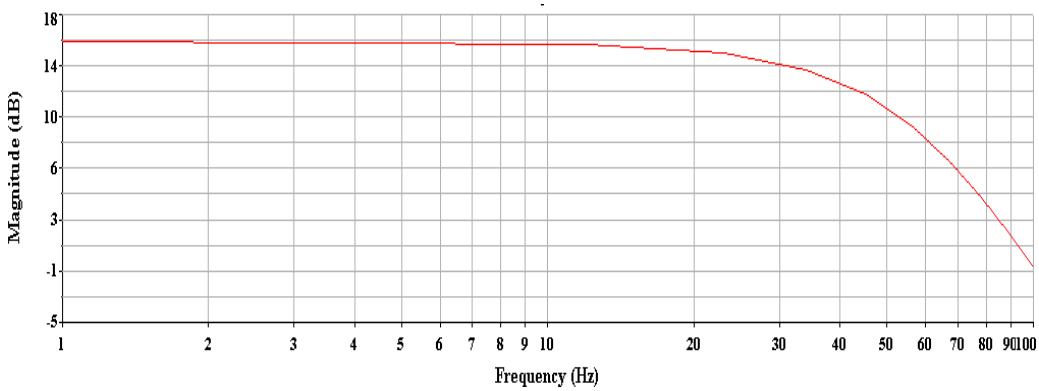

(a)

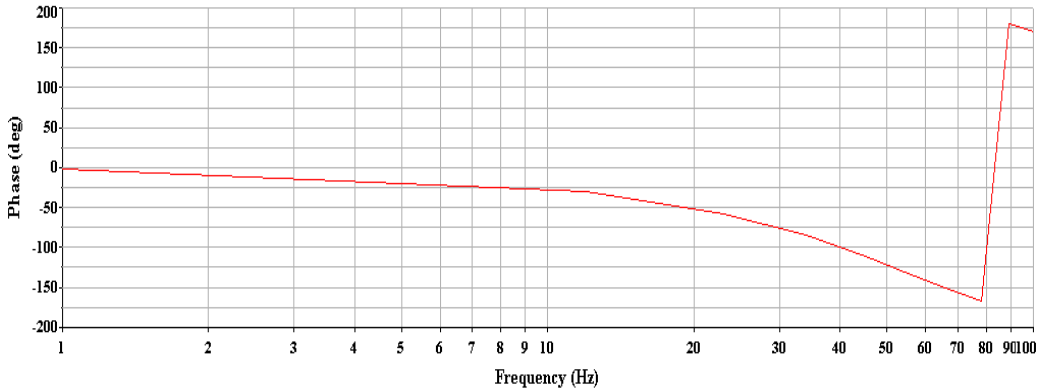

(b)

Figure 6-3 : Frequency characteristics of the designed 3rd order active 40Hz low-pass filter. a) Magnitude response (in dB), b) Phase response (in degrees)

6.4 Digital Hardware

In order to perform digital signal processing, the amplified EEG signals should be discretized and transmitted to a computer. Usually, the digitization of the signal is done via commercial analog to digital converters (ADC's) or using data acquisition cards which are more expensive than the ADC's. When ADC is used in the design, a microcontroller is needed for transferring the digitized signal to the computer. The transfer can be done either with serial or parallel communication depending on the hardware the microcontroller and computer both support.

For today's computers, Universal Serial Bus (USB) is the most common and maybe the only communication platform due to its speed in transfer. And with the development in technology, low cost microcontrollers with USB hardware are available in the market which makes it easy to implement a USB communication with the computer.

As stated in the introduction section in this chapter, it is aimed to design the EEG hardware as minimum number of components as possible. Therefore, the digital hardware is composed of PIC18F4553, a compact microcontroller with a high ADC resolution and Full Speed (FS) USB hardware [79]. The hardware schematics of the digital circuitry can be found in Appendix B.

6.5 Isolation

Isolation in medical systems is necessary for two reasons. The most important one is that the electrical equipment can harm the subject when the isolation is poor. Possible leakage currents can flow through subject's body which can lead to permanent disorders or even to deaths. In order to protect the subject from these problems, subject has to be electrically isolated from the environment properly. This can be performed by using isolated supplies like batteries or isolation transformers for the analog amplifier which can decrease the risk of electrical shock [83]. Moreover, the amplifier circuitry should be isolated from digital the circuitry and the recording system due to possible reverse currents coming from the computer side which can also harm the subject. In this design, standard batteries are used in the analog circuitry for providing the supply isolation.

Isolation is also important for removing the effects of the noise caused by power network, electrical equipments and high speed electronic devices like computers. So, the analog and digital circuits should be electrically separated from those devices by employing proper signal isolation in the system. Moreover, the ADC's used in these systems are usually affected from the signal oscillations in the

analog circuitry. This is mainly caused by the ground nodes the analog and digital circuits are referenced and when they are implemented as the same node, the ADC's usually can not convert the signals accurately. Therefore, the analog and digital grounds should also be isolated.

The signal isolation can be done with galvanic isolators, analog and digital optocouplers, transformers or the isolation amplifiers in the circuit. In this design, the amplified EEG signals are isolated from the digital circuitry with analog optocouplers [80]. The reason for using optocouplers is that they occupy less space in the circuit and cost less as compared with other isolator types. Moreover, as the microcontroller used in this design has built-in USB device hardware, the isolation can not be done digitally. Therefore, the analog optocoupling is preferred and this provides an advantage of ground isolation between the analog and digital circuits which results in better digitization of the signal at the ADC stage.

6.6 EEG Cap Design

In commercial EEG systems, the electrodes are placed on an elastic head cap according to the 10-20 electrode placement system [41], [43]. These caps are suitable only for passive ring electrodes in which the electrodes are covered with a conductive gel. Figure 6-5 shows a commercial EEG cap produced by Neuroscan.

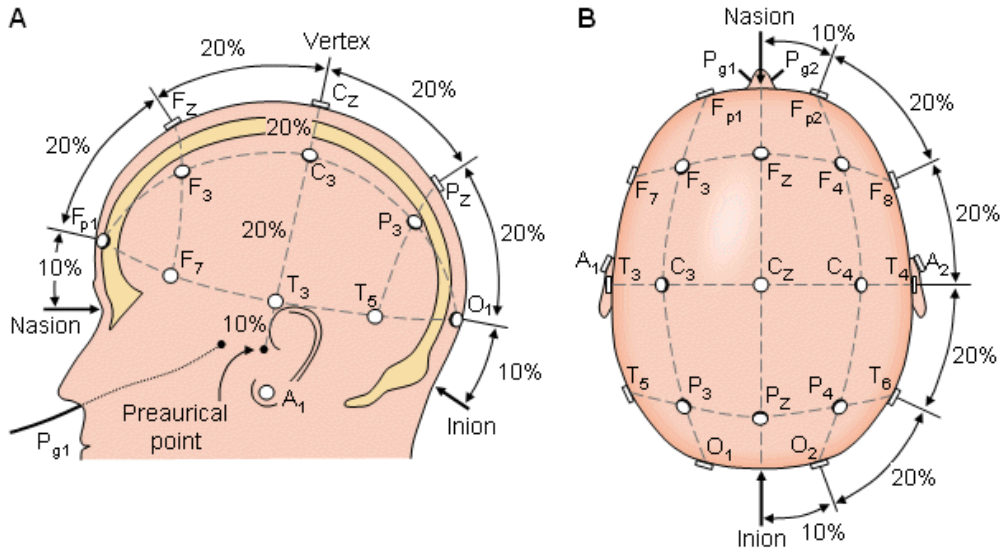

Figure 6-4 : International 10 – 20 Electrode Placement System. The naming comes from the percentage ratio of the distance between two consecutive electrodes according to the distance between Inion and Nasion points of the human scalp [41].

Figure 6-5: 19 Channel EEG cap produced by Compumedics Neuroscan [81].

However, when active electrodes are to be used in the system, the electrodes may not be easily attached to the scalp due to their size and weight of the material in the electrodes. For this reason, a cap design is performed for active electrodes in which the placement of the electrodes is easy and the effect of common mode noise is theoretically reduced (Figure 6-6).

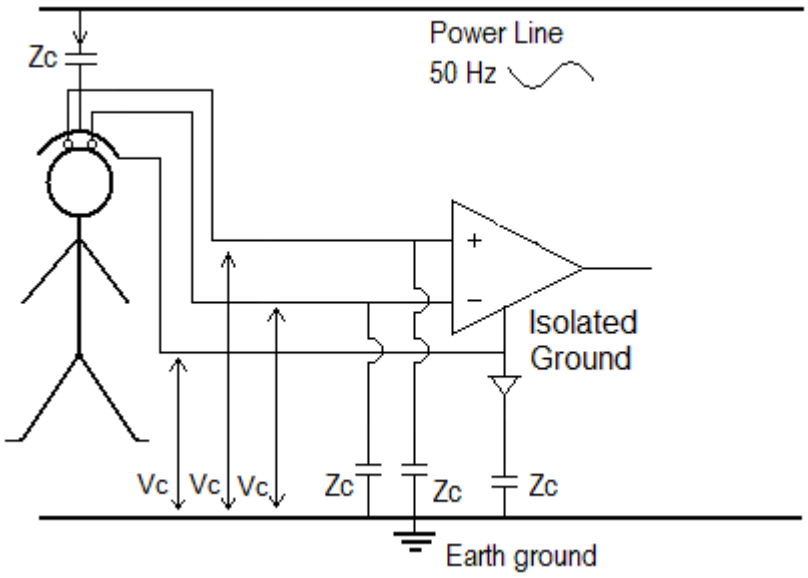

Figure 6-6 : The effect of the designed EEG cap on reducing the common mode voltage induced on the body. The common mode voltage with respect to the amplifier ground is decreased as the distance between the amplifier ground and the electrode leads is small. Furthermore, the leakage currents are more likely to flow through the cap instead of the body with this configuration.

The designed EEG cap in Figure 6-7 is composed of three layers. The outer layer is a Teflon material for holding and fixing the active electrodes on the scalp. In the middle layer, there is a thin aluminum film which is used for a conductive path to the analog ground. This film acts as a protective layer for the displacement currents which can generate a common mode voltage in the preamplifier stage. The inner layer is a soft tissue made up of Styrofoam which provides a soft contact between the cap and the subject. 10 active electrodes are located on the

cap according to 10-20 electrode placement system [41],[43] as shown in Figure 6-7.

(a)

(b)

Figure 6-7 : Pictures of the designed EEG cap. The active electrodes can easily be placed onto the scalp of the subject.

6.7 Experiment Controller and EEG Interface Design

Monitoring and recording of the EEG signals are performed by a computer program which acts usually as the main controller in these systems. Therefore, in the last part of the EEG design, the computer program of the system will be explained.

The system flowchart of the computer software is given in Figure 6-8. It is composed of several small software blocks that control the EEG signal acquisition, recording, monitoring and experimenting BCI applications.

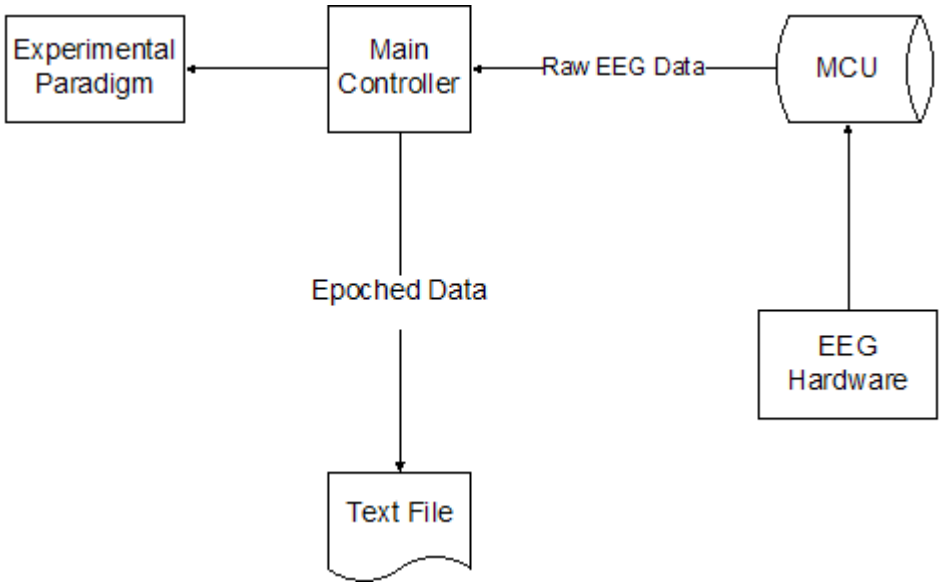

Figure 6-8: The flowchart of the controller software. MCU stands for the microcontroller unit which is the PIC18F4553 device [79].

These operations are managed in separate threads in order not to interfere with each other and affect the flow of the overall system. The threads are created by using multimedia timers which provide the highest resolution (1ms) for event scheduling in programs. Being available in most of the computers, multimedia timers can be managed in all Windows based operating systems. As it provides a high resolution and priority for timing, the sampling of the analog EEG signals,

monitoring and recording of the data and the intensification timing in spelling paradigm are all done with the multimedia timer instances.

The program is prepared in Visual Studio .NET 2005 which provides a useful framework for computer applications based on object oriented programming (OOP). It is controlled with a friendly graphical user interface allowing the EEG operator to manage the EEG sessions easily.

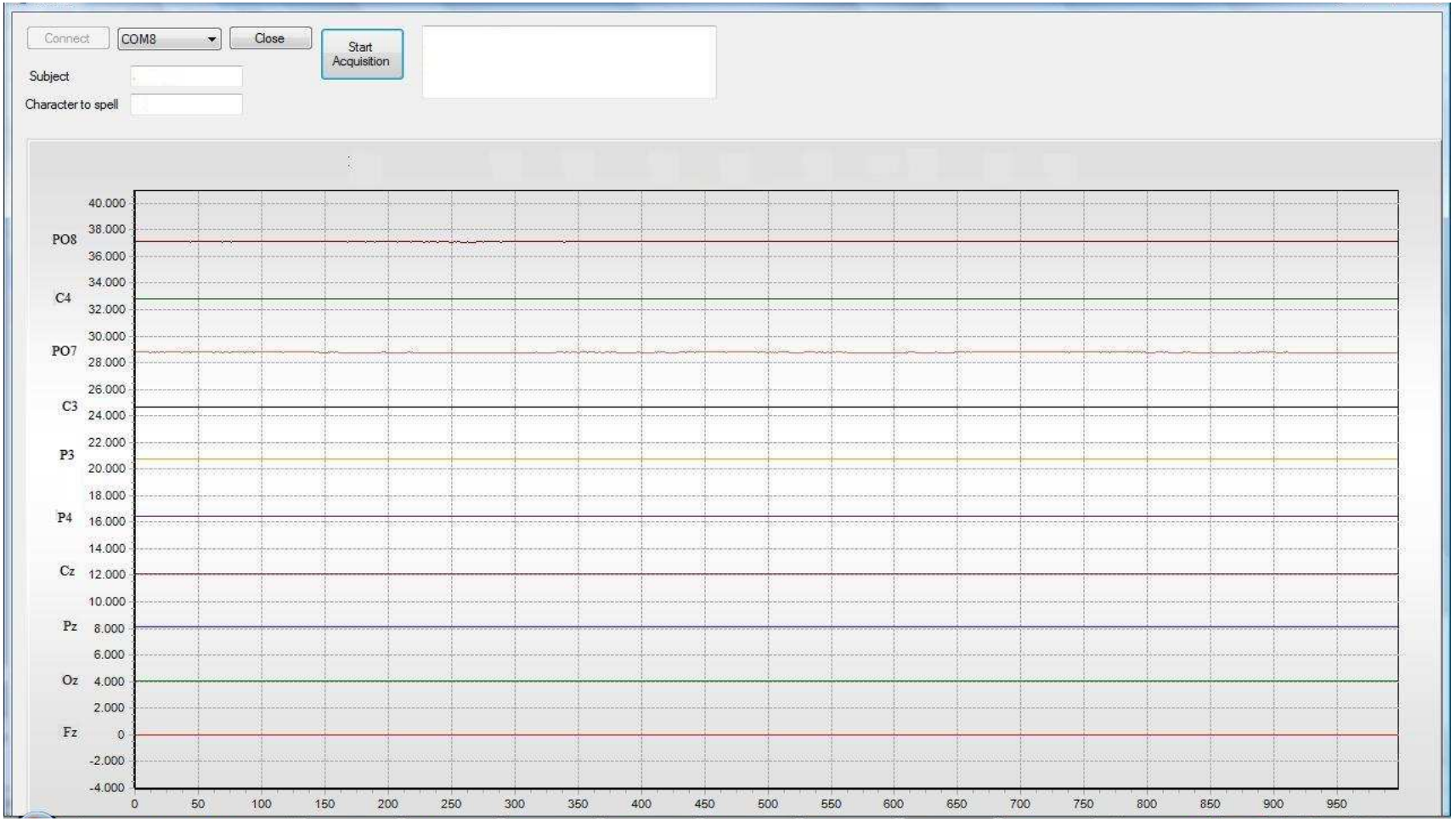

Figure 6-9 : Signal monitoring interface of the designed system. It is operated with the P300 Speller user interface.

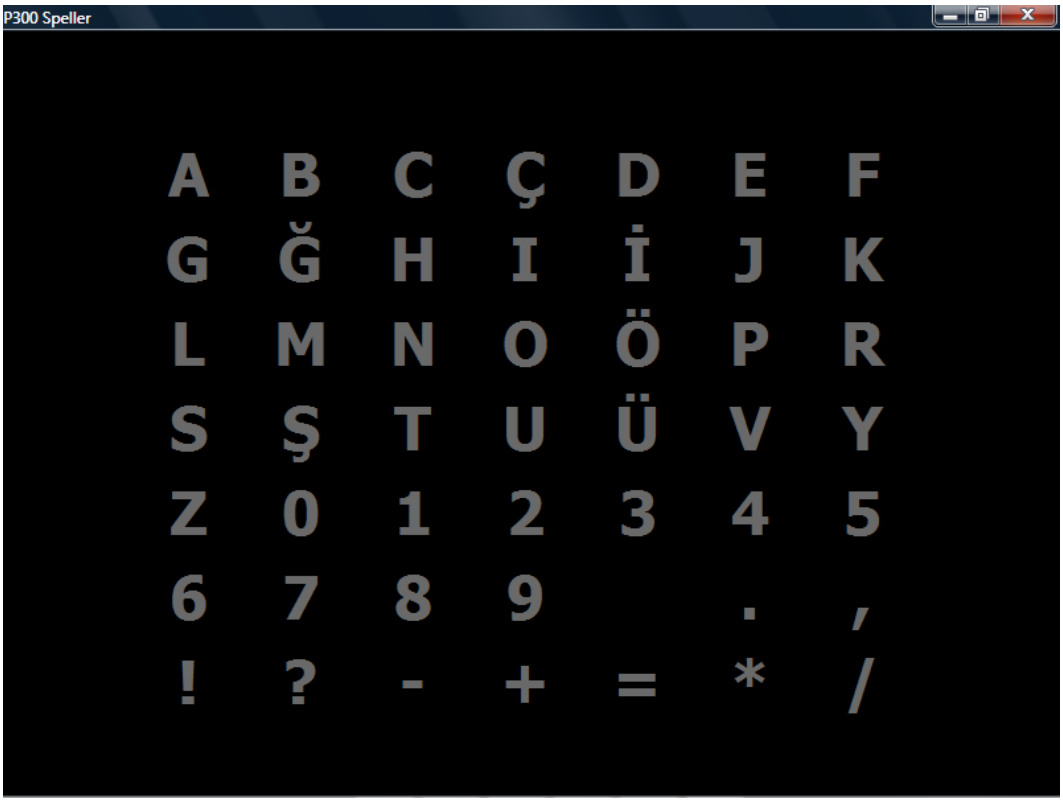

Figure 6-10 : Graphical user interface prepared for the P300 Speller.

CHAPTER 7

RESULTS

As stated in the introduction chapter, the Spelling Application is investigated in several aspects which can mainly be summarized as the application type of classification methods [77] (the analysis of classification performance by separating the observations of row and column intensifications), the comparison of Wiener filtering with standard filtering techniques and the effect of probability estimation method by application of Maximum Likelihood Estimation in the prediction mechanism of the target character. These aspects will be addressed in this result chapter by performing the analysis case by case on several Spelling Paradigm datasets.

In this study, the methodologies are tested on one of the BCI competition datasets (the P300 Speller dataset of BCI Contest II [18]). An experimental dataset is obtained for the spelling application at Dokuz Eylül University, in a shielded EEG laboratory environment. Furthermore, a successful experimentation is performed with the designed hardware at the Brain Research Laboratory of Electrical and Electronics Department of Middle East Technical University. The results of the presented methods will be provided after giving a brief explanation of each dataset.

7.1 Results on the BCI Competition II: Dataset IIb

The P300 Speller datasets for BCI Competition II and III are provided by Wadsworth BCI [14], in which the measurements are obtained with the BCI2000 system [15]. The datasets are publicly available at [18] and [20]. Here in this thesis, only the results for the dataset of BCI Competition II [18] are presented since the implemented methodologies could not be properly integrated to the dataset of BCI Competition III due to the size of the provided dataset in this contest and memory requirements of the employed methodologies.

In these experiments, the spelling matrix consists of 36 characters which are distributed on 6 rows and 6 columns of the matrix (Figure 3-1). The intensification procedure for each spelled character is performed by flashing a row or column for 100ms and after that showing a blank screen (no intensified rows and columns) for 75ms. Therefore, a single intensification lasts for 175ms (5.7Hz) and as there are 6 row and 6 column intensifications, one trial of intensification is completed after 2.1 seconds (175ms x 12 intensifications). After each trial, a blank screen is presented for 2.5 seconds to inform the subject that the trial is completed and the next trial is coming up. The intensification procedure is repeated for 15 trials so that the whole procedure takes nearly 69 seconds to complete the spelling session of a single character ((2.1s of trial duration+ 2.5s blank screen time) x 15 trials).

In both datasets, the EEG signals are digitized at a sampling rate of 240Hz and in the dataset of BCI contest III only, the signals are band-pass filtered by hardware with cut-off frequencies 0.1Hz and 60Hz. The information provided in these datasets consists of the raw EEG data measured from 64 channels (Figure 7-1), the codes of the intensification (Figure 7-2) and the target characters that are spelled during those sessions.

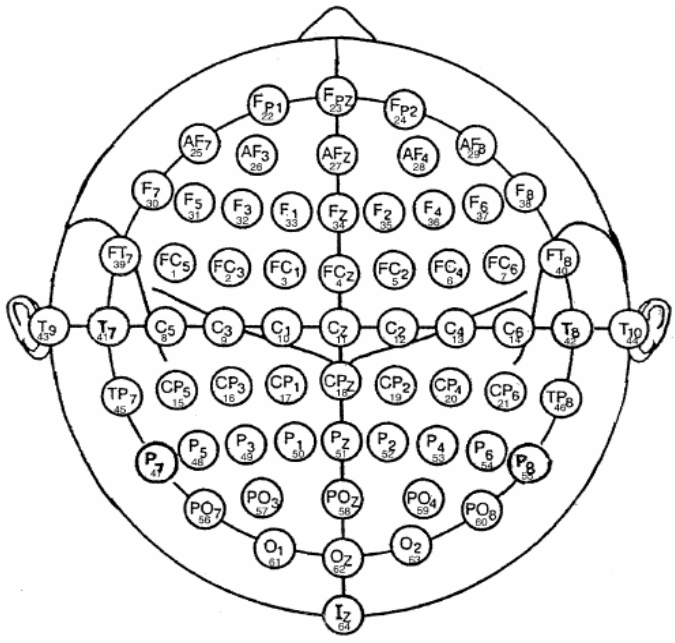

Figure 7-1 : The EEG channels used in the measurements in P300 Speller datasets of [18] and [20].

Figure 7-2 : Epoch information in [18] and [20]. The row and column intensifications are epoched with the ongoing EEG during the paradigm according to the demonstrated encoding scheme.

The P300 Speller dataset of BCI Contest II [18] includes three spelling sessions from one subject; two for training and one for testing the algorithms prepared for this problem. Each session is composed of several runs in which the 3-5 letter words are spelled[4]. The contents of these sessions are provided in Table 7-1 and Table 7-2.

Table 7-1: Contents of the Training Sessions in Spelling Paradigm Dataset of BCI Contest II

	Session 1					**Session 2**					
Runs	**1**	**2**	**3**	**4**	**5**	**1**	**2**	**3**	**4**	**5**	**6**
Words	CAT	DOG	FISH	WATER	BOWL	HAT	HAT	GLOVE	SHOES	FISH	RAT

Table 7-2: Contents of the Test Session in Spelling Paradigm Dataset of BCI Contest II

	Session 3							
Runs	**1**	**2**	**3**	**4**	**5**	**6**	**7**	**8**
Words	FOOD	MOOT	HAM	PIE	CAKE	TUNA	ZYGOT	4567

As stated in chapter 3, the basis of this study relies on the success of the algorithm proposed by Kaper *et al* [4]. In their work, they have employed Support Vector Machines (SVM) [77] with a feature set configuration consisting of 10 EEG channels (Figure 7-3 (a)). Moreover, commercial P300 Speller systems employ even less number of electrode configuration in their methods [42] (Figure 7-3 (b)). Therefore, in this thesis, after the presentation of each stimulus, the EEG time segments of 600ms duration from the channels in Figure 7-3 (a) are extracted. As in [4], a long feature vector consisting of 1440 elements (600ms x 240Hz x 10 channels / 1000) is constructed to compare the methodologies presented. Since it is only possible to perform offline analysis on the dataset, the

[4] The data of the 6th run of Session 2 is somehow corrupted; it contains some bugs related to the recording process. Therefore, it is excluded in forming the classification model and hence in providing the results here.

results here will be provided with cross-validation accuracy on the training set and prediction accuracy on both training and test sets.

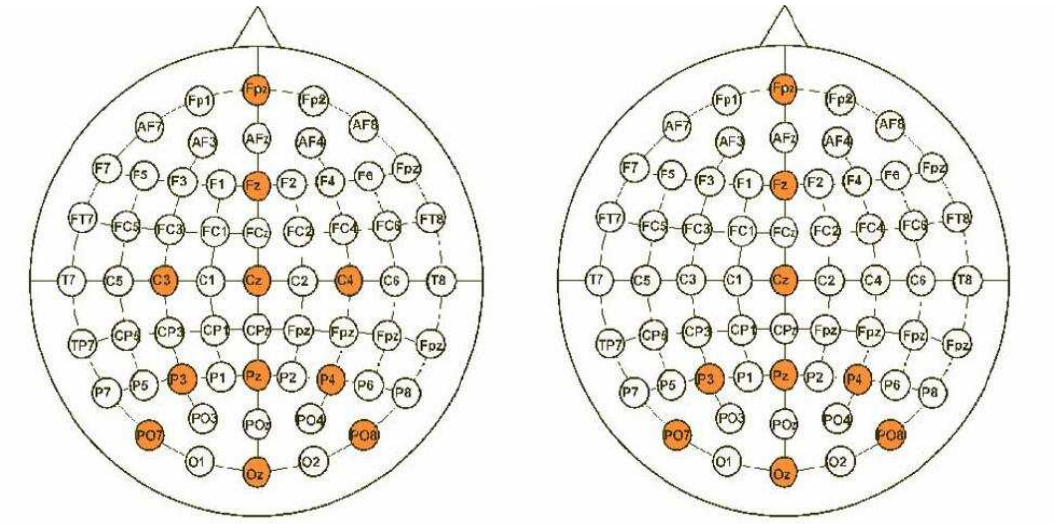

(a) (b)

Figure 7-3: The electrode configurations used in existing P300 Speller Systems [42].

7.1.1 Separation of Row and Column Intensifications

In Kaper's study [4], using a single SVM classifier, the classification results for the test set in Table 7-2 are reported as 100% accuracy for all characters after 5 repetitions. Here, the same methodology is applied but in this case also the responses to row and column intensifications are treated separately. As the method of band-pass filtering has not been given in [4], a Butterworth filter of order 10 with cutoff frequencies 0.5Hz and 30Hz is applied to produce the results. The results for the 5 – fold cross validation values on the training set is given in Table 7-3 (C=20.007, σ = 27.359 for all).

Table 7-3: The 5 - fold Cross Validation Values on the Training Set

No Row and Column Separation (reported by Kaper)	84.5%	
No Row and Column Separation (observed)	78.1197%	
With Row and Column Separation	Rows	74.7009%
	Columns	82.6496%

The difference between the observed and reported values on cross validation ratios might arise from several factors. As there are 1:5 ratio on the number of target and non-target observations, one should perform a selection from the non-target observations to train the classifier so that the number of samples from each class is the same. Otherwise, the classifier would naturally decide that all new coming samples belong to the class with highest probability of occurrence (which is the non-target class). Therefore, the group selected to train the classifier may not be the same as in [4], as the selection procedure is random. However, in order to preserve the consistency in presenting the results here, the selected training group is fixed for all simulations of the methodologies in each investigated dataset.

Another factor possibly affecting the difference in cross-validation results might be the application of normalization. Kaper implemented simple scaling (explained in section 5.3.4) on the filtered observations, that is, the samples are scaled to the interval of [-1,1]. However, this normalization may lead to improper adjustment of the data for our case. The reason is that, the non-target signals, in general, have lower amplitude as compared to the target signals. When simple scaling is applied, it is highly probable that a non-target signal resembles to a target one. Therefore, in this study, Gaussian normalization is preferred as it preserves the shape of the observed signals better. Furthermore, it is also applied in the method of Rakotomamonjy [6] in which the data is normalized according to the statistical properties of the observations.

As stated at the beginning of this section, the filter type has not been explained clearly in [4]. The difference in the cross-validation values might also be caused by this reasoning. Rakotomamonjy [6] applied an 8th order band-pass Chebyshev Type 1 filter with cutoff frequencies 0.1Hz and 10Hz in their study for BCI contest III. Both of these filter types are compared with the proposed Wiener filtering in the following sections.

The 5-fold cross-validation values in Table 7-3 indicate that the rows and column observation groups may not always be classified with the same accuracy. The reason for this might be that the subject may exhibit different responses to row and column intensifications. As the subject's perception to row and column flashings may differ, they should be treated and trained in separate classifiers to increase the level of commonness and homogeneity in the training model. Therefore, the 5-fold cross-validation is performed on row and column groups independently and optimum parameters (the regularization parameter C in SVM and the variance parameter σ in Gaussian RBF) providing the maximum cross validation ratio are found (76.9231% for rows and 84.2735% for columns) for each of them as $C_r = 100$, $\sigma_r = 120$ and $C_c = 40$, $\sigma_c = 60$ (see Table 7-4 below for the comparison).

7.1.2 The Effect of Wiener Filtering

As discussed in chapter 3, the optimum frequency bands for P300 speller are determined by estimating a Wiener filter for all EEG channels of interest. The Wiener filters are produced by estimating a 10th order linear phase FIR implementation for the frequencies found by the analysis of the spectral powers.

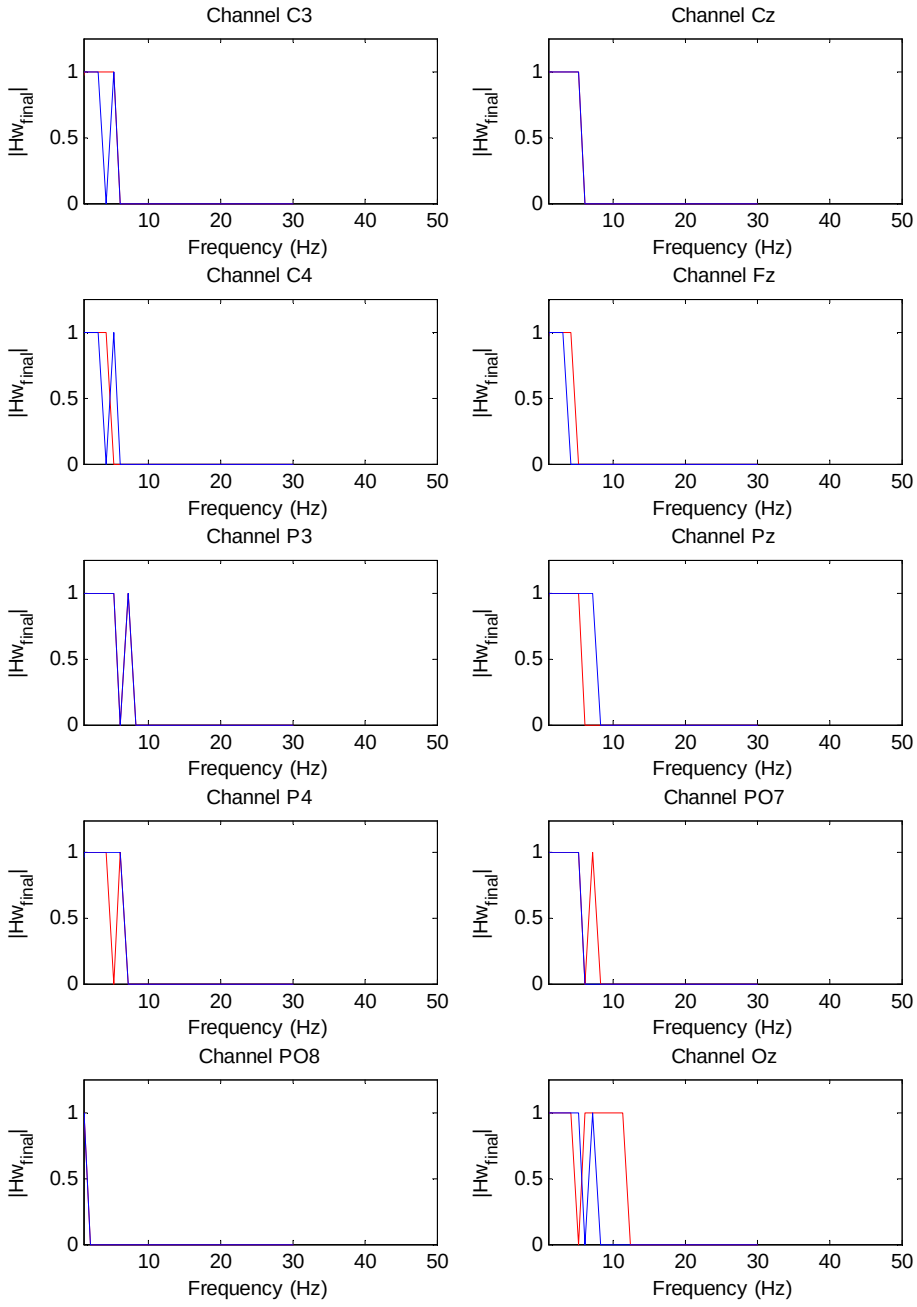

Figure 7-4 : Estimated Wiener filters for the predetermined 10 EEG channels. Wiener filter estimates are shown in red and blue for the row and column groups, respectively. In some channels the filter estimates for both groups overlap (Cz, P3 and PO8).

As one can observe from Figure 7-4, the frequency band for the target signals actually covers a narrower range for this dataset. When the classifier is trained with the same parameters (Table 7-4) on the training set, the 5-fold cross validation values have increased on both row and column groups.

Table 7-4: Maximum 5 - fold cross - validation values found on the training set

$C_r = 100$, $\sigma_r = 120$ $C_c = 40$, $\sigma_c = 60$	Rows	Columns
10^{th} order Butterworth - 0.5Hz-30Hz filtered training set	76.9231%	84.2735%
10^{th} order Wiener filtered training set	77.9487%	86.5812%

The target character prediction accuracy results of Wiener and Butterworth preprocessing on the training and test sets are presented in Figure 7-5 and Figure 7-6.

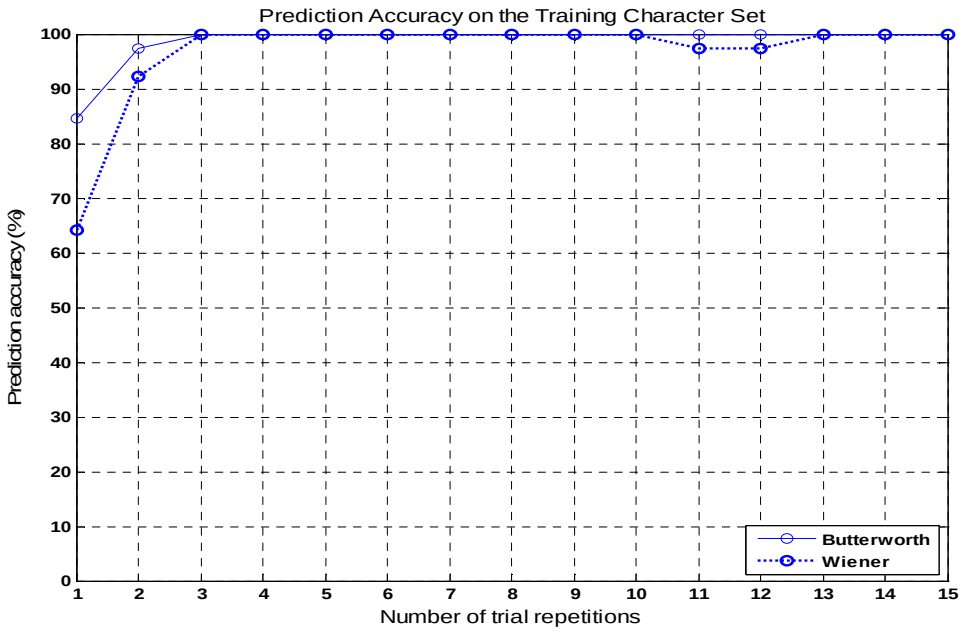

Figure 7-5: Prediction accuracy of the target characters on the training set (39 characters). Solid: preprocessed with 10th order Butterworth filter. Dotted: preprocessed with 10th order FIR Wiener filter.

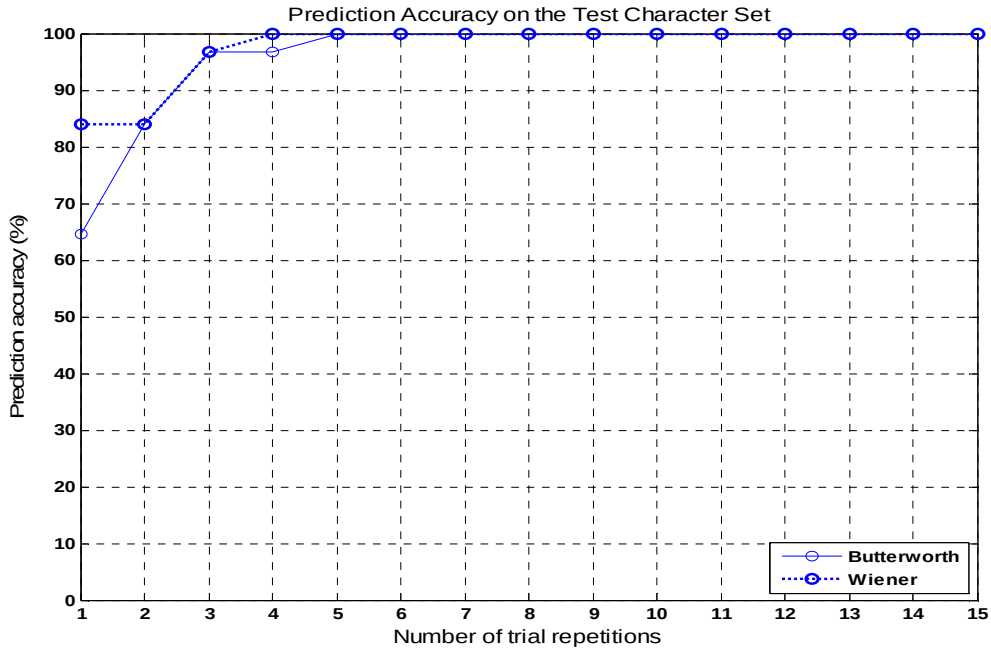

Figure 7-6: Prediction accuracy of the target characters on the test set (31 characters). Solid: preprocessed with 10th order Butterworth filter. Dotted: preprocessed with 10th order FIR Wiener filter.

From Figure 7-6, it is clear that preprocessing with Wiener filtering has better classification performance on the test set as compared to Butterworth filtering. Even using 2 trials of repetitions, prediction with Wiener filtering is over 80% for 31 characters. Furthermore, according to Kaper's results, the accuracy of prediction is below 80% within 2 repetitions and equal to 100% only after 5 trials (Figure 7-7). Filtering with Wiener approach has increased the prediction accuracy to 100% with only 4 trial repetitions.

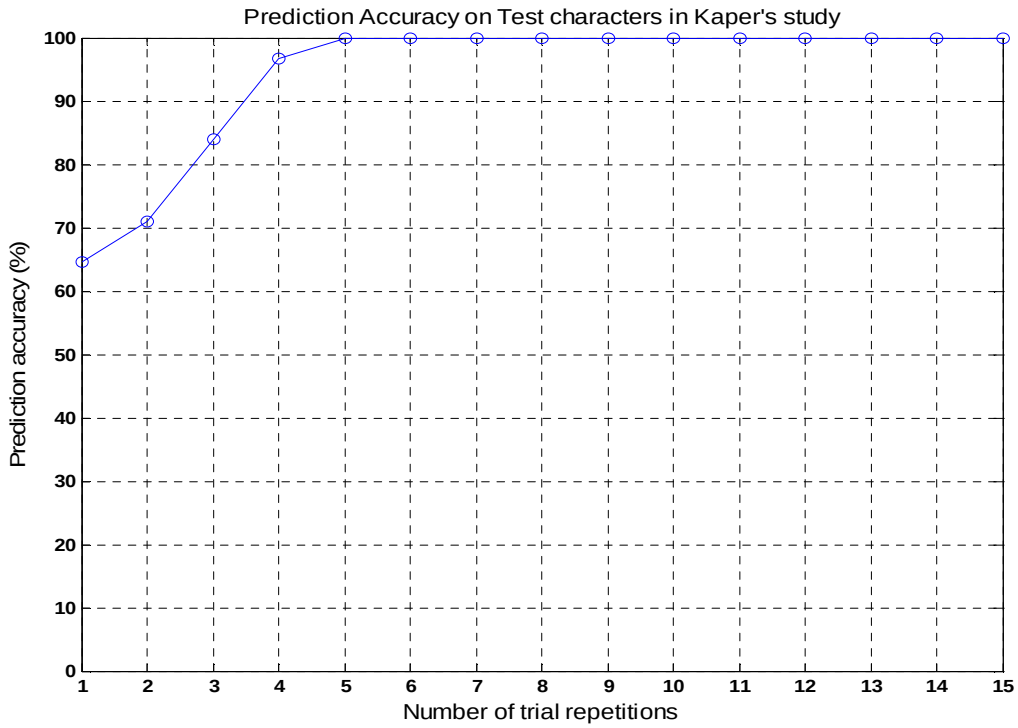

Figure 7-7 : Target character prediction accuracy on the test set reported by Kaper [4].

7.1.3 Prediction with MLE of SVM outputs

One can note from Figure 7-5 that the prediction accuracy with Wiener filtering on the training set shows some inconsistency with the increasing number of trial repetitions; between 10th and 13th repetitions, a single character is false

predicted. This is a common error in the prediction mechanism which could also happen in the Butterworth case. The reason is that the results here are presented with the common P300 Speller methodology of scoring the output of the SVM classifier [4] (see section 5.4.2). In this technique, the SVM output giving the maximum value among the 6 samples in a trial can be considered as from the target class even if it is predicted as a non-target observation by SVM. Therefore, if one also uses the information provided by SVM (the samples predicted as target by SVM), the class-conditional density of target prediction is better estimated (explained in section 5.4.2). This prediction approach provides a threshold mechanism which prevents the persistent classification of the target character in a real world application case. The results on the training and test sets with ML prediction of the SVM outputs are given in Figure 7-8 and Figure 7-9.

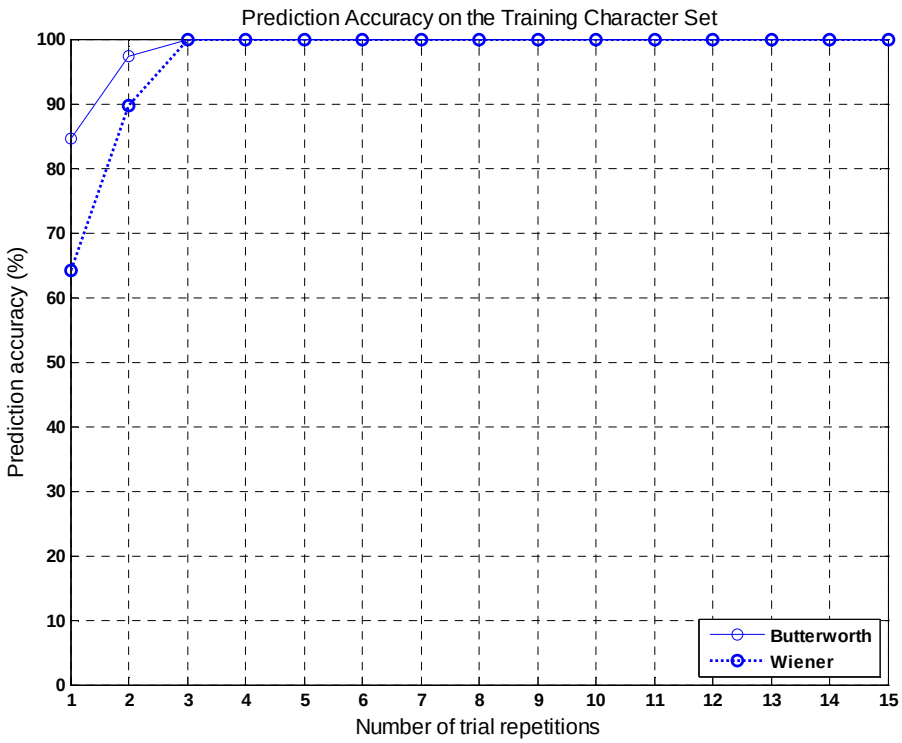

Figure 7-8 : Prediction accuracy of realistic MLE of SVM outputs on the training set (39 characters). Solid: preprocessed with 10th order Butterworth filter. Dotted: preprocessed with 10th order FIR Wiener filter.

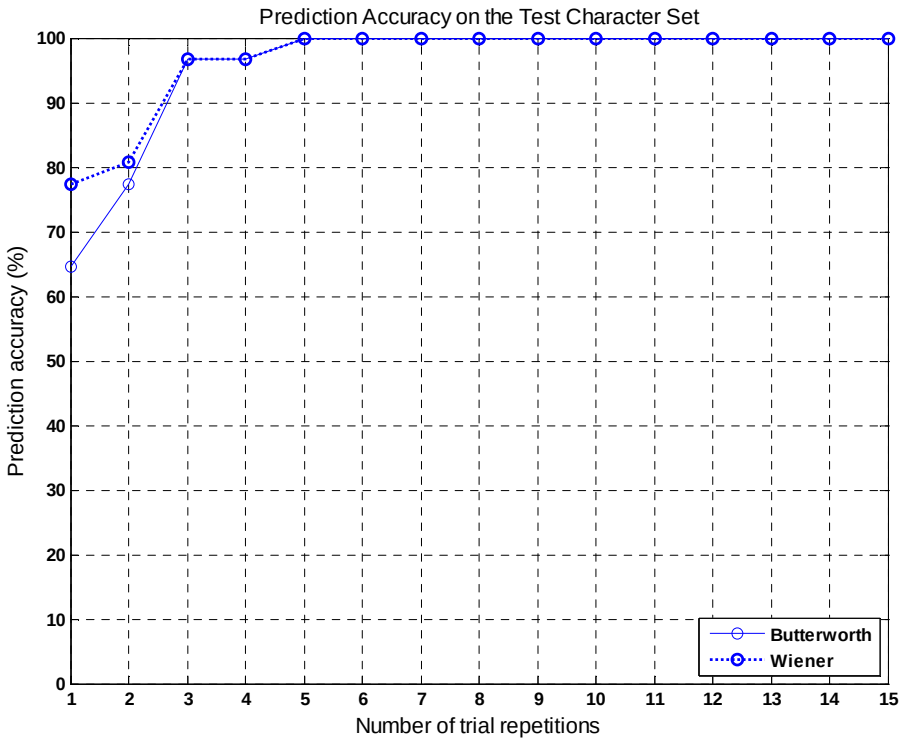

Figure 7-9 : Prediction accuracy of realistic MLE of SVM outputs on the test set (31 characters). Solid: preprocessed with 10th order Butterworth filter. Dotted: preprocessed with 10th order FIR Wiener filter.

In this case, the results for both filter types became nearly similar. However, in order to prevent the false and continuous prediction in Spelling Paradigm one should include the target class output information supplied by the main classifier which is the SVM in our case. On the other hand, with these results also, Wiener filtering is more preferable as it provides higher prediction accuracy on the test set in less number of trial repetitions.

7.2 Results on Experimental Datasets

7.2.1 P300 Speller Experiment at 9 Eylül University

In order to obtain a practical dataset for this study, first, the experimental setup of the P300 speller has been implemented and realized in the shielded EEG rooms of Brain Dynamic Research Laboratories of 9 Eylül University.

Figure 7-10 : Pictures from the P300 Speller experiment at 9 Eylül University

The instrument used to measure the electrical activity of the brain is a 64 channel EEG device of Neuroscan Systems which provides 1 kHz sampling of EEG signals with active noise cancellation. The intensification algorithms for the Spelling Paradigm experimental interface are integrated with the epoching mechanism of the EEG system.

The experiment is performed on a healthy subject of age 24 (Figure 7-10) who did not have any experience on evoked potential experiments. She is asked to stay relaxed on a comfortable chair in front of a monitor on which the 6x6 spelling matrix is presented. All operations are managed within the control room and in case of a fatigue or any other problems related to the subject, she is monitored on one of the screens in the control room.

In this experiment, the spelling application is performed for 35 characters in one session which lasted about 2 hours. The procedure for spelling each character is explained as follows:

- The subject is asked to focus on the predetermined characters on the 6x6 spelling matrix which are explained to the subject outside of the shielded room via microphone. She is supposed to realize and silently count the number of target row and column intensifications.
- As in the case of BCI Competition datasets, 15 trial repetitions are used in spelling each character. For each trial, the intensifications are block randomized for 6 rows and 6 columns.
- Since the subject had no experience on Spelling Paradigm, in order to provide easy realization of the intensifications, the flashing duration is set to 270ms (170ms on, 100ms off). The blank period between the trials is kept at 2.5 seconds.

The characters spelled during the experiment are given in Table 7-5. The first 15 characters are used to construct the classification model and the remaining 20 characters are reserved for offline prediction.

Table 7-5: The characters spelled in the experimentation performed at 9 Eylül University

	Training Set (15 characters)	Test Set (20 characters)
Spelled words	HECE BALKAR UGRAS	BERNA URUN EKIM DEVRIM 7

As stated at the beginning of this section, the sampling rate of the recording EEG system is 1 kHz which is nearly 4 times higher than that of the BCI contest datasets. This results in a much longer feature vector, some of which, in fact, may be redundant for classifying the target responses. Regarding the presented results on the dataset of BCI Competitions II, the optimal frequency bands for detecting the P300 responses lie mainly below 20Hz. Therefore, it is also possible to apply downsampling to the EEG signals which is also employed in [6]. By this way, the construction of the Wiener filter and SVM classification model will be much faster as the computational power decreases with less number of feature samples. Here, the results will be presented on downsampled data while investigating the effects of Wiener and other filtering methodologies.

For the first case where the data is downsampled to 100Hz by taking the average of blocks of consecutive 10 samples, the vector of interest is constructed with 600 ms long EEG segments from the predetermined 10 channels in Figure 7-3. Therefore, the input space consists of 600 elements (600ms x 100Hz / 1000Hz x 10 channels). The Wiener filters estimated from the downsampled raw EEG data for each channel are shown in Figure 7-11.

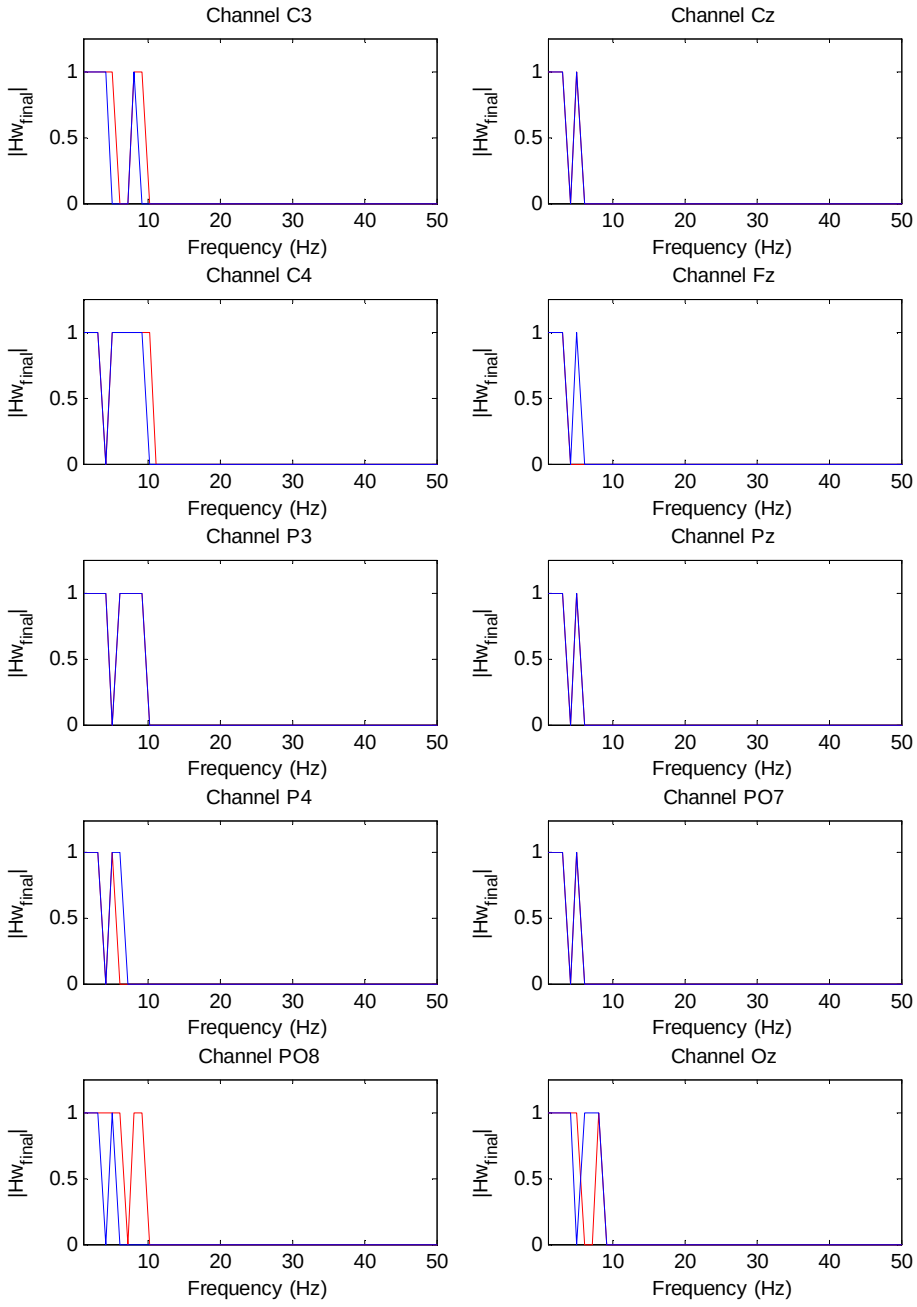

Figure 7-11 : Estimated Wiener filters for the predetermined 10 EEG channels (using downsampled raw EEG data). The estimates are shown in red for row, and blue for the column groups.

The results for 5-fold cross-validation accuracy on the training set are given in Table 7-6.

Table 7-6: The 5 - fold Cross Validation Values of SVM on the Training Set, preprocessed with investigated filtering techniques

$C_r = C_c = 20.007$, $\sigma_r = \sigma_c = 27.359$	Rows	Columns
10^{th} order Butterworth - 0.5Hz-30Hz	77.6786%	82.1429%
8^{th} order Butterworth - 0.5Hz-30Hz	79.2411%	84.1518%
10^{th} order Chebyshev I - 0.1Hz-10Hz	82.5893%	89.2857%
8^{th} order Chebyshev I - 0.1Hz-10Hz	85.0446%	87.0536%
Estimated Wiener filter	84.8214%	87.7232%

One can note from Table 7-6 that the cross-validation accuracy is higher in low frequency band-pass filtered cases which are the 10^{th} and 8^{th} order Chebychev and Wiener filters (see Figure 7-11 for the frequency range of the estimated filters). When the prediction accuracy is calculated over the training and test sets as in Figure 7-12, Figure 7-13, Figure 7-14, Figure 7-15 and Figure 7-16, Chebyshev filters are observed to be more successful than other filtering schemes.

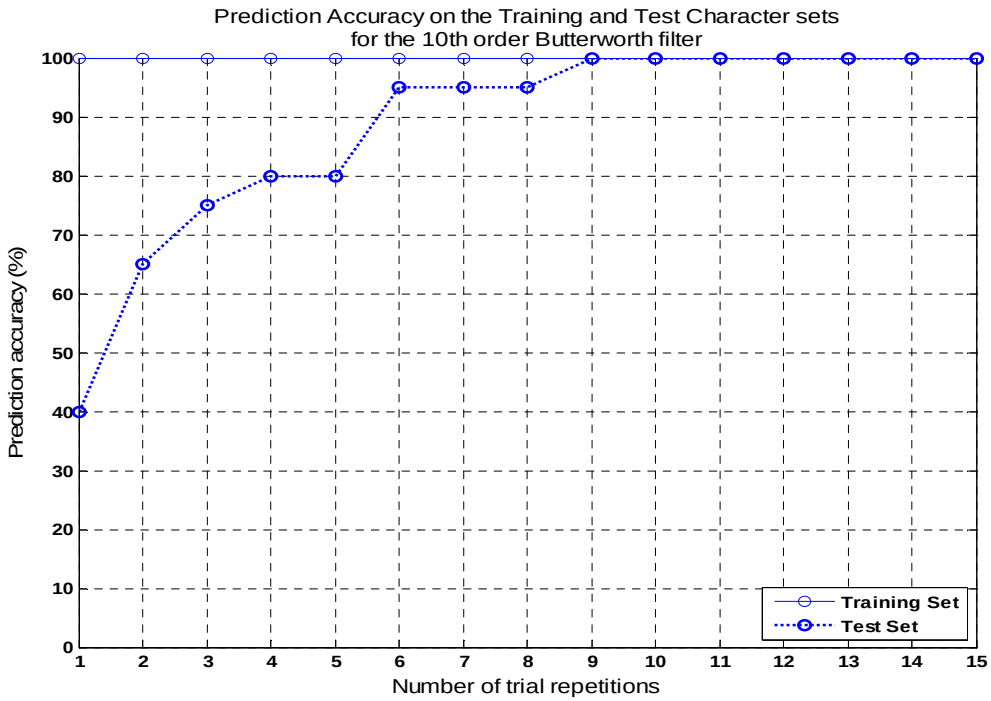

Figure 7-12 : Prediction accuracy of realistic MLE of SVM outputs. Preprocessed with 10th order Butterworth filter. Solid: training set (15 characters). Dotted: test set (20 characters)

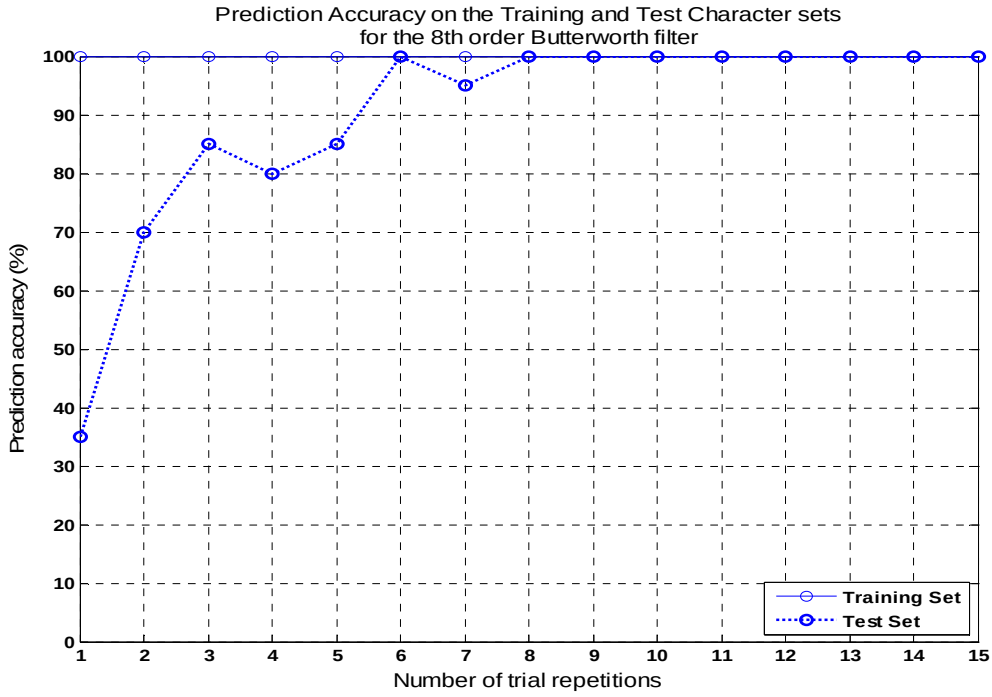

Figure 7-13 : Prediction accuracy of realistic MLE of SVM outputs. Preprocessed with 8th order Butterworth filter. Solid: training set (15 characters). Dotted: test set (20 characters)

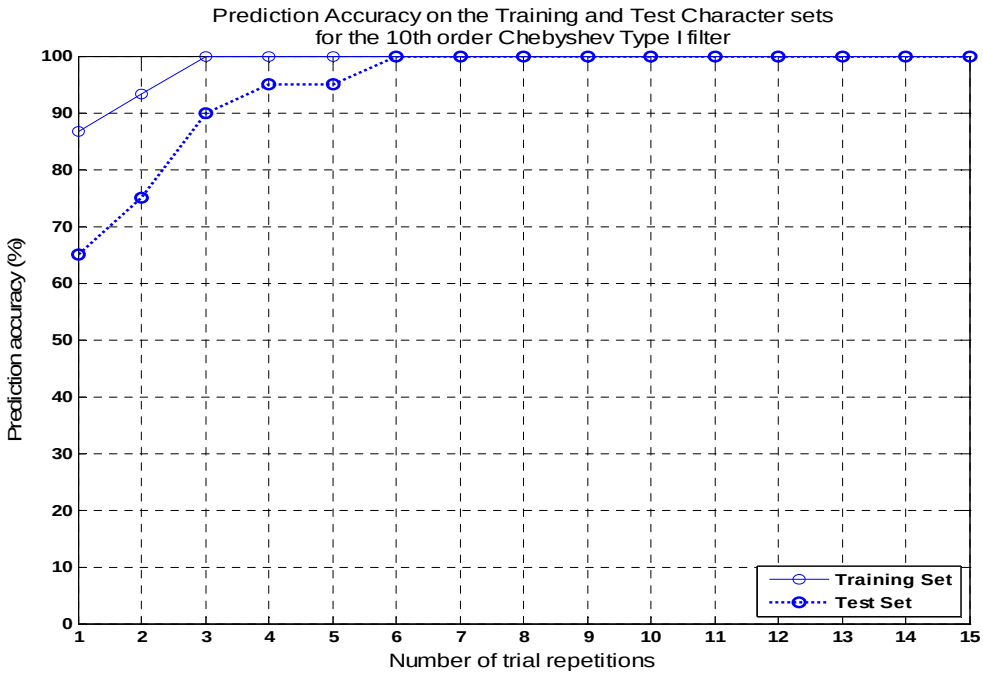

Figure 7-14 : Prediction accuracy of realistic MLE of SVM outputs. Preprocessed with 10th order Chebyshev Type I filter. Solid: training set (15 characters). Dotted: test set (20 characters).

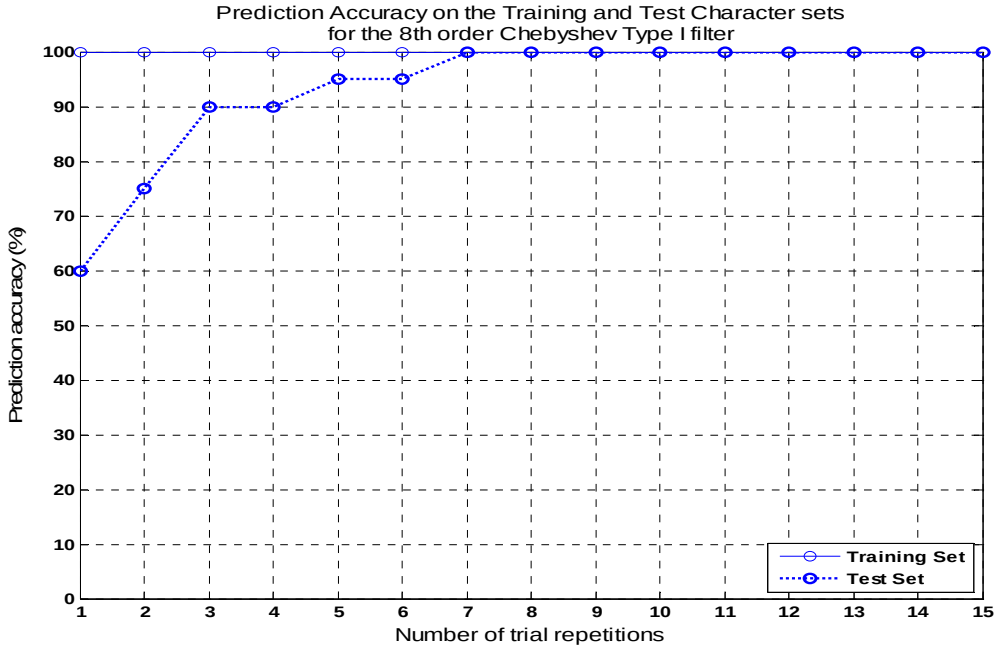

Figure 7-15 : Prediction accuracy of realistic MLE of SVM outputs. Preprocessed with 8th order Chebyshev Type I filter. Solid: training set (15 characters). Dotted: test set (20 characters).

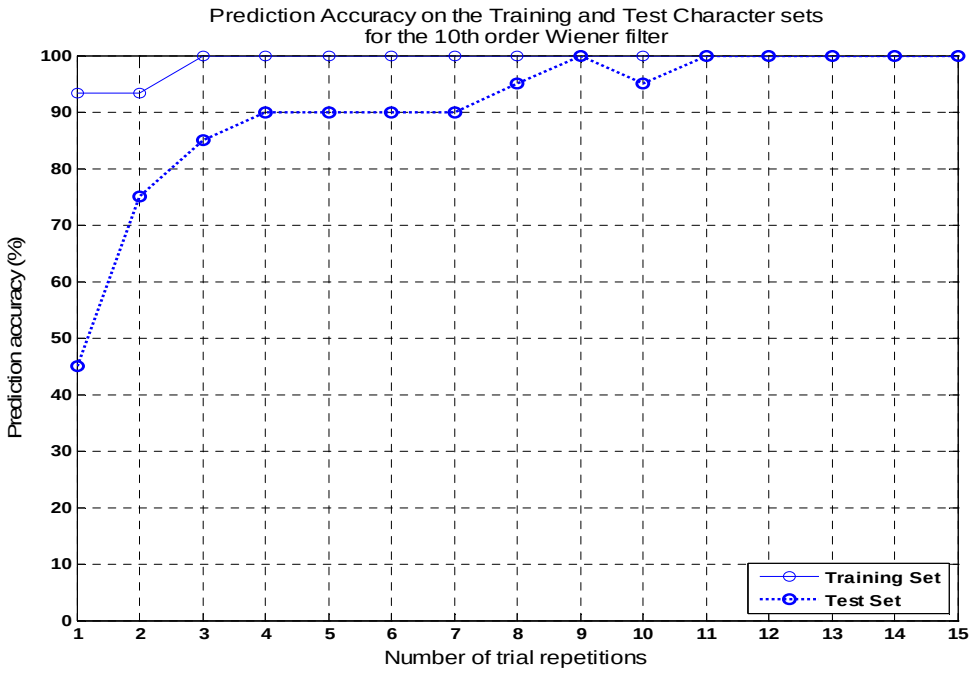

Figure 7-16 : Prediction accuracy of realistic MLE of SVM outputs. Preprocessed with 10th order Wiener filter. Solid: training set (15 characters). Dotted: test set (20 characters).

However, one should note that the evaluation of the prediction accuracy is performed for the parameters given in the literature [4]. When the case is investigated for the optimum regularization and variance parameters (C and σ) providing the highest cross-validation values (Table 7-7), filtering with Wiener approach becomes as successful as the Chebyshev case (Figure 7-17, Figure 7-18, Figure 7-19, Figure 7-20 and Figure 7-21).

Table 7-7: The 5 - fold Cross Validation Values of SVM on the Training Set for optimum parameters, preprocessed with investigated filtering techniques

$C_r = 80,\ C_c = 100,\ \sigma_r = 100,\ \sigma_c = 120$	**Rows**	**Columns**
10th order Butterworth - 0.5Hz-30Hz	81.0268%	82.3661%
8th order Butterworth - 0.5Hz-30Hz	81.4732%	84.5982%
10th order Chebyshev I - 0.1Hz-10Hz	87.0536%	89.2857%
8th order Chebyshev I - 0.1Hz-10Hz	83.7054%	85.9375%
10th order Wiener filter	84.8214%	88.8393%

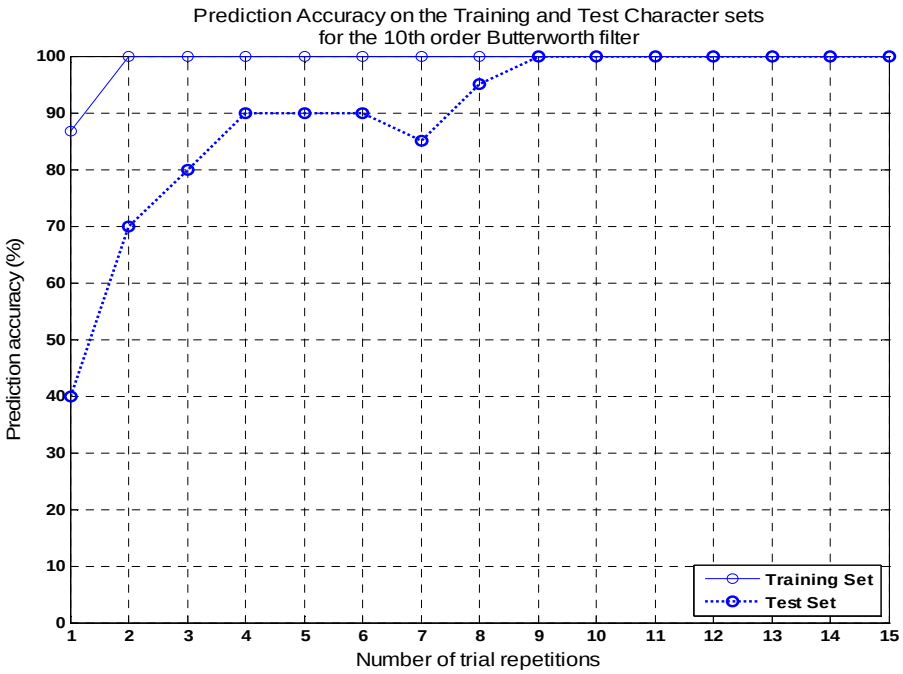

Figure 7-17 : Prediction accuracy of realistic MLE of SVM outputs. Preprocessed with 10th order Butterworth filter, trained with optimum parameters in Table 7-7. Solid: training set (15 characters). Dotted: test set (20 characters).

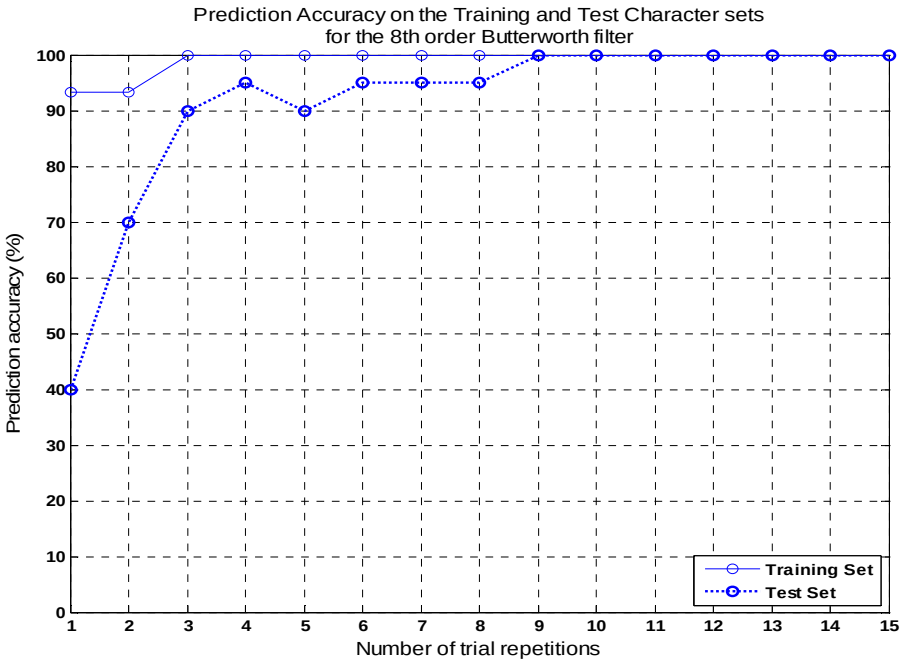

Figure 7-18 : Prediction accuracy of realistic MLE of SVM outputs. Preprocessed with 8th order Butterworth filter, trained with optimum parameters in Table 7-7. Solid: training set (15 characters). Dotted: test set (20 characters).

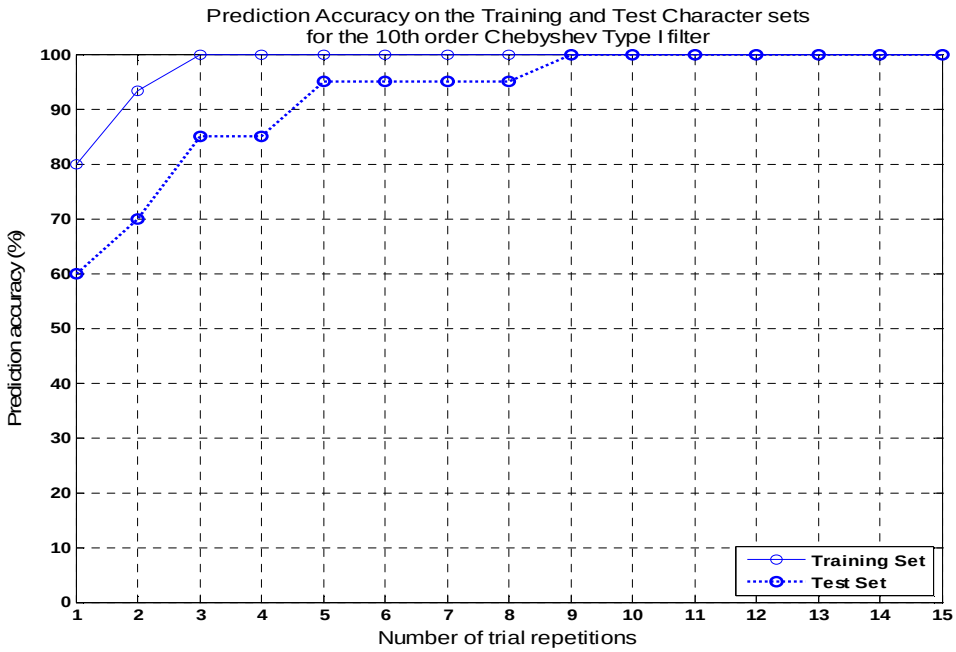

Figure 7-19 : Prediction accuracy of realistic MLE of SVM outputs. Preprocessed with 10th order Chebychev Type I filter, trained with optimum parameters in Table 7-7. Solid: training set (15 characters). Dotted: test set (20 characters)

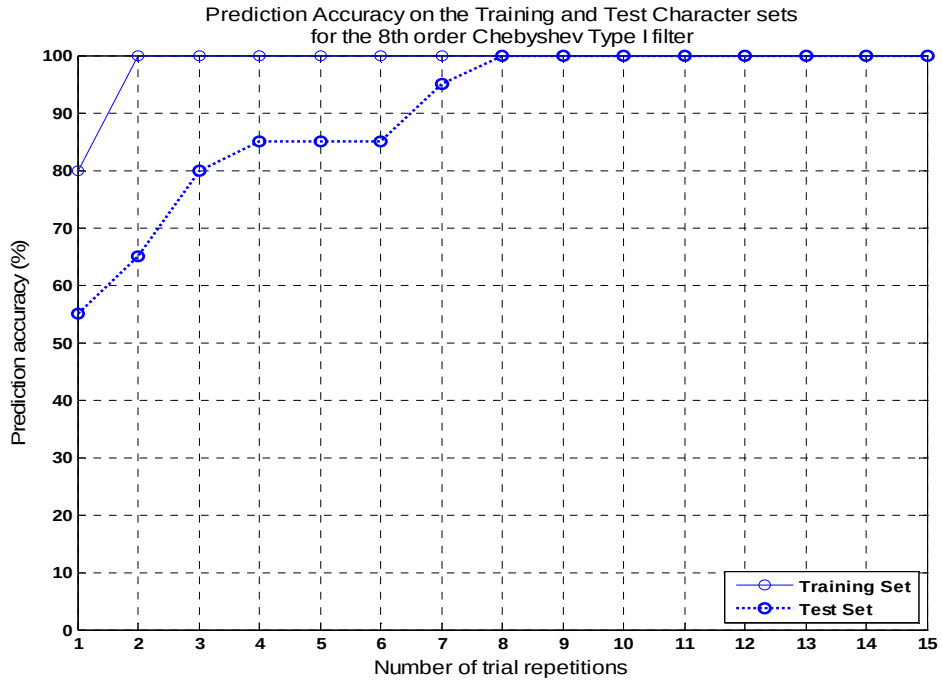

Figure 7-20 : Prediction accuracy of realistic MLE of SVM outputs. Preprocessed with 8th order Chebychev Type I filter, trained with optimum parameters in Table 7-7. Solid: training set (15 characters). Dotted: test set (20 characters)

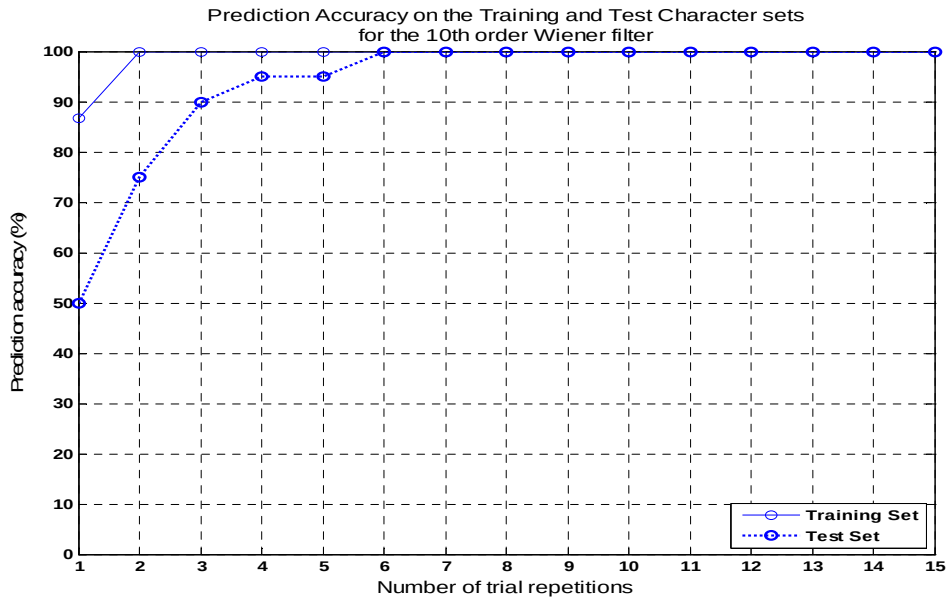

Figure 7-21 : Prediction accuracy of realistic MLE of SVM outputs. Preprocessed with 10th order Wiener filter, trained with optimum parameters in Table 7-7. Solid: training set (15 characters). Dotted: test set (20 characters).

From Table 7-7, the 5-fold cross-validation accuracy has increased for all filtering schemes (especially for the Chebyshev cases). In this case however, the prediction performance with Chebyshev filtering has decreased to 8 trial repetitions for 100% accuracy in the test set (Figure 7-19 and Figure 7-20). On the other hand, the accuracy with the Wiener filtering technique has increased to 6 trial repetitions for perfect prediction and became comparable with the result in the previous case of Chebyshev. However, it should be underlined here that, the Wiener filter estimation is performed on the raw EEG data. That is, the noisy frequency components in the unfiltered signal might affect the estimation procedure involved in Wiener filter model. The performance of the approach can be further increased with low-pass filtering the EEG signals first (like an equiripple filter between 0-50Hz) and then estimating the Wiener filter. The final forms of the estimated Wiener filters for the low-pass filtered case are given in Figure 7-22.

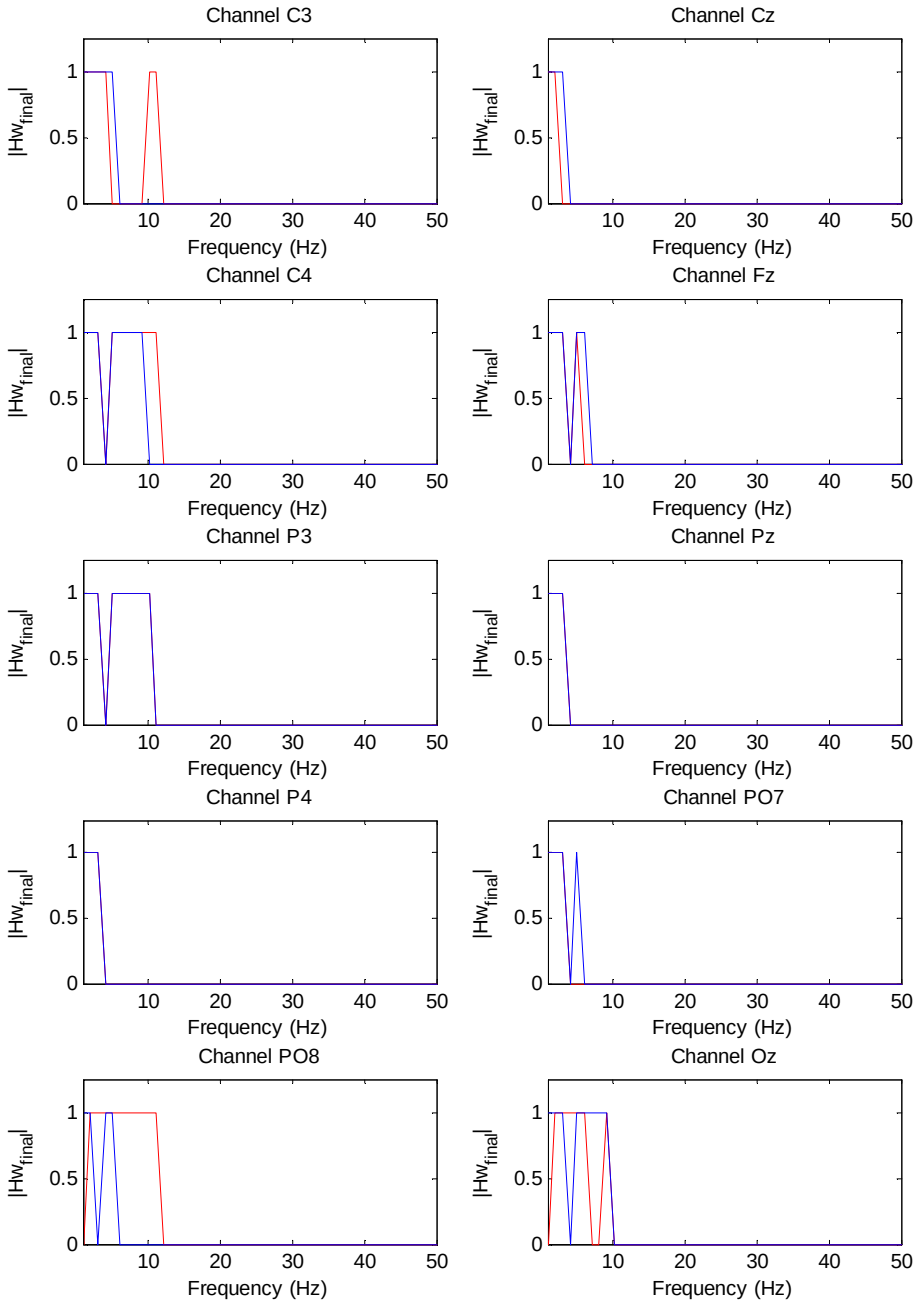

Figure 7-22 : Estimated Wiener filters for the predetermined 10 EEG channels (estimated from the downsampled, 50Hz low-pass filtered EEG data). The estimates are shown in red for row, and blue for the column groups.

The cross-validation and prediction accuracy results for this case are given in Table 7-8, Figure 7-23 and Figure 7-24.

Table 7-8: The 5 - fold Cross Validation Values of SVM on the lowpass + Wiener preprocessed Training Set, (1) with the parameters in the literature and (2) optimum parameters searched using the dataset.

		Rows	Columns
(1)	$C_r = C_c = 20.007, \sigma_r = \sigma_c = 27.359$	82.5893%	89.0625%
(2)	$C_r = 80,\ C_c = 100,\ \sigma_r = 100,\ \sigma_c = 120$	83.0357%	89.7321%

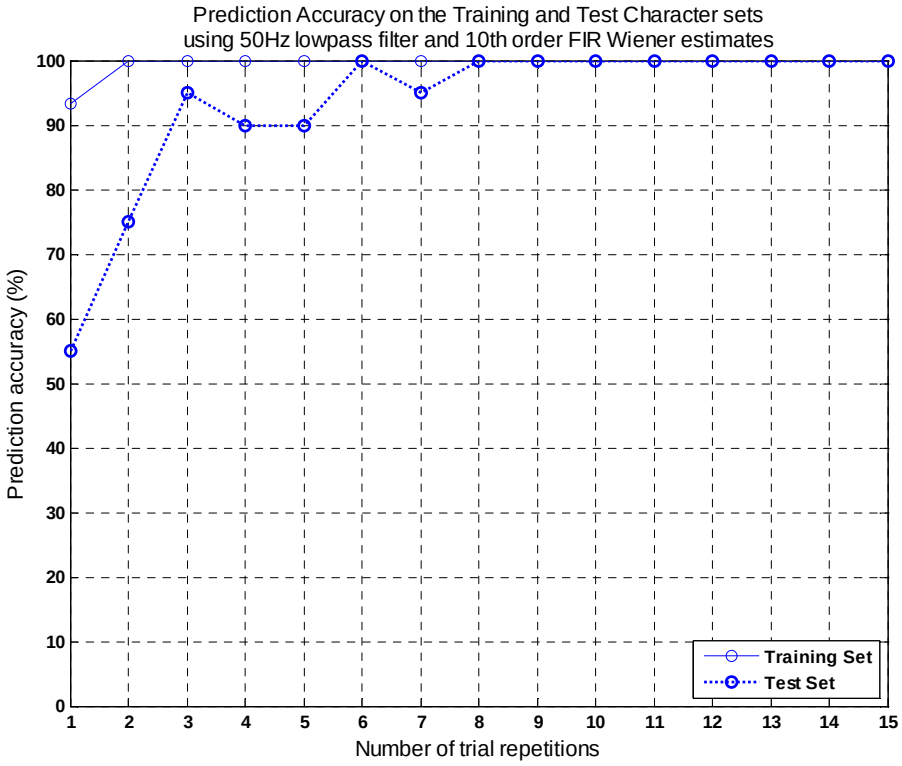

Figure 7-23 : Prediction accuracy of realistic MLE of SVM outputs. Preprocessed with 50Hz low pass + 10th order Wiener filter, trained with the parameters of Table 7-8 (1). Solid: training set (15 characters), Dotted: test set (20 characters).

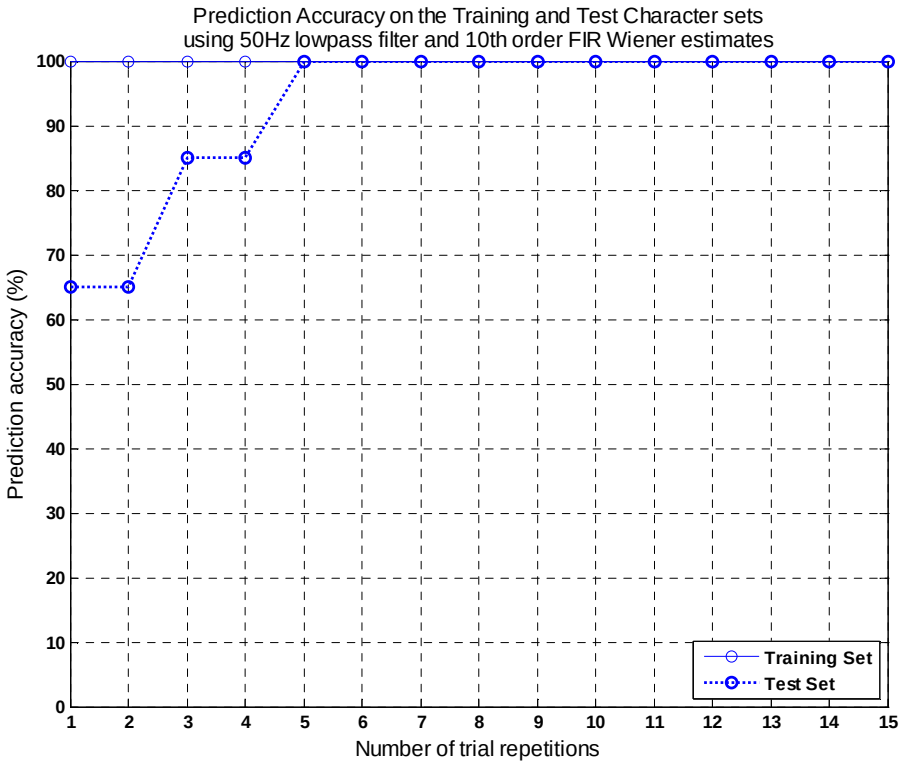

Figure 7-24 : Prediction accuracy of realistic MLE of SVM outputs. Preprocessed with 50Hz low pass + 10th order Wiener filter, trained with the parameters in Table 7-8 (2). Solid: training set (15 characters). Dotted: test set (20 characters).

As can be seen from Figure 7-24, the prediction accuracy on the test set has increased to 100% using only 5 trial repetitions which gives an idea of increase in the accuracy of Wiener filter estimation with prefiltering. It is also surprising that the presented model has also shown 100% prediction accuracy in a single trial on the training set. This result, in general, implies that the classification model is not so accurate and has suffered from overfitting (see section 5.2.3). However, as it can be observed from the results on the test set, this is not the case and Wiener filter approach outperformes among the discussed preprocessing methods in terms of the improvement of prediction accuracy.

7.2.2 Experimentation with the Designed Hardware

In the final section of this chapter, the results obtained from the Spelling experiment with the designed EEG system are presented. The experiment is conducted on a single subject with the conditions and procedure stated below:

- The measurement environment had no electrical shielding. Two continuously running PC clusters of 8 computers each were working nearby the recording room.
- The experiment was conducted in a dark environment.
- The subject was asked to sit relaxed on a standard chair without arms.
- A 7x7 spelling matrix composed of Turkish letters and other alphanumeric characters were presented to the subject (Figure 7-26).
- The EEG signals were measured using the designed active electrodes located on the predetermined positions on the scalp (Figure 7-3). The ground and the active reference electrodes are positioned on FPz and right ear respectively.
- For each spelled character, the recording of EEG signals was started after a 10 seconds of preparation time. During this interval, the subject got ready for the intensification sequences.
- The intensifications were randomized in blocks of 14 for 7 rows and 7 columns. The interstimulus interval was set to 250ms in which a row or column was flashed on for 150ms and then flashed off for 100ms.
- A total of 15 trial repetitions were employed for all the characters in the spelling session. The break time between the trials was adjusted to 1 second. Therefore, the spelling run for each character lasted about 77.5 seconds (10 seconds preparation time + (14 intensifications x 250 ms + 1000 ms break) x 15 repetitions).
- As the experiment employed 14 different intensifications and 15 trial repetitions for each character, a spelling run consists of 210 observations out of which there are 30 target and 180 non-target observations (2 targets

in a single trial x 15 repetitions and 12 non-targets in a single trial x 15 repetitions).

- The EEG signals were digitized at a sampling rate of 1 kHz and recorded in separate files for each spelled character.
- The experiment was offline performed for spelling of 20 characters which are distributed to the training and test sets as in Table 7-9.

Figure 7-25 : Pictures from the experiment on P300 Speller conducted in Brain Research Laboratory of Electrical and Electronics Eng. Dept., METU

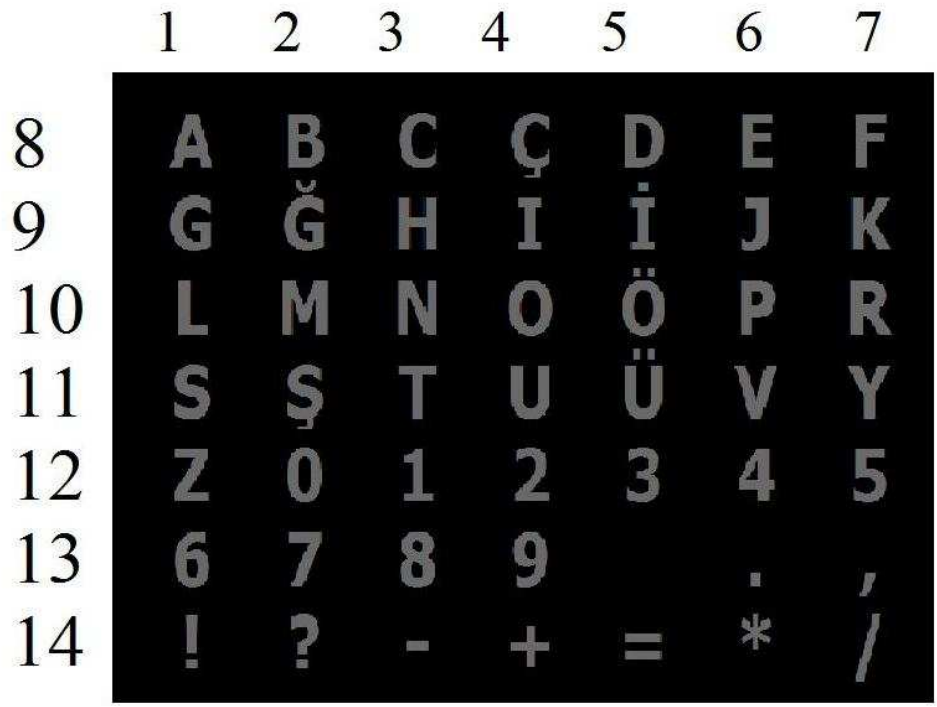

Figure 7-26 : The spelling matrix and stimulus codes used in the experimentation performed with the designed hardware.

Table 7-9: The characters spelled in the experimentation conducted with the designed hardware

	Training Set (9 characters)	Test Set (11 characters)
Spelled words	BERNA29BA	BFKRTL7ÜHP3

7.2.2.1 Results on the EEG measurements

For visualization of the recorded target and non-target responses, the averaged EEG signals from each class are shown in Figure 7-27 and Figure 7-28. From these figures, it is clear that the developed EEG system accurately measured the target P300 and non-target responses during the experiment.

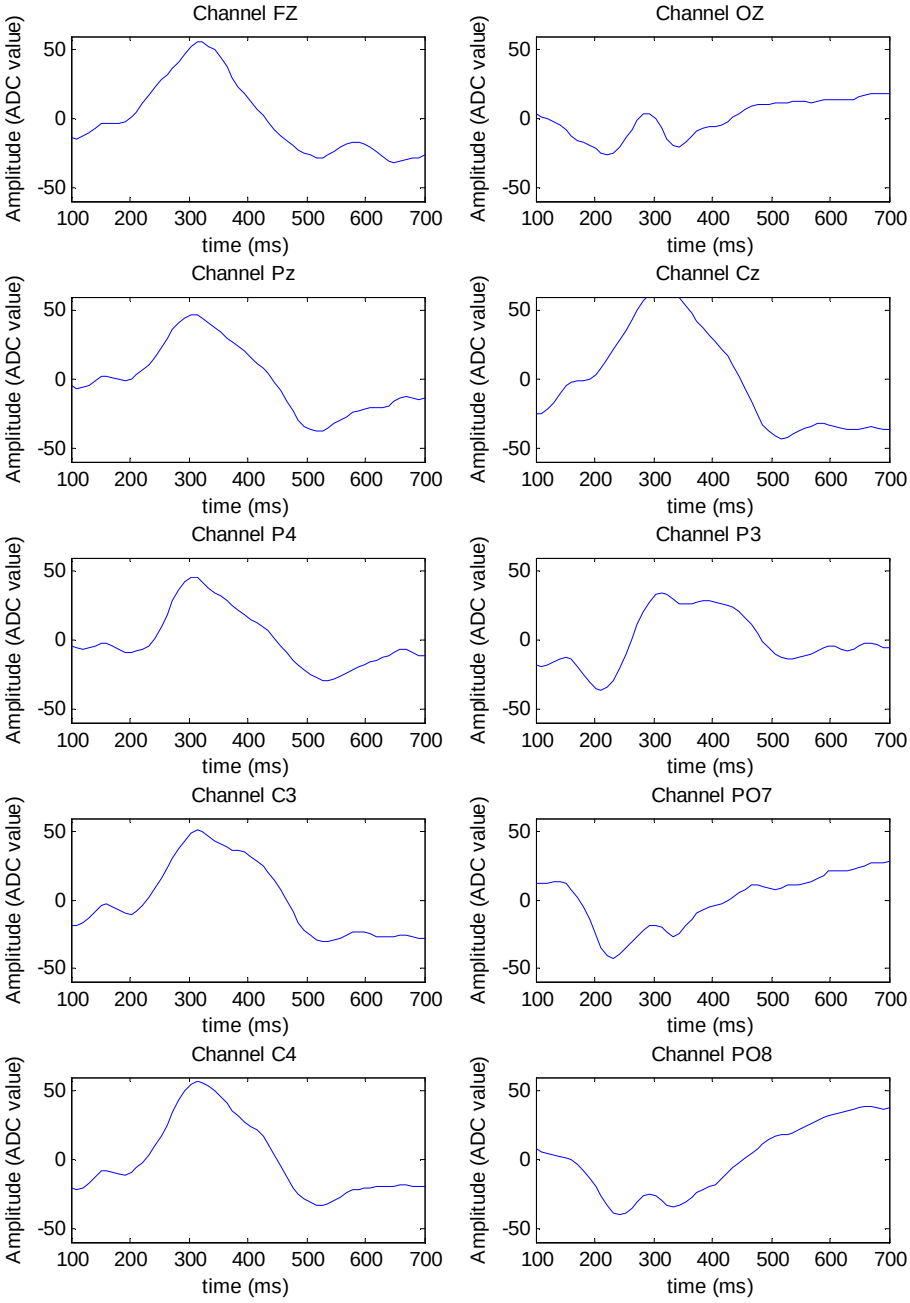

Figure 7-27 : Averaged target responses measured in the P300 Speller experiment conducted with the designed hardware.

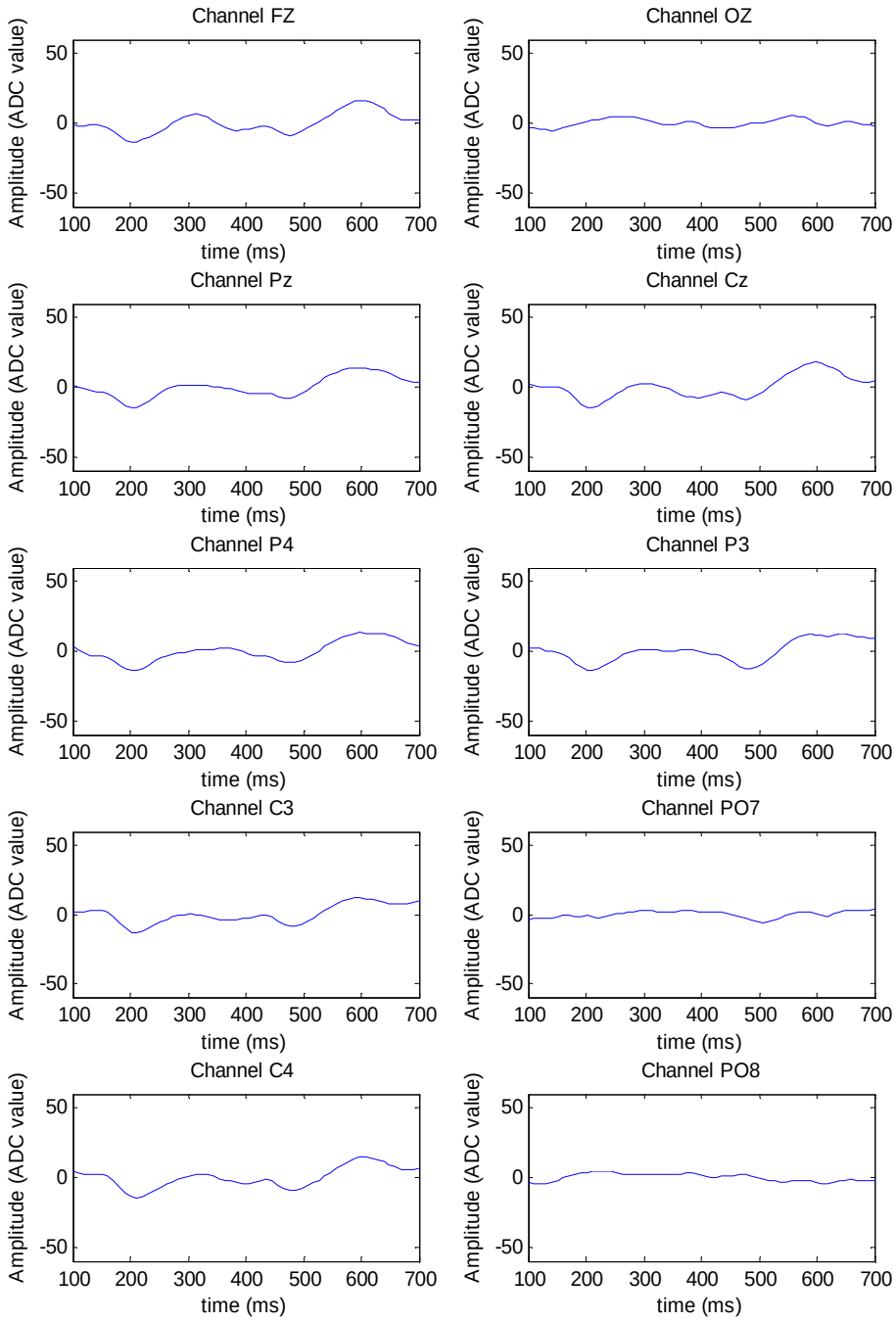

Figure 7-28 : Averaged non-target responses measured in the P300 Speller experiment conducted with the designed hardware

7.2.2.2 Offline Analysis Procedure

The steps followed in preprocessing and classification of these datasets is summarized below:

Preprocessing

Single trial extraction: EEG time segments of 600ms length, 100ms after the presentation of visual stimuli are extracted.

Filtering: Although the EEG hardware employs active analog band-stop and low-pass filters in its design, the extracted time segments are digitally filtered with an equiripple low pass filter with a cutoff frequency of 50Hz.

Decimation: In order to reduce the dimensionality of the input space, the filtered time segments are downsampled to 100Hz by taking the average of every 10 consecutive samples. Therefore, the number of time samples for each channel has been reduced to 60.

Wiener filter estimation: The decimated observations are separated into row and column groups and for each group the Wiener filter estimation is performed.

Construction of the feature vector: All Wiener filtered EEG segments are concatenated by channel for each observation and a long feature vector is constructed with 600 elements (60 samples x 10 channels).

Training

Grouping row and column observations: The preprocessed observations are separated into row and column groups and for each group the data is divided into target and non-target classes.

Selection of observations: From each trial, 1 target and 1 non-target observation is selected to construct the SVM classifier for each group.

Search of parameters: For maximum cross-validation accuracy on the training set, the regularization parameter C and the variance parameter σ are searched for both groups between the interval [10, 200] with increments of 5. This is a time consuming procedure and once the optimum values are found these parameters are kept as constants for the SVM classifiers.

7.2.2.3 Results of the Proposed Methodologies

The estimated Wiener Filters are shown in Figure 7-29. One can note that the optimum frequency bands for the row and column groups can show difference in some of the EEG channels.

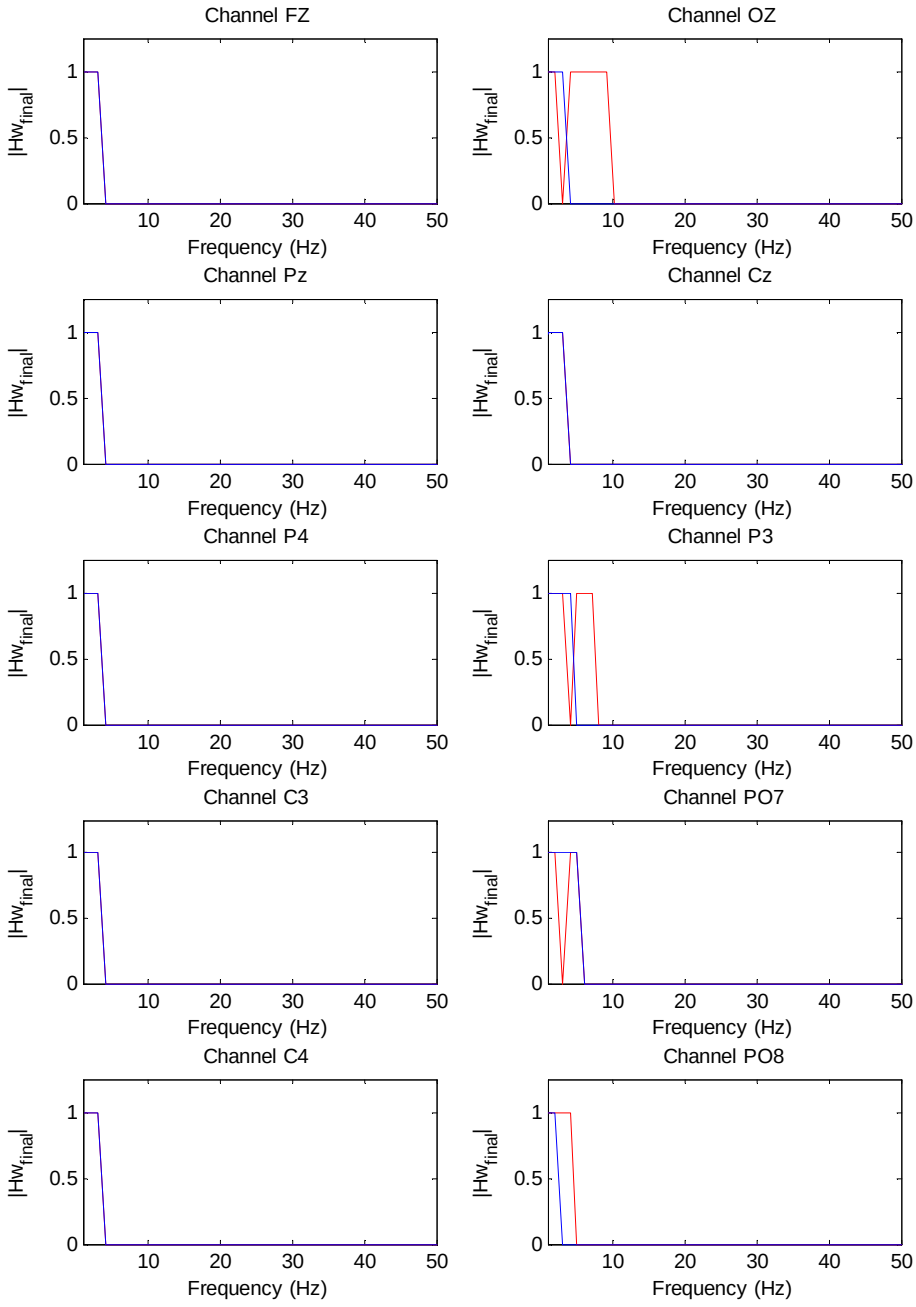

Figure 7-29 : Estimated Wiener filters for the predetermined 10 EEG channels on the experiment data performed with the designed hardware. The filters are estimated from the downsampled, 50Hz low-pass filtered EEG data and are shown in red for row, blue for the column groups.

The maximum cross-validation accuracies are obtained as 87.037% and 85.1852% for the row and column groups on the training set using the optimum values $C_r = 60$, $C_c = 100$ and $\sigma_r = 90$, $\sigma_c = 120$ for the searched parameters. The prediction accuracies on the training and test sets are shown in Figure 7-30.

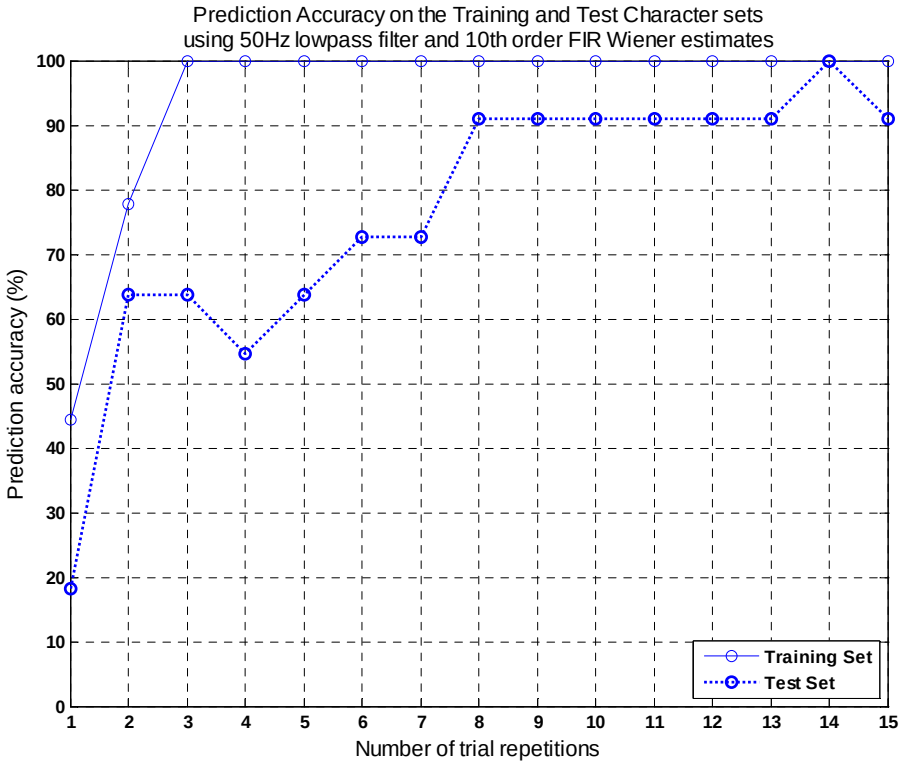

Figure 7-30 : Prediction accuracy of realistic MLE of SVM outputs on the experiment data. Preprocessed with 50Hz low pass + 10th order Wiener filter, trained with the optimal parameters. Solid: training set (9 characters). Dotted: test set (11 characters)

Here, one should remember that the test set is composed of 11 characters. Therefore, only one character has been false predicted after 8 trial repetitions. This can be seen on the predicted characters in Table 7-10 more clearly.

Table 7-10: Predicted characters in the test set with respect to the trial repetition number

Trials	Predicted Characters
1	ĞKKR6G,T9ÖI
2	BFPMTL7Ü8PÇ
3	BFRRTG7Ü8PD
4	FFRRTG7Ü8PD
5	FEKRT!7ÜHPD
6	BEKRTG7ÜHPD
7	B,KRTG7ÜHPD
8	BFKRTL7ÜHPD
9	BFKRTL7ÜHPD
10	BFKRTL7ÜHPD
11	BFKRTL7ÜHPD
12	BFKRTL7ÜHPD
13	BFKRTL7ÜHPD
14	BFKRTL7ÜHP3
15	BFKRTL7ÜHPD

The only misclassified character in Table 7-10 after 8 trials (omitting the exception in the 14th repetition) is the last one in which the subject informed that she was not well concentrated on the character in the spelling session due to the headache she suffered from. Omitting this case, the methodologies predicted the characters with 100% accuracy using only 8 trials.

CHAPTER 8

CONCLUSION

In this thesis, the implementation of the P300 Speller system is performed by the development of a P300 based BCI system. Several experiments are conducted with the designed system in which the measurements are realized with the active electrodes. Convincing performance is obtained in these experiments as the system was able to measure the P300 patterns required for the spelling application.

Wiener filtering, a statistical signal processing technique, is employed as a signal enhancement method on the P300 speller for the first time in the literature. The optimum frequency bands for P300 detection is investigated by estimating the Wiener filters for the target and non-target observations. It is applied to several P300 Speller datasets and observed to be more successful than the other filtering techniques in terms of target character prediction accuracy. Furthermore, the rows and columns of the spelling matrix are treated in separate groups in order to investigate the difference in classification accuracies between these two intensification types. In the P300 Speller dataset of BCI Competition II, the target characters in the test set are predicted with 100% accuracy within 4 trials which is higher than that of the prediction results of competition winners. On the other hand, the prediction of the target characters with the designed system is performed after 8 trials in order to obtain a perfect accuracy for all characters.

8.1 General Observations and Discussion

Several results are deducted from the observations on the investigated Spelling Paradigm datasets. The first and maybe the most important observation is that the brain responses to row and column intensifications are not classified with equal accuracy. One can see from the cross-validation results that, (although treated in the same way) the row groups usually have lower classification accuracy than the column group for equal regularization and variance parameters (see section 7.1.1). Even for the optimal values of the cross-validation results, the row group is observed to be more misclassified than the column one. Although not presented here, the single vector classification results were also higher for the column group for each of the observed training and test sets. To give an example, in the experimental study with the designed system, the misclassified character was lying on the same column with the predicted character after 8 repetitions. The column prediction was correct, but not the row. Therefore, it can be inferred that the human perception to the row and column intensifications can be different for each subject in terms of the brain's responses which is an open research topic for the neurophysiologists and psychologists interested in BCI. Furthermore, in order to satisfy a successful classification scheme, these intensification groups should be trained and classified separately on two classification modalities.

Another important deduction is that the optimum frequency band for P300 detection is in fact narrower than the normal EEG frequency range (0-45Hz). The unnecessary frequency components outside this range can be eliminated for better classification results. Whether the filtering technique is performed with Wiener approach or not, filtering the out-of-range components considerably increases the performance of the classification. Filtering with Wiener approach only provides the frequency information that is optimal in detection of the measured signal.

Furthermore, one should note that the application of Wiener filtering on the P300 Speller problem is only meaningful with the assumptions described in chapter 4.

The stationarity of the signal patterns are of special importance in this methodology. Unlike the common sense that the EEG measurements are non-stationary signals [2], in this study, they are treated as stationary by employing a WSS model of the P300 pattern and the noise signals. This modality is proven to be valid for the P300 detection problem in Spelling Paradigm as the results show that the filtering with the Wiener approach yielded the best classification performance in SVM among the other preprocessing techniques (see sections 7.1.2 and 7.2.1). Furthermore, the presented approach is performed by the estimation of the Wiener filters from the raw EEG data. It can be further improved by estimating these after prefiltering the raw EEG signal first, with a low-pass filtering method as described in section 7.2.1.

The performance of the classification depends on many parameters like the selection of the training group, the type of normalization and the separation of the row and column intensification groups. The cross-validation results, hence the accuracy of the trained models is considerably affected by the samples selected to train the classifiers. In order to perform a rational comparison between the preprocessing and other methods, it is highly necessary to use the same group in training the classifiers for all investigated filtering cases. Otherwise, the performance of the classification method could vary (even for the same method) in the second run of the algorithm.

In addition, the results presented in this thesis are obtained by performing a Gaussian normalization on the datasets. The preprocessing methodologies in the literature could have higher performance in here if they were investigated for all normalization types discussed in section 5.3.4. However, the results for these cases are believed to be variable on every P300 Speller dataset as the feature patterns concerned here are more likely to be random signals. The shape and amplitude of these signals might not be as well preserved as the Gaussian normalization when compared to other normalization types. A deeper study is needed to validate this assumption though.

Another important factor is that the classification results might not show the same behaviour among the preprocessing techniques. That is, the parameters which are optimal for one technique may not be as much optimal as the other one. Therefore, they should be investigated for the cases in which they exhibit the maximum cross validation accuracy on the training set. However, fortunately in the presented results, all preprocessing techniques exhibited nearly the same behavior in classification accuracies (except the Chebyshev case in section 7.2.1).

Finally, it should be underlined here that the performance of the overall system is more dependent on the employed discriminative classification method. In most cases, the target characters can be predicted by using a powerful classifier exhibiting a 100% accuracy (may be at the 15^{th} trial repetition) without any preprocessing method. Therefore, the main success of this system is determined by the SVM classifier [77]. Other methodologies can only serve slight improvements in speed of the system as compared among each other.

8.2 Advantages of the Developed System and Methods

The proposed methodologies provide several advantages for the spelling application in terms of practicality in the EEG measurements and preprocessing mechanisms. The active electrodes employed in the system eliminate the need for skin preparation stage applied in the passive counterpart. Using active electrodes provides longer EEG measurements, thus improves the usability of a BCI system. On the other hand, filtering with the Wiener approach increases the classification accuracy as it offers the optimal frequency bands for P300 detection. Since it is performed on a dataset with only class label information, it automatically determines the frequencies comprising the user specific target signals which can also be considered as a feature extraction methodology in this scheme. Therefore, one can apply the Wiener filtering on similar binary classification models even if there is no prior information on how to filter the data.

The decision mechanism for an online P300 speller can be improved by the methodology proposed in section 5.4.2. The off states of the subject can be determined by this method so that the BCI system becomes more practical as it does not need a continuous response from the subject.

8.3 Future Work

The thesis can be further improved with the future studies on the following topics:

- The developed system for the moment is applicable for only offline measurements and analysis. The controlling mechanisms should be upgraded to realize an online P300 based BCI system. Furthermore, the system and the methods are only tested on a single healthy subject. More experimentation should be performed with the designed hardware and the presented methodologies on other healthy or disabled subjects.

- The only BCI application investigated in this thesis is the P300 Speller. However, one can increase the number of application types in this systems by implementation other BCI applications based on P300 detection. This is a simple task since the hardware supports all the mechanisms required for a P300 based BCI system. A slight modification on the presented methodologies may be required depending on the specific BCI application to be implemented.

- Currently, the active electrodes and the EEG cap can not be properly operated on every subject due to the fixed size of the cap. The placement of the electrodes can be disturbing for the subject as the material used in the electrodes for contacting the scalp is sharp in order to reach the scalp through hair. The materials used in their design should be improved to be easily and confortably used by everybody. The hardware can be improved

by using surface mount devices in construction of the circuits so that they are much smaller in size. By this way, the whole system can be attached on the EEG cap.

- As well as the P300 based BCI applications, other paradigms can be implemented within the system. After all, a complete BCI system can be realized by including the wheelchair application, P300 Speller and other assistive BCI systems in a compact framework as shown in Figure 8-1.

Figure 8-1: A compact BCI system for the disabled. In the future work, different BCI paradigms can be implemented on a single hardware system in which the basic needs of the patients are satisfied.

REFERENCES

[1] Wolpaw J.R., Birbaumer N., McFarland D.J., Pfurtscheller G., Vaughan T.M., "Brain Computer Interfaces for Communication and Control", *Clinical Neurophysiology*, **113**: 767-791, March 2002

[2] Lotte F., Congedo M., Lecuyer A., Lamarche F., Arnaldi B., "A Review of Classification Algorithms for EEG-Based Brain-Computer Interfaces", *Journal of Neural Engineering*, **4**: R1-R13, January 2007

[3] Farwell L.A., Donchin E., "Talking off the top of your head: Toward a Mental Prosthesis Utilizing Event-Related Brain Potentials", *Electroencephalography and Clinical Neurophysiology*, **70**: 510-523, 1988

[4] Kaper M., Meinicke P., Grossekathoefer U., Lingner T., Ritter H., "BCI Competition 2003 – Dataset IIb: Support Vector Machines for the P300 Speller Paradigm" *IEEE Transactions on Biomedical Engineering*, Vol. 51, No. 6, June 2004

[5] Kaper M., Ritter H., "Progress in P300-based Brain-Computer Interfacing", *IEEE International Workshop on Biomedical Circuits and Systems*, 2004

[6] Rakotomamonjy A., Guigue V., "BCI Competition III: Dataset II – Ensemble of SVMs for BCI P300 Speller", *IEEE Transactions on Biomedical Engineering*, Vol.55, No.3, March 2008

[7] Bostanov V., "BCI Competition III - Data Sets Ib and IIb: Feature Extraction From Event-Related Brain Potentials with the Continuous Wavelet Transform and the t-Value Scalogram", *IEEE Transactions on Biomedical Engineering*, Vol. 51, No. 6, June 2004

[8] Xu N., Gao X., Hong B., Miao X., Gao S., "BCI Competition 2003 – Data Set IIb: Enhancing P300 Wave Detection Using ICA-based Subspace Projections for BCI Applications", *IEEE Transactions on Biomedical Engineering*, Vol. 51, No. 6, June 2004

[9] Krusienski D.J., Sellers E.W., Cabestaing F., Bayoudh S., McFarland D.J., Vaughan T.M., Wolpaw J.R., "A Comparison of Classification Techniques for the P300 Speller", *Journal of Neural Engineering*, **3**: 299-305, 2006

[10] Guan J., Chen Y., Huang M., "Classification of Single-Trial Potentials Evoked by Imitating-Natural-Reading Using v-SVM", *International Journal of Computational Intelligence Research*, Vol.2, No.1: 110-114, 2006

[11] Guger C., Schlög A., Neuper C., Walterspacher D., Strein T., Pfurtscheller G., "Rapid Prototyping of an EEG-Based Brain-Computer Interface (BCI)", *IEEE Transactions on Neural Systems and Rehabilitation Engineering*, Vol.9, No. 1, March 2001

[12] Müller G.R., Neuper C., Pfurtscheller G., "Implementation of a Telemonitoring System for the Control of an EEG-Based Brain-Computer Interface", *IEEE Transactions on Neural Systems and Rehabilitation Engineering*, Vol.11, No. 1, March 2003

[13] Moore M.M., "Real-World Applications for Brain-Computer Interface Technology" *IEEE Transactions on Neural Systems and Rehabilitation Engineering, Vol.11, No. 2, June 2003*

[14] Wolpaw J.R., McFarland D.J., Vaughan T.M., Schalk G., "The Wadsworth Center Brain-Computer Interface (BCI) Research and Development Program", *IEEE Transactions on Neural Systems and Rehabilitation Engineering*, Vol.11, No. 2, June 2003

[15] Schalk G., McFarland D.J., Hinterberger T., Birbaumer N., Wolpaw J.R., "BCI2000: A General-Purpose Brain-Computer Interface (BCI) System", *IEEE Transactions on Biomedical Engineering*, Vol. 51, No. 6, June 2004

[16] Fabiani M., Gratton G., Karis D., Donchin E., "The Definition, Identification and Reliability of Measurements of the P300 component of the Event-Related Brain Potential", *Advances in Psychophysiology*, Vol. 2 JAI Press, 1988

[17] Blankertz B., Müller K.R., Curio G., Vaughan T.M., Schalk G., Wolpaw J.R., Schlögl A., Neuper C., Pfurtscheller G., Hinterberger T., Schröder M., Birbaumer N., "The BCI Competition 2003: Progress and Perspectives in Detection and Discrimination of EEG Single Trials", *IEEE Transactions on Biomedical Engineering*, Vol.51, No.6, June 2004

[18] Blankertz B., BCI Competition II (2003) – P300 Speller Dataset (webpage). Available online at: http://www.bbci.de/competition/ii/ , Documentation: http://www.bbci.de/competition/ii/albany_desc/albany_desc_ii.pdf

[19] Blankertz B., Müller K.R., Krusienski D.J., Schalk G., Wolpaw J.R., Schlögl A., Pfurtscheller G., Millan J.R., Schröder M., Birbaumer N., "The BCI Competition III: Validating Alternative Approaches to Actual BCI Problems", *IEEE Transactions on Neural Systems and Rehabilitation Engineering*, Vol.14, No.2, June 2006

[20] Blankertz B., BCI Competition III (2005) – P300 Speller Dataset (webpage). Available online at: http://www.bbci.de/competition/iii/ , Documentation: http://bbci.de/competition/iii/desc_II.pdf

[21] Lin Z.L., Zhang C.S., "Enhancing Classification by Perceptual Characteristics for the P300 Speller Paradigm", *Proceedings of the 2nd International IEEE EMBS Conference on Neural Engineering – Arlington/Virginia* – March 16-19, 2005

[22] Thulasidas M., Guan C., Wu J., "Robust Classification of EEG Signals for Brain-Computer Interface", *IEEE Transactions on Neural Systems and Rehabilitation Engineering*, Vol. 14, No. 1, 2006

[23] Garrett D., Peterson D.A., Anderson C.W., Thaut M.H., "Comparison of Linear, Nonlinear, and Feature Selection Methods for EEG Signal Classification", *IEEE Transactions on Neural Systems and Rehabilitation Engineering*, Vol. 11, 141-4, 2003

[24] Blankertz B., Curio G., Müller K.R., "Classifying Single Trial EEG: Towards Brain Computer Interfacing", *Advanced. Neural Information Processing Systems,* Vol. 14, 157-64

[25] Schlögl A., Lee F., Bischof H., Pfurtscheller G., "Characterization of Four-Class Motor Imagery EEG Data for the BCI-competition 2005", *Journal of Neural Engineering,* Vol. 2, L14-22, 2005

[26] Zhang H., Guan C., Wang C., "A Statistical Model of Brain Signals with Application to Brain-Computer Interface", *Proceedings of the 2005 IEEE, Engineering in Medicine and Biology 27th Annual Conference, Shanghai, China*, September 1-4, 2005

[27] Hoffman U., "Bayesian Machine Learning Applied in a Brain Computer Interface for Disabled Users", *Doctoral Thesis, École Polytechnique Federale De Lausanne,* 2007

[28] Hoffmann U., Vesin J-M., Ebrahimi T., Diserens K., "An Efficient P300-Based Brain-Computer Interface for Disabled Subjects", *Journal of Neuroscience Methods,* **167**, pp:115-125, 2008

[29] Hoffmann U., Garcia G.N., Vesin J-M., Ebrahimi T., "Application of the Evidence Framework to Brain-Computer Interfaces", In: *Proceedings of the IEEE Engineering in Medicine and Biology Conference,* (2004),

[30] Liu Y., Zhou Z., Hu D., Dong G., "T-weighted Approach for Neural Information Processing in P300 based Brain-Computer Interface". *International Conference on Neural Networks and Brain, 2005,* Vol.3, pp.1535-1539, 13-15 October. 2005

[31] Serby H., Yom-Tov E., Inbar G.F., "An Improved P300-Based Brain-Computer Interface", *IEEE Transactions on Neural Systems and Rehabilitation Engineering,* Vol. 13, No. 1, March 2005

[32] Hayes M.H., "Statistical Digital Signal Processing and Modeling", *John Wiley & Sons, Inc.,* 1996

[33] Therrien C.W., “Discrete Random Signals and Statistical Signal Processing”, *Prentice Hall Signal Processing Series*, 1992

[34] Duda R.O., Hart P.E., “Pattern Classification and Scene Analysis”, *John Wiley & Sons, Inc.*, 1973

[35] Bishop C.M., “Neural Networks for Pattern Recognition”, *Clerdon Press-Oxford*, 1995

[36] Vapnik V., “The Nature of Statistical Learning Theory”, *Springer-Verlag, New York*, 1995

[37] Vapnik V., “Statistical Learning Theory”, *John Wiley and Sons, Inc., New York*, 1998

[38] Burges C.J.C., “A Tutorial on Support Vector Machines for Pattern Recognition”, *Data Mining Knowledge Discovery*, Vol. 2, pp: 121-167, 1998.

[39] Cortes C., Vapnik V., “Support-Vector Network”, *Machine Learning*, Vol. 20, pp:273–297, 1995

[40] Schölkopf B., Smola A., Müller K.R., “Nonlinear Component Analysis as a Kernel Eigenvalue Problem”, *Neural Computation*, **10**(5): 1299–1319, 1998

[41] Malmivuo J., Plonsey R., “Bioelectromagnetism – Principles and Applications of Bioelectric and Biomagnetic Fields”, [Online book], Chapter 13, Available at: http://www.bem.fi/book/13/13.htm#03

[42] Guger C., “Brain Computer Interface”, Lecture notes in *The 4th International Summer School on Emerging Technologies in Biomedicine: Advanced Methods for the Estimation of Human Brain Activity and Connectivity, Applications to Rehabilitation Engineering, Patras, Greece*, 29 June – 4 July 2008.
http://heart.med.upatras.gr/school2008/Materials.html

[43] Jasper H.H. The ten-twenty electrode system of the International Federation. Electroencephalogr. Clinical Neurophysiology, **(10)** pp:370-375. 1958

[44] Wolpaw J.R, "Brain-Computer Interface Technology: A Review of the First International Meeting", *IEEE Transactions on Rehabilitation Engineering*, 8(2):164–173, 2000

[45] Kübler A., Mushahwar V.K., Hochberg L.R., Donoghue J.P., "BCI Meeting 2005 – Workshop Clinical Issues and Applications", *IEEE Transactions on Neural Systems and Rehabilitation Engineering*, Vol. 14, No.2, June 2006

[46] Mason S.G., Birch G.E., "A General Framework for Brain-Computer Interface Design", *IEEE Transactions on Neural Systems and Rehabilitation Engineering*, Vol. 11, No. 1, March 2003

[47] Cincotti F., Bianchi L., Birch G., Guger C., Mellinger J., Scherer R., Schmidt R.N., Suarez O.Y., Schalk G., "BCI Meeting 2005 – Workshop on Technology: Hardware and Software", *IEEE Transactions on Neural Systems and Rehabilitation Engineering*, Vol. 14, No.2, June 2006

[48] EEG systems: http://archlab.gmu.edu/people/cbaldwi4/EEG.jpg

[49] Mobile EEG systems: http://www.gtec.at/content.htm

[50] Leuthardt E.C., Miller K.J., Schalk G., Rao R.P.N., Ojemann J.G., "Electrocorticography-Based Brain Computer Interface – The Seattle Experience", *IEEE Transactions on Neural Systems and Rehabilitation Engineering*, Vol. 14, No.2, June 2006

[51] Wilson J.A., Felton E.A., Garell P.C., Schalk G., Williams J.C., "ECoG Factors Underlying Control of a Brain-Computer Interface", *IEEE Transactions on Neural Systems and Rehabilitation Engineering*, Vol. 14, No.2, June 2006

[52] Hill N.J., Lal T.N., Schröder M., Hinterberger T., Wilhelm B., Nijboer F., Mochty U., Widman G., Elger C., Schölkopf B., Kübler A., Birbaumer N., "Classifying EEG and ECoG Signals Without Subject Training for Fast BCI Implementation: Comparison of Nonparalyzed and Completely Paralyzed Subjects", *IEEE Transactions on Neural Systems and Rehabilitation Engineering*, Vol. 14, No.2, June 2006

[53] Thakor N.V., "Frontiers of Neuroengineering", Lecture notes in *The 4th International Summer School on Emerging Technologies in Biomedicine:*

Advanced Methods for the Estimation of Human Brain Activity and Connectivity, Applications to Rehabilitation Engineering, Patras, Greece, 29 June – 4 July 2008.
http://heart.med.upatras.gr/school2008/Materials.html

[54] Lebedev M.A., Nicoleis M.A., "Brain-machine interfaces: Past, present and future", *Trends in Neurosciences,* Vol.29, No.9, pp: 536-546, September 2006.

[55] Magnetoencephalography - SQUID, http://en.wikipedia.org/wiki/SQUID

[56] Lal T.N., Schröder M, Hill N.J., Preissl H., Hinterberger T., Mellinger J., Rosenstiel W., Birbaumer N., Hofmann T., Schölkopf B., "A Brain-Computer Interface with Online Feedback Based on Magnetoencephalography", *Proceedings of the 22nd International Conference on Machine Learning, Bonn, Germany,* 2005

[57] Kauhanen L., Nykopp T., Lehtonen J., Jylanki P., Heikkonen J., Rantanen P., Alaranta H., Sams M., "EEG and MEG Brain-Computer Interface for Tetraplegic Patients", *IEEE Transactions on Neural Systems and Rehabilitation Engineering,* Vol.14, No.2, pp.190-193, June 2006

[58] The picture of a commercial Magnetoencephalographm.
http://www.elekta.com/assets/functional_mapping/images/meg_side.jpg

[59] Weiskopf N., Mathiak K., Bock S.W., Scharnowski F., Veit R., Grodd W., Goebel R., Birbaumer N., "Principles of a Brain-Computer Interface (BCI) Based on Real-Time Functional Magnetic Resonance Imaging (fMRI)", *IEEE Transactions on Biomedical Engineering,* Vol.51, No.6, June 2004

[60] Choi, S.H., Lee M., "Brain Computer Interface Using EEG Sensors Based on an fMRI Experiment", In *International Joint Conference on Neural Networks, Vancouver, Canada,* July 2006

[61] Choi, S.H., Lee M., Wang Y., Hong B., "Estimation of Optimal Location of EEG Reference Electrode for Motor Imagery Based BCI Using fMRI", *Proceedings of the 28th IEEE EMBS Annual International Conference, New York, USA,* August 2006

[62] Coyle S., Ward T., Markham C., McDarby G., "On the Suitability of Near-Infrared (NIR) Systems for Next-Generation Brain-Computer Interfaces", *Physiological Measurement,* Vol. 25, pp. 815–822, August 2004

[63] Wolpaw J.R., Loeb G.E., Allison B.Z., Donchin E., Nascimento O.F.D., Heetderks W.J., Nijboer F., Shain W.G., Turner J.N., "BCI Meeting 2005

– Workshop on Signals and Recording Methods", *IEEE Transactions on Neural Systems and Rehabilitation Engineering*, Vol. 14, No.2, June 2006

[64] Gao X., Xu D., Cheng M., Gao S., "A BCI-Based Environmental Controller for the Motion-Disabled", *IEEE Transactions on Neural Systems and Rehabilitation Engineering*, Vol. 11, No.2, June 2003

[65] Maggi L., Parini S., Piccini L., Panfili G., Adreoni G., "A Four Command BCI System Based on the SSVEP Protocol", In *Proceedings of the 28th IEEE EMBS Annual International Conference, New York, USA,* August 2006

[66] Nielsen K.D., Cabrera A.F., Nascimento O.F.D., "EEG Based BCI—Towards a Better Control. Brain-Computer Interface Research at Aalborg University", *IEEE Transactions on Neural Systems and Rehabilitation Engineering*, Vol. 14, No.2, June 2006

[67] Pfurtscheller G., Neuper C., "Motor Imagery and Direct Brain-Computer Communication", *Proceedings of the IEEE* , Vol.89, No.7, pp.1123-1134, July 2001

[68] Townsend G., Graimann B., Pfurtscheller G., "Continuous EEG Classification During Motor Imagery—Simulation of an Asynchronous BCI", *IEEE Transactions on Neural Systems and Rehabilitation Engineering*, Vol. 12, No.2, June 2004

[69] Curran E., Sykacek P., Stokes M., Roberts S., Penny W., Johnsrude I., Owen A., "Cognitive Tasks for Driving a Brain-Computer Interfacing System: A Pilot Study", *IEEE Transactions on Neural Systems and Rehabilitation Engineering,* Vol.12, No.1, pp.48-54, March 2004

[70] Pfurtscheller G., "Event-related desynchronization (ERD) and event related synchronization (ERS)," In *Electroencephalography: Basic Principles, Clinical Applications and Related Fields, 4th ed., E. Niedermeyer and F. H. Lopes da Silva, Eds. Baltimore, MD: Williams & Wilkins,* 1999, pp. 958–967

[71] Pfurtscheller G., da Silva F.H.L, "Functional Meaning of Event-Related Desynchronization (ERD) and Synchronization (ERS)," In *Event-Related Desynchronization, Handbook of Electroenceph. and Clin. Neurophysiol., rev ed,. Amsterdam, The Netherlands: Elsevier,* 1999, Vol. 6, pp. 51–65

[72] Lalor E.C., Kelly S.P., Finucane C., Burke R., Smith R., Reilly R.B., McDarby G., "Steady-state VEP-based brain-computer interface control in an immersive 3D gaming environment", *EURASIP Journal on Applied Signal Processing*, **(19)**:3156–3164, 2005

[73] OpenVIBE, A Software for Brain Computer Interfaces and Real Time Neurosciences, Webpage: http://openvibe.inria.fr/

[74] Electroencephalogram: http://en.wikipedia.org/wiki/Electroencephalogram

[75] Control of a wheelchair with BCI
http://www.utar.edu.my/ipsr/img/brain3.JPG

[76] Control of a robotic arm with BCI
http://en.wikipedia.org/wiki/File:Monkey_using_a_robotic_arm.jpg

[77] Chang C.-C., Lin C.-J., "LIBSVM: A Library for Support Vector Machines". Online available at: http://www.csie.ntu.edu.tw/~cjlin/libsvm/

[78] Uşaklı A.B., Gençer N.G., "USB-Based 256-Channel Electroencephalographic Data Acquisition System for Electrical Source Imaging of the Human Brain", *Instrumentation Science and Technology*, **35**: 255-273, 2007

[79] Microchip Technology Inc., "PIC18F2458/2553/4458/4553 Datasheet, 28/40/44-Pin High-Performance, Enhanced Flash, USB Microcontrollers with 12-Bit A/D and nanoWatt Technology". Available at: ww1.microchip.com/downloads/en/DeviceDoc/39887b.pdf

[80] Vishay Semiconductors, "IL300, Linear Optocoupler, High Gain Stability, Wide Bandwidth", Documentation:
http://www.vishay.com/docs/83622/83622.pdf

[81] Compumedics – Neuroscan, Quik-Caps,
http://www.neuroscan.com/cart/Details.cfm?ProdID=188&category=6

[82] Erdoğan H.B., "A 10 channel EEG system for BCI applications, Technical Documentation", Electrical and Electronics Engineering Dept., Brain Research Laboratory, METU, will be available at: http://www.eee.metu.edu.tr/~biomed/brl/index.html

[83] Webster J.G., "Medical Instrumentation: Application and Design", *John Wiley and Sons Inc., 3rd ed.* 1997

APPENDIX A

PROOF OF WIDE SENSE STATIONARITY OF A SINUSOIDAL RANDOM PROCESS

A random process $x(n)$ is said to be a wide-sense stationary process if the following conditions are satisfied [32]:

1. The mean of the process $\mu_x(n)$ is a constant.
2. The autocorrelation $R_x(n_1, n_2)$ is a function of $(n_1 - n_2)$.

Consider the random process given by

$$x(n) = \sum_i A_i e^{jw_i n + \varphi_i} \tag{B.1}$$

where A_i's and w_i's are deterministic (amplitude and frequency) parameters defining the sinusoid. Here, the phase parameters φ_i's are random variables whose distribution is assumed to be uniform between 0 and 2π. That is,

$$f_{\varphi_i}(\varphi_i) = \begin{cases} \dfrac{1}{2\pi} & 0 \le \varphi_i \le 2\pi \\ 0 & \textit{elsewhere} \end{cases} \tag{B.2}$$

Proof of Condition 1

$$
\begin{aligned}
\mu_x(n) &= E\{x(n)\} \\
&= E\left\{\sum_i A_i e^{j(w_i n+\varphi_i)}\right\} \\
&= \sum_i A_i E\left\{e^{j(w_i n+\varphi_i)}\right\} \\
&= \sum_i A_i e^{jw_i n}\int_{-\infty}^{+\infty} e^{j\varphi_i} f_{\varphi_i}(\varphi_i)d\varphi_i \\
&= \sum_i A_i e^{jw_i n}\int_{0}^{2\pi} e^{j\varphi_i}\frac{1}{2\pi}d\varphi_i \\
&= \sum_i A_i e^{jw_i n}\frac{1}{2\pi}\underbrace{\left(e^{j\varphi_i}\Big|_{\varphi_i=0}^{2\pi}\right)}_{=0} \\
&\Rightarrow \mu_x(n) = 0
\end{aligned}
\qquad \text{(B.3)}
$$

It can be seen that the mean of the random process is constant. Therefore, the first condition for WSS is satisfied.

Proof of Condition 2

$$
\begin{aligned}
&R_x(n_1,n_2) = E\{x(n_1)x^*(n_2)\} \\
&= \int\left(\sum_i A_i e^{j(w_i n_1+\varphi_i)}\right)\left(\sum_k A_k e^{-j(w_k n_2+\varphi_k)}\right) f_{\varphi_1,\ldots,\varphi_N}(\varphi_1,\ldots,\varphi_N)d\varphi_1\ldots d\varphi_N
\end{aligned}
\qquad \text{(B.4)}
$$

Here, it can be assumed that φ_i's are independent random variables so that their joint probability density can be represented as a product of their marginal densities:

$$
f_{\varphi_1,\ldots,\varphi_N}(\varphi_1,\ldots,\varphi_N) = f_{\varphi_1}(\varphi_1)f_{\varphi_2}(\varphi_2)\ldots\ldots f_{\varphi_N}(\varphi_N) \qquad \text{(B.5)}
$$

$$\Rightarrow R_x(n_1,n_2)=$$
$$\int\left(\sum_i A_i e^{j(w_i n_1+\varphi_i)}\right)\left(\sum_k A_k e^{-j(w_k n_2+\varphi_k)}\right) f_{\varphi_1}(\varphi_1) f_{\varphi_2}(\varphi_2)\ldots f_{\varphi_N}(\varphi_N)\, d\varphi_1\ldots d\varphi_N \tag{B.6}$$

One can note from the above expression that the integral of the cross-multiplication of exponential terms yields to 0 unless $i \neq k$. That is,

$$\int_0^{2\pi} A_i A_k e^{j(w_i n_1+\varphi_i)} e^{-j(w_k n_2+\varphi_k)} f_{\varphi_1}(\varphi_1)\ldots f_{\varphi_N}(\varphi_N)\, d\varphi_1\ldots d\varphi_N =$$
$$A_i A_k e^{jw_i n_1} e^{-jw_k n_2}\left(\frac{1}{2\pi}\right)^N \underbrace{\int_0^{2\pi} e^{j(\varphi_i-\varphi_k)}}_{=0} = 0 \tag{B.7}$$

Therefore,

$$\Rightarrow R_x(n_1,n_2)=\sum_i A_i^2 e^{jw_i(n_1-n_2)} \int_0^{2\pi} \underbrace{e^{j(\varphi_i-\varphi_i)}}_{=1} f_{\varphi_1}(\varphi_1)\ldots f_{\varphi_N}(\varphi_N)\, d\varphi_1\ldots d\varphi_N$$
$$=\sum_i A_i^2\left(\frac{1}{2\pi}\right)^N e^{jw_i(n_1-n_2)} \tag{B.8}$$

which is a function of (n_1-n_2). Therefore, $x(n)$ is WSS process as it also satisfies the second condition.

APPENDIX B

EEG HARDWARE SCHEMATICS

The circuit diagram of the designed active electrode is shown in Figure B - 1. It is composed of two voltage buffers and a first order high-pass filter with cutoff frequency of 0.1Hz.

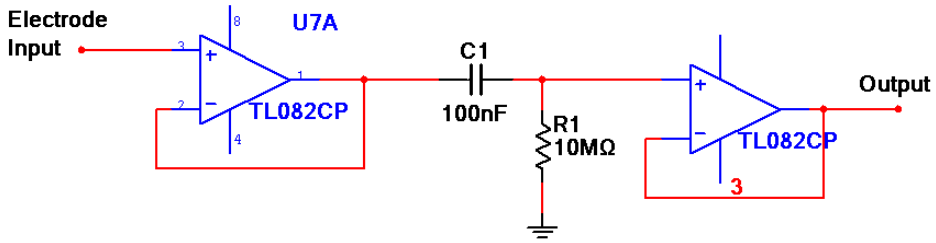

Figure B - 1: Circuit diagram of the active electrode

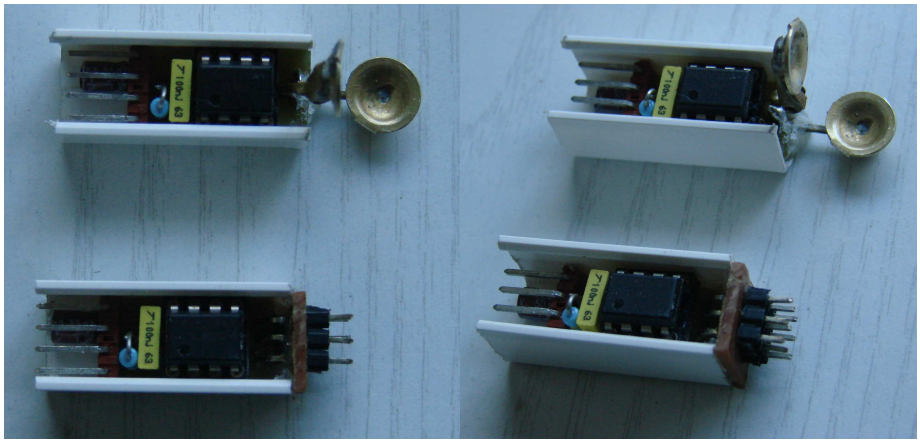

Figure B - 2: The pictures of the active electrodes. The electrode with the ring shaped contact is used for reference and attached to the right ear.

The EEG signals are amplified differentially with the preamplification stage in which the differential gain is adjusted to 50. The output signal is filtered to remove the DC offsets. The circuit diagram of the preamplifier circuitry is given in Figure B - 3.

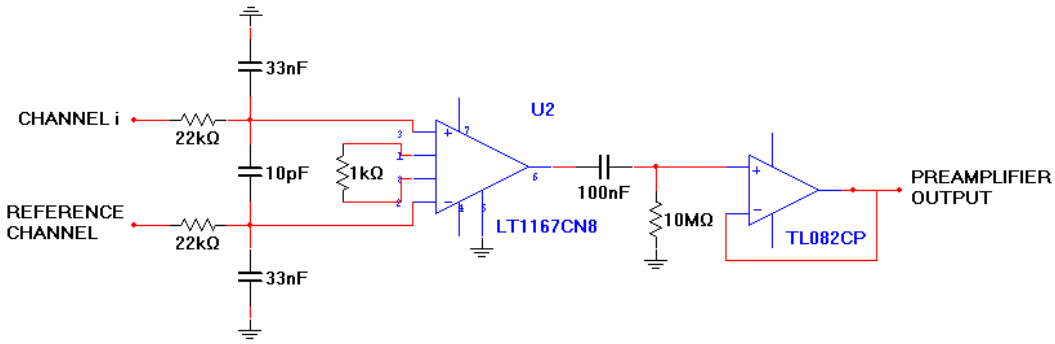

Figure B - 3: The preamplifier circuitry in the EEG amplifier.

Two active filters are used in the analog circuitry. The amplified signal is first filtered with a band-stop filter with frequency of 50Hz to remove the effect of the power line noise and after the notch filter, the signal is processed with a third order low-pass filter to remove the unnecessary components in the EEG frequency range. For this purpose, the cut-off frequency of the low-pass filter is set to 40Hz. The filter is designed according to Bessel filter specifications to obtain a flat group delay for all frequencies in the range. The circuit diagrams of the filter circuits are given in Figure B - 4 and Figure B - 5.

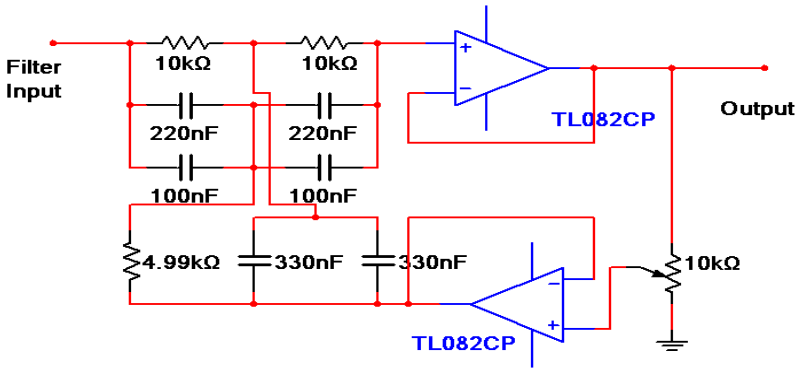

Figure B - 4: Active 50Hz notch filter. It is used to remove the effect of the power line noise.

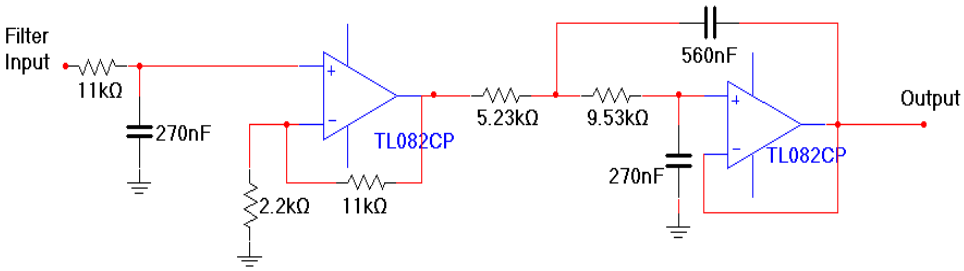

Figure B - 5: 3rd order Bessel low-pass filter with 40Hz cut-off frequency.

The whole schematics of the designed EEG amplifier is shown in Figure B - 6.

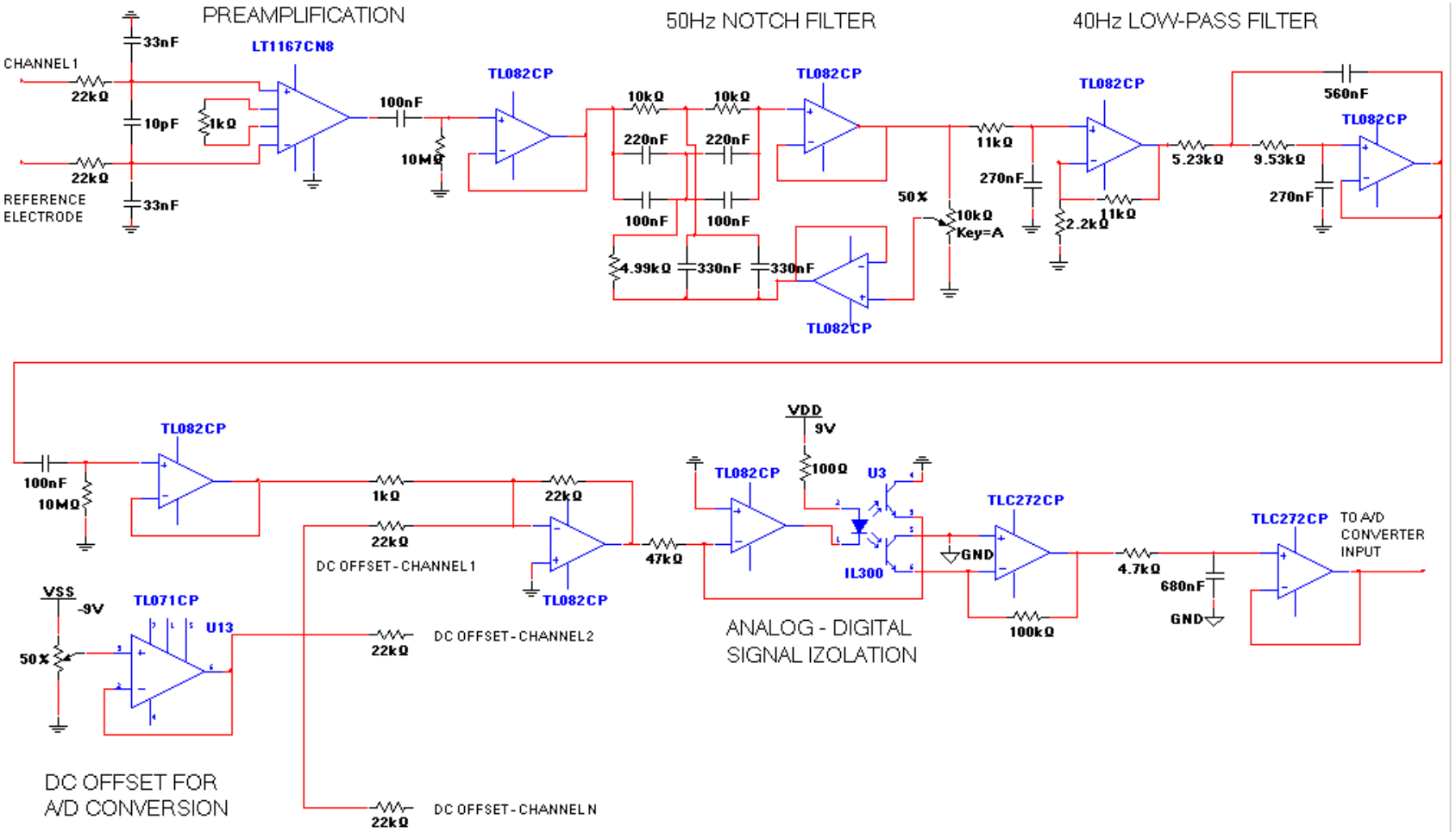

Figure B - 6: The circuit diagram of the designed EEG amplifier.

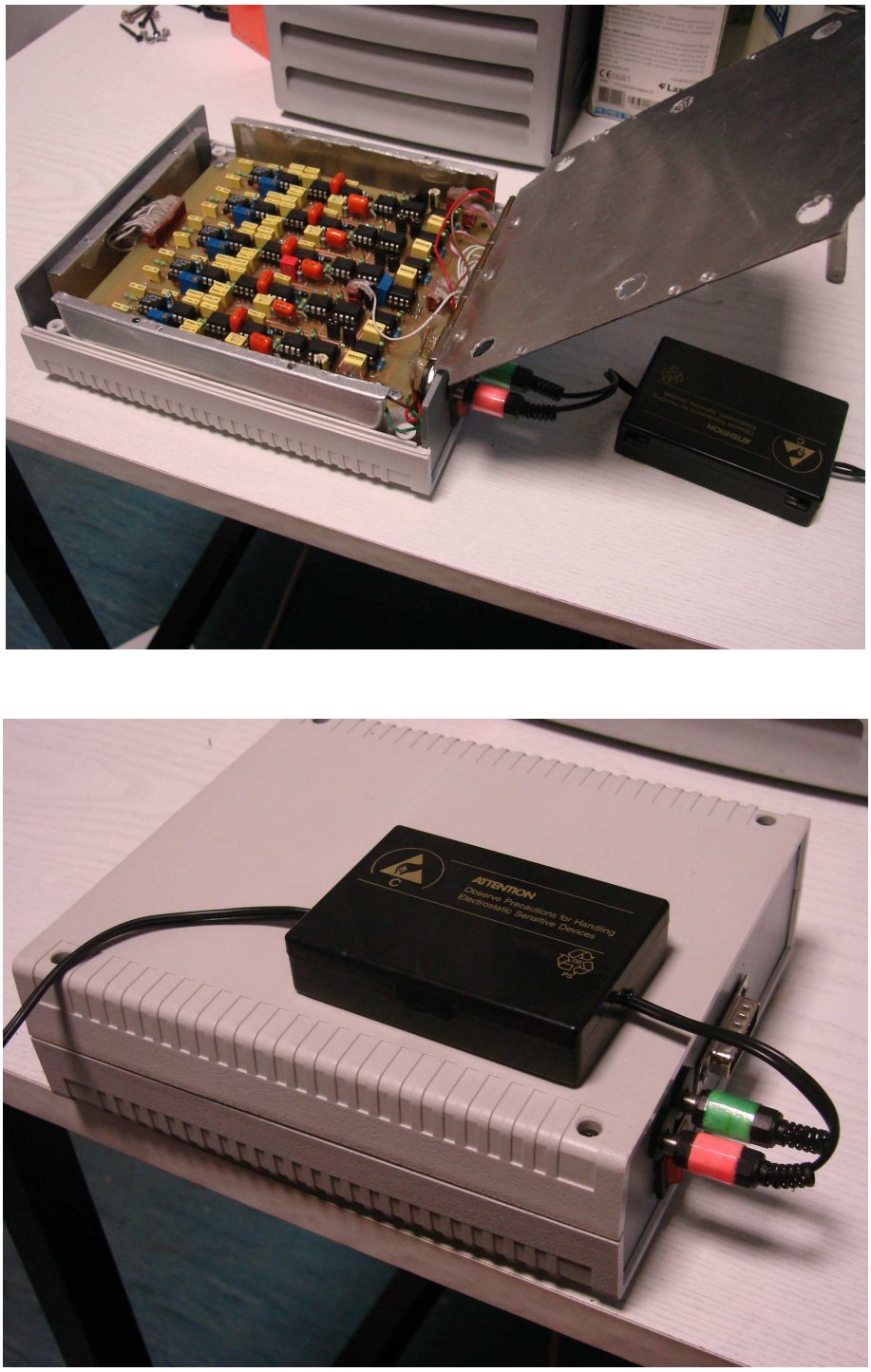

Figure B - 7: Pictures of the printed EEG amplifier. The system is supplied by two batteries. These supplies are regulated with a power circuitry included in the black box shown in the picture.

The schematics of the digital hardware is shown in Figure B - 8.

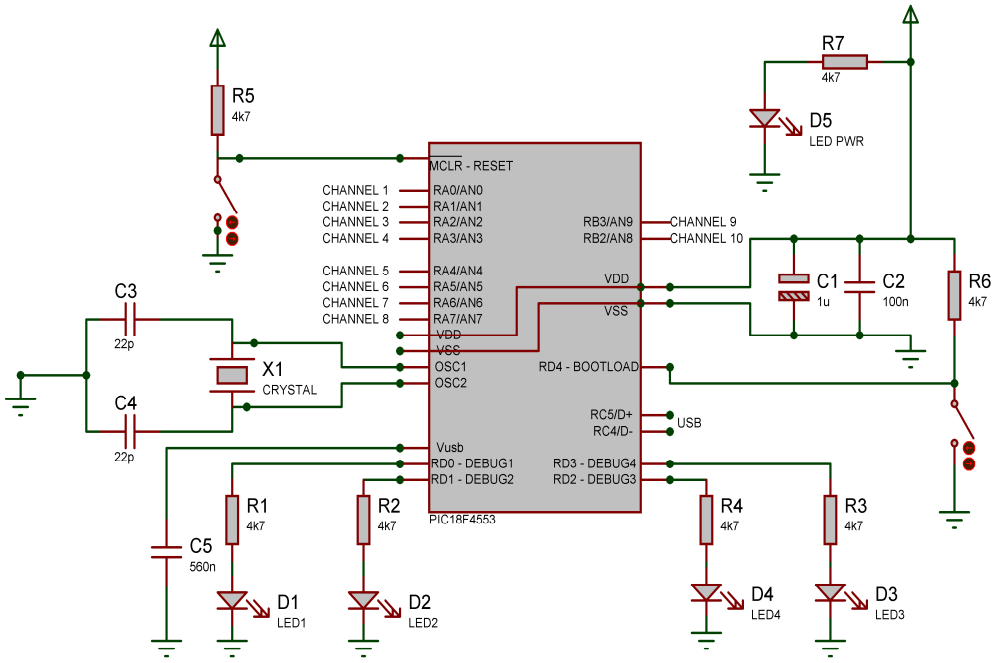

Figure B - 8: The circuit used in the digital hardware. The circuit is mainly composed of a compact microcontroller, PIC18F4553, which is used to perform A/D conversion and USB transfer.

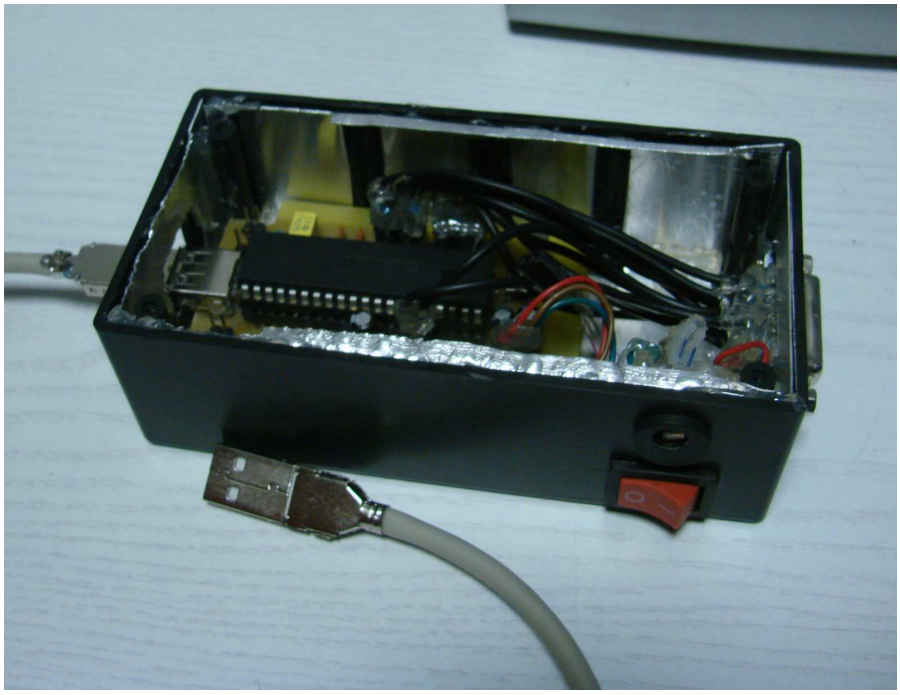

Figure B - 9: Pictures of the digitizing system. The analog signals are digitized by A/D conversion and sent to the computer via USB.

Figure B - 10: Pictures from the experiments performed with the designed EEG system.

B.1 Performance Tests

Several tests are performed to measure the performance of the designed amplification system. Here, basic tests will be presented such as Magnitude Response, Common Mode Rejection Ratio (CMRR), test signal outputs and outputs from ongoing EEG signals. One can find detailed information on these and other specifications in the technical documentation of the designed system [82].

The differential mode gain with respect to frequency is given in Figure B - 11.

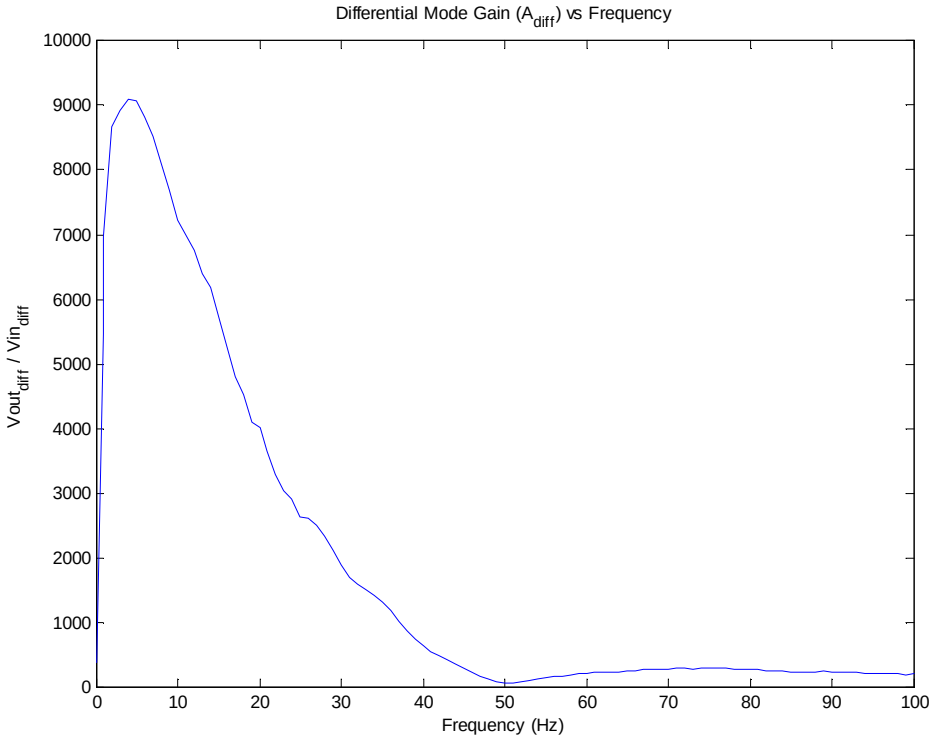

Figure B - 11 Magnitude response of the designed EEG system. The system has maximum gain between 1 and 10 Hz.

As can be seen in Figure B - 11, the system has a non linear differential gain for the frequency range. It has the minimum gain near 50Hz in order to reduce the effect of power line noise. The CMRR of the system with respect to frequency is demonstrated in Figure B - 12.

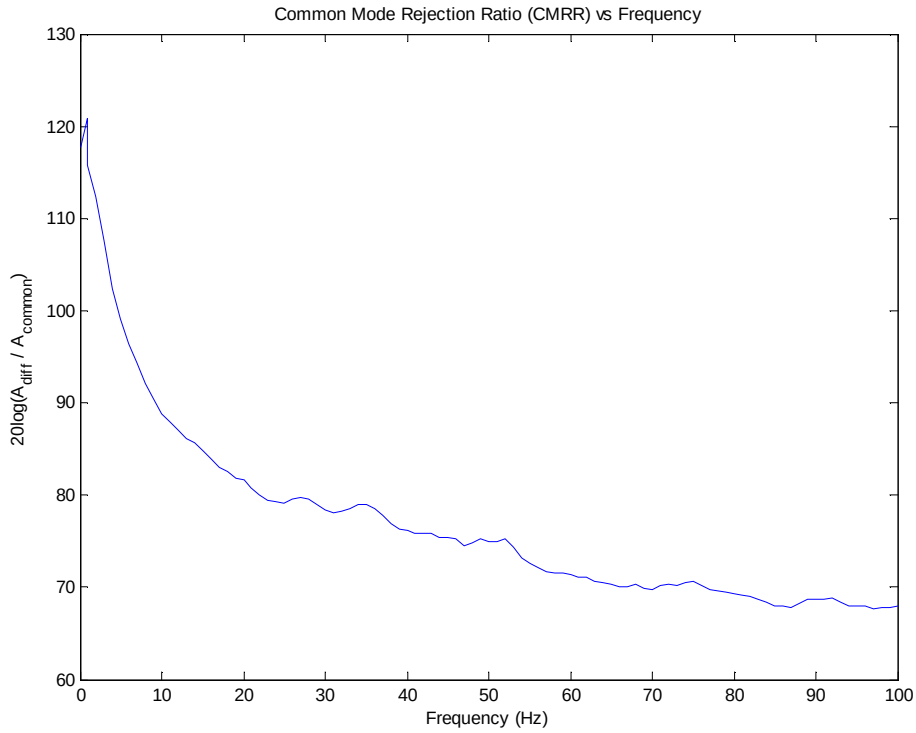

Figure B - 12: Common Mode Rejection Ratio (CMRR) of the designed EEG amplifier. The system exhibits rejection of the common mode signal higher than 80dB in the frequency range of 0.1-20Hz

Several test signals are applied to the designed system, the outputs of which are shown in Figure B - 13, Figure B - 14 and Figure B - 15. In all cases, a sinusoidal waveform with an amplitude of $100\,\mu V$ (with different frequencies) is given as the input to simulate the EEG signal. The outputs for these cases are given in terms of A/D conversion results with an offset for each EEG channel to see all waveforms in one plot. Note that the amplitude of the output decreases as the frequency is increased. This is due to the nonlinear differential gain of the amplification system shown in Figure B - 11.

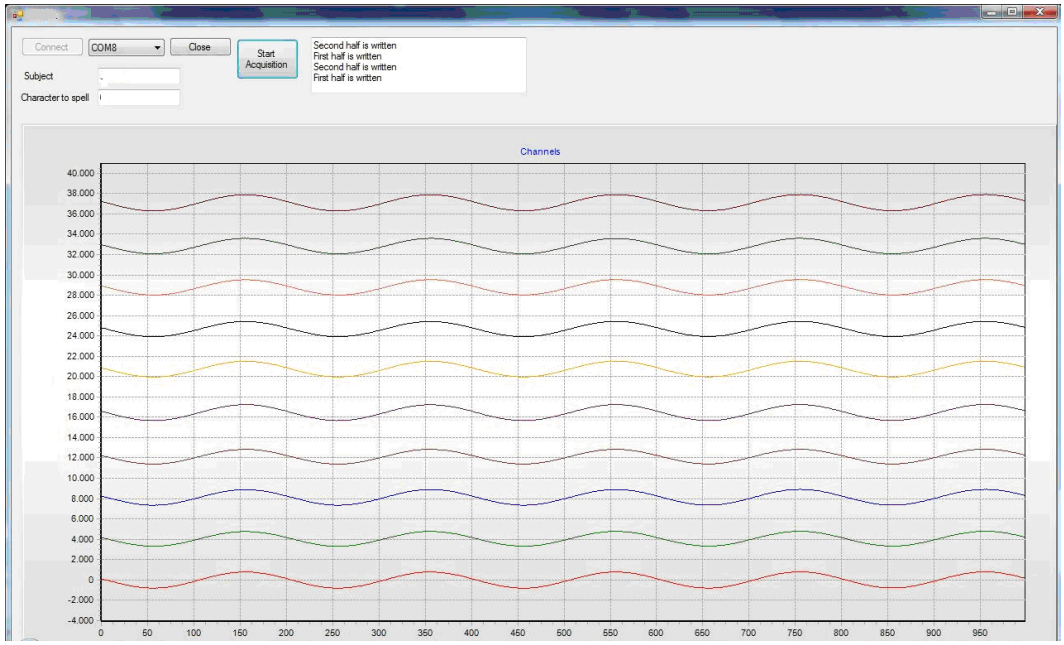

Figure B - 13: The output of the EEG system for a 100uV test signal with frequency 5Hz.

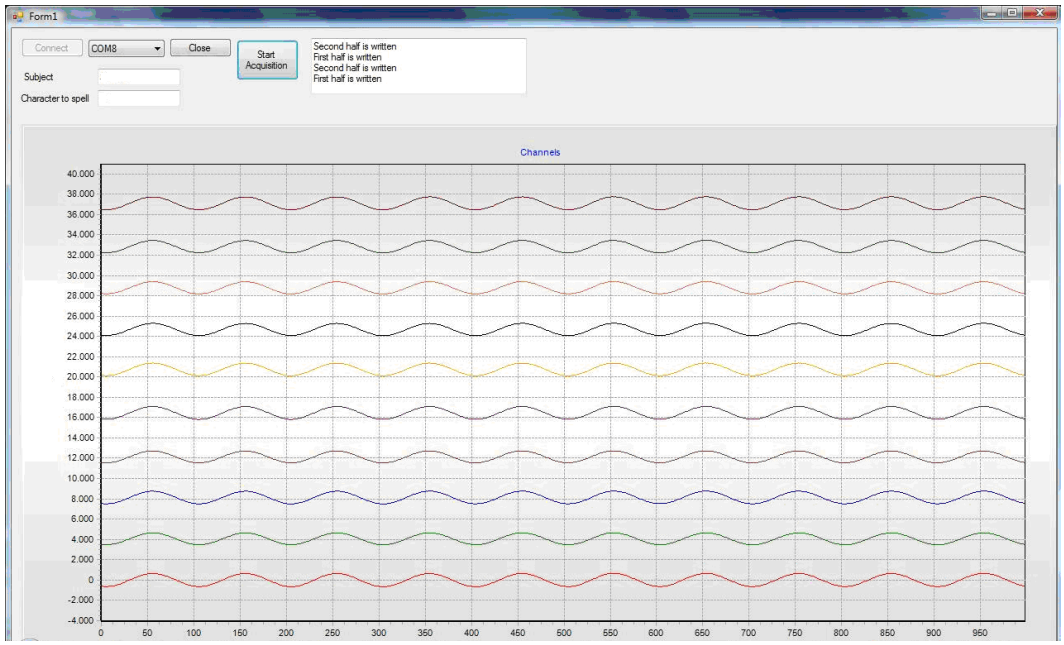

Figure B - 14: The output of the EEG system for a 100uV test signal with frequency 10Hz.

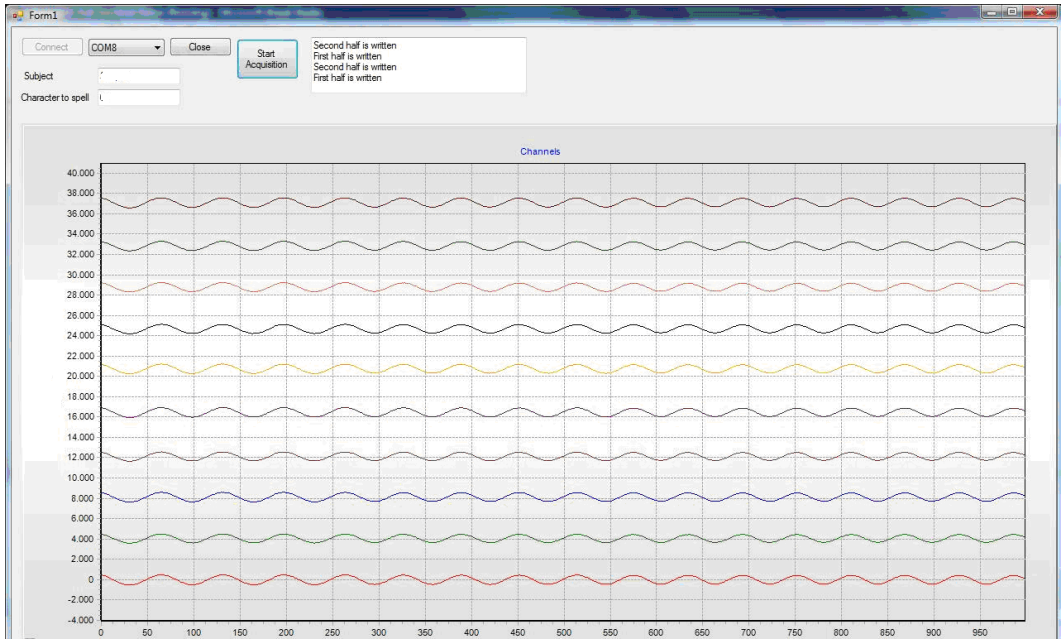

Figure B - 15: The output of the EEG system for a 100uV test signal with frequency 17Hz.

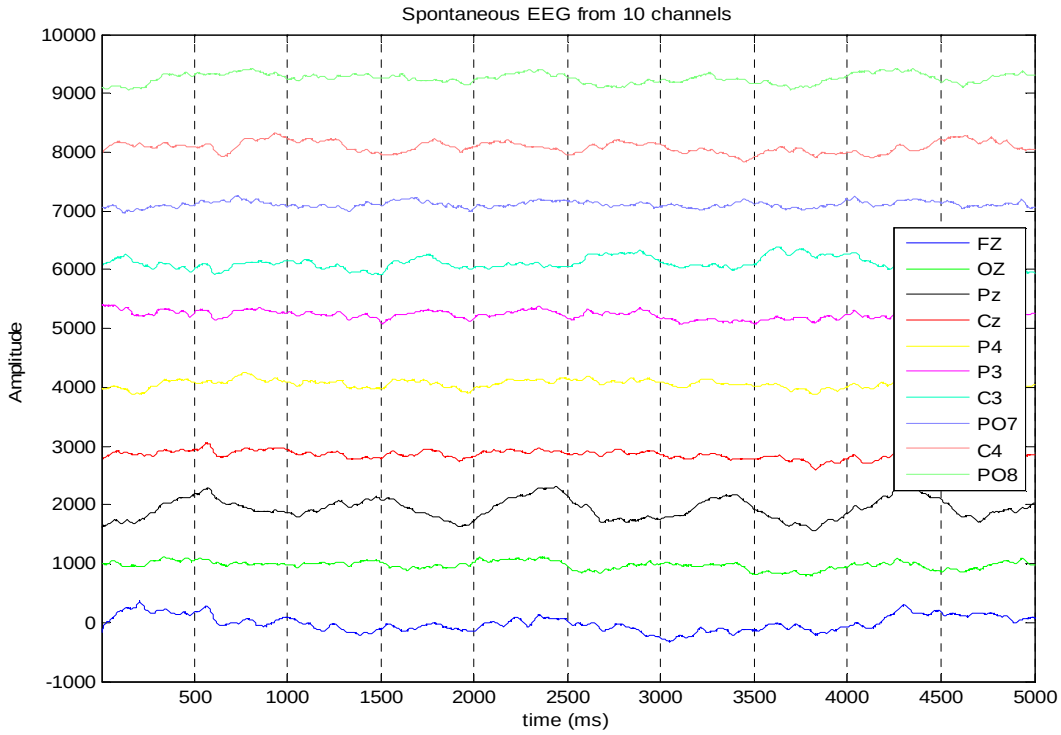

Figure B - 16: Offline visualization of the spontaneous EEG signal recorded by the system from 10 channels. The amplitude of the signals is given in terms of the A/D conversion results. An artificial offset is given for all channels in order to visualize them in one plot.